

Maria Dyrseth

Development, Design and Production of a Wingsail for an Autonomous Surface Vessel

Master's thesis in Mechanical Engineering

Supervisor: Andreas Echtermeyer

July 2020

NTNU
Norwegian University of Science and Technology
Faculty of Engineering
Department of Mechanical and Industrial Engineering



Maria Dyrseth

Development, Design and Production of a Wingsail for an Autonomous Surface Vessel

Master's thesis in Mechanical Engineering
Supervisor: Andreas Echtermeyer
July 2020

Norwegian University of Science and Technology
Faculty of Engineering
Department of Mechanical and Industrial Engineering



Abstract

During the last years, there has been a rising interest in exploring the health of the marine ecosystem. Climate changes due to rising waters, growing marine industry and shipping, plastic waste in the ocean, and pollution from cities, are only some of the topics that have been focused on. Today, the survey of the oceans is mostly done by scientific vessels with a crew or by vessels towing instrumental equipment. The scientific measurements done by the scientific vessels provide high-quality, but with a high cost. Vessels that tow equipment will only map the oceans in the areas where vessels usually travel. With Autonomous Unmanned Surface Vessels, much larger areas can be mapped, which can contribute to the goal of providing more data related to our oceans.

This thesis covers the whole development process, from concept and design to production of all parts of a hollow composites wingsail for an Autonomous Measurement Boat at the Norwegian University of Science and Technology. The design process was done utilizing a structural parametric study, together with composites modeling and Computational Fluid Dynamics (CFD) for creating a realistic wind pressure load. By using simulation-based composite layup optimization early in the design process, the time to achieve a high-performing design are reduced. The results from the final design showed that the wind pressure load at the maximum design wind velocity of 20 m/s acting on the wingsail, produced a maximum stress, in fiber direction S11 of 21.37 MPa. The stress occurred in the mast and is just 1.66 % of the strength. The weight target was met with the wingsail weighing 19 kg while having a maximum deformation of 3.371 mm at the maximum design wind of 20 m/s.

The thesis also describes the manufacturing of all the parts of the wingsail, which was done by the author herself. Medium-Density Fiberboard was used as mould material, creating moulds for the outer shell and internal "ribs" of the wingsail. Carbon Fibre Reinforced Plastic (CFRP) parts were made utilizing common composites manufacturing methods such as filament winding, Vacuum Assisted Resin Infusion and out-of-autoclave pre-impregnated fibers.

Sammendrag

I løpet av de siste årene, har det vært en økt interesse i å undersøke det marine økosystemets helse. Klimaendringer der økte havnivåer, en økende marin industri og shipping, plastikkavfall i havet og forurensing fra byer, er bare noen av feltene som har blitt fokusert på. I dag, blir undersøkelser på havet er hovedsakelig gjort av forskningsbåter der personell må være tilstede, eller av instrumentelle utstyr slept av båter. De undersøkelsene som blir gjort av slike forskningsbåter er av høy kvalitet, men også med en høy kostnad med tanke på at den må være bemannet. I tillegg vil båtene som sleper instrumentelle utstyr, kun undersøke i de områdene der båter som regel kjører. Med en autonom, ubemannet overhavsbat vil mye større områder kunne bli utforsket, som kan bidra til målet om å få samlet inn mer data relatert til havet vårt.

Denne masteroppgaven omhandler hele utviklingsprosessen, fra konsept og design, til produksjon av alle deler av et hul kompositt vingeseil for en autonom målingsbat ved Norges teknisk-naturvitenskapelige universitet. Designprosessen var gjort ved å benytte strukturelle parameterstudier, sammen med komposittmodellering og numerisk fluiddynamikk for å lage et realistisk vindtrykk på vingeseilet. Bruk av simuleringsbasert kompositt-optimering i de tidlige designfasene, gjør at tiden for å oppnå et høyt ytende design er redusert. Resultatene fra det ferdige designet viste at maksimale vindtrykket ved 20 m/s som virker på vingeseilet, produserer en maksimal spenning i fiberretning på 21.37 MPa. De største spenningene på vingeseilet oppstod i masten og er på kun 1.66 % av styrken. Vektmaatlet var innfridd da alle delene på seilet veide totalt 19 kg med en maksimal deformasjon på 3.371 mm ved maksimal designet vindlast på 20 m/s.

Opgaven beskriver også produksjonen av alle delene av vingeseilet der alt ble utført av forfatteren selv. Medium-Density Fiberboard ble brukt som støpeformmateriale for begge vingeskallene og de interne avstiverstagene. Karbonfiberdelene ble lagd med velkjente komposittproduksjonsmetoder som vikling, vakuuminfusjon og med pre-impregnert egnet til støp utenfor av autoklav.

Acknowledgements

I would like to dedicate a big thanks to my supervisor Professor Andreas Echtermeyer who has been supporting me along the way, as well as Erik Sæther and Sondre Østli Rokvam at the composites group for all the help for helping me get a better knowledge within composites production. A special thanks to the companies Fritzoe Engros, ReThink and Hagemans Nordic which made me bring this work to life.

Last but not least, I would like to thank Christer Kobbevik Oldeide for his valuable engineering advises and endless support, and my mom and dad for always being supportive and encouraging.

Contents

Abstract	i
Sammendrag	iii
Acknowledgements	v
Nomenclature	xvi
Symbols	xvii
1 Introduction	1
1.1 Background and motivation	1
1.2 Problem Description	1
1.3 Project Scope	1
1.4 Requirements for the autonomous surface vessel	2
1.5 Various Configurations of Sail	3
1.5.1 Rigid Sail with Foam Core	3
1.5.2 Rigid Sail with Ribs	3
1.5.3 Symmetric Airfoil	4
1.5.4 Cambered Airfoil	4
1.5.5 Tapered Wing Profile	4
1.5.6 Rectangular Wing Profile	4
1.5.7 Chosen Concept: Symmetric, Rectangular Wingsail with Ribs	5
1.6 Thesis structure	5
2 Theory	7
2.1 Loads on the Sail	7
2.2 Airfoil	8
2.3 CFD	9
2.4 Structural Analysis	10
2.5 Composites	10
2.5.1 Typical Definitions for Composites	12
2.6 Manufacturing Methods	12

2.6.1	Filament Winding of Tubes	12
2.6.2	Vacuum Assisted Resin Transfer	13
2.6.3	Pre-preg "Out-of-Autoclave"	14
3	Methods and Procedure - Design	16
3.1	Overview	16
3.2	Deciding Airfoil Profile	16
3.3	Deciding Wing Area	19
3.4	Overview CFD and Structural Optimization	21
3.5	CAD Setup	21
3.6	CFD Setup	22
3.6.1	CFD Mesh	22
3.6.2	Solver	22
3.6.2.1	6.5 m/s	22
3.6.2.2	20 m/s	23
3.7	Structural Optimization Setup	24
3.7.1	Design Requirements	24
3.7.2	Overview	24
3.7.3	Mesh	25
3.7.4	Material	25
3.7.5	Boundary Conditions, Load and Interactions	26
3.7.6	Regions	26
3.7.7	Composite Layup	27
3.7.8	Parameter Study Values	27
3.8	Structural Mechanical Setup in Abaqus	29
3.8.1	Overview	29
3.8.2	Material	29
3.8.3	Properties and Composite Layup	29
3.8.4	Load and Interactions	30
3.8.4.1	Importing Loads From Ansys to Abaqus	30
3.8.4.2	Interactions	30
3.8.5	Boundary Conditions	30
3.8.6	Mesh	31

3.8.7	Buckling Analysis Setup	31
4	Methods and Procedure - Production	32
4.1	Overview	32
4.2	Mould Production	32
4.2.1	Mainsail Mould	32
4.2.2	Rib Mould	36
4.3	Carbon Fiber Reinforced Polymer Production	37
4.3.1	Mainsail CFRP Production	37
4.3.2	Spars CFRP Production	39
4.4	Mast CFPR Production	41
4.4.1	Mast Extraction	45
4.5	Electronics Box	46
4.6	Electronics Routing	47
4.7	Assembly	48
5	Results and Discussion - Design	50
5.1	CFD	50
5.1.1	CFD Validation	50
5.2	FEA	53
5.2.1	Structural Optimization	53
5.2.2	Results for Candidate 1	57
5.3	Validation - Mechanical Analysis Abaqus	57
5.3.1	Buckling Results	58
5.3.2	Material Data	58
5.3.2.1	XPREG XC110 410 g Prepreg	58
5.3.2.2	GRAFIL 34-700 24K	59
5.3.2.3	Pyrofil TR30S	59
5.3.3	Mesh Sensitivity Analysis	59
5.4	Summary of Results	61
6	Results and Discussion - Production	62
6.1	Mainsail	63
6.2	Mast	65

6.3	Ribs	67
6.4	Electronics Box	68
7	Conclusion	70
8	Further work	71
8.1	Controlling Sail Orientation	71
8.2	Assembly	72
8.3	Testing	72
8.4	Sensors and Electronics	73
8.5	Mast Foot	73
8.6	UV-coating	74
	References	75
	Appendices	78
A	Modeling, Setup, Procedures and Results	78
A.1	CFD Setup	78
	A.1.1 2D-analysis	78
	A.1.2 3-D	86
A.2	Structural analysis	87
	A.2.1 Mesh	87
	A.2.2 Setup composite layup	87
B	FEM Validation Setup in Abaqus	90
B.1	Part	90
B.2	Properties	91
	B.2.1 Materials	91
	B.2.2 Ribs, Mast and Main Sail	93
	B.2.3 Glue	95
B.3	Assembly	95
B.4	Step	95
	B.4.1 Static	95
	B.4.2 Buckling	95
B.5	Interactions	95

	B.5.1	Glued Connections	95
	B.5.2	Mast Interface	96
B.6		Loads	96
B.7		Mesh	97
	B.7.1	Ribs	97
	B.7.2	Mast	98
	B.7.3	Main Sail	99
	B.7.4	Glue	100
C		FEM Validation Results from Abaqus	101
	C.1	Global Result @ 6.5m/s Wind Speed	101
	C.2	Mast Result @ 6.5m/s Wind Speed	102
	C.3	Spant Result @ 6.5m/s and 20m/s Wind Speed	103
	C.4	Global Result @ 20m/s Wind Speed	104
	C.5	Mast Result @ 20m/s Wind Speed	105
	C.6	Glue Result @ 20m/s Wind Speed	106
D		Ansys Mechanical Additional Results	107
E		Material Data Test	110
	E.1	Rib CFRP Specimen Preparation	110
	E.2	Mainsail CFRP Specimen Preparation	110
	E.3	Strain Gauges	110
	E.4	Tensile Test	110
	E.5	Results	111
F		Provided Data	112
G		Scripts	113
	G.1	Abaqus Automatic Meshing Script	113
	G.2	Polynomial Regression Python Script	117
H		Machine Drawings for Testrig	120
	H.1	Testrig Frontplate	121
	H.2	Testrig Backplate	122
	H.3	Testrig Strammer	123
I		Datasheets	124
	I.1	Cascol Indoor 3304	125
	I.2	Medium-Density Fiberboard	127

I.3	GRAFIL 34-700 Filament Winding Fiber	128
I.4	Mitsubishi-Rayon Pyrofil TR30S 3K	129
I.5	Tencate - Carbon 205 gsm 2x2 Twill TR30S T 3K	130
I.6	XPREG XC110 Out-Of-Autoclave Component Prepreg System	133
I.7	XPREG XC110 Out-Of-Autoclave Component Prepreg System - Processing Guide	136
I.8	EPIKOTE Resin MGS RIMR 135 Data Sheet	137
I.9	TEKNOSEAL 4002 Sealer Data Sheet	146
I.10	TEKNOTHERM 4350 Topcoat Datasheet	147
I.11	SprayMax 2k Clear Coat	148
I.12	Chemlease 2185 Release Agent	151

List of Figures

1	Wingsail produced as a sandwich structure with foam core	3
2	Wing with spars, ribs and wing skin	3
3	Symmetric airfoil profile	4
4	Cambered airfoil profile	4
5	Various configurations of planform's for straight wings	5
6	Forces acting on a wingsail.	8
7	Definition of an airfoil.	8
8	Airfoil nomenclature	9
9	Different patterns of woven Carbon Fibers	11
10	Overview of layers and the respective orientations for a laminate	12
11	Filament Winding Overview	13
12	VART Schematics Overview	14
13	Overview of the production method for Out-of-Autoclave Prepreg	15
14	(a) Wingprofile for the non-symmetric profile NACA2412, (b) Wingprofile for the symmetric profile NACA0018	16
15	(a) NACA2412 Lift coefficient vs alpha from XFOIL, (b) NACA0018 Lift coefficient vs alpha from XFOIL.	17
16	NACA0021 profile	18
17	(a) NACA0018 Lift coefficient/ Drag coefficient vs alpha from XFOIL, (b) NACA0021 Lift coefficient/ Drag coefficient vs alpha from XFOIL.	19
18	Hull resistance for different cases vs vessel velocity for the 2 meter long hull.	20
19	Design Approach Overview	22
20	Overview of the structural setup.	25
21	Overview of the imported pressure imported from CFD.	26
22	Overview of the various regions of the wingsail	27
23	Mainsail mould components before (a) and after (b) milling	33
24	Mainsail mould after milling assembly	33
25	Overview cutting and gluing MDF	34
26	MDF milling	35
27	Mainsail mould after assembly of milled components and filler applied	36
28	Rib mould before and after milling	37

29	Production schematics	38
30	Mainsail Production	38
31	Production schematics of ribs	40
32	Rib production	40
33	Curing Cycle Ribs	41
34	Stainless steel mandrel	42
35	PAN carbon fiber being wound onto the mandrel	43
36	Completed filament winding process	44
37	Profiles attached to the mast	45
38	Overview of the mast extraction configuration	46
39	Electronics top cover	47
40	Electronics box main room and placement in wingsail	47
41	Internal routing of cables	48
42	Assembly schematics	49
43	Lift force vs alpha from CFD-analysis of the wingsail of area 2.88 m^2 with K-KL- omega turbulence model.	50
44	Comparison of Cl/Cd and Cl vs alpha from XFOIL, k-omega SST model and k-kl- omega model	51
45	Comparison of Cd vs alpha from XFOIL, k-omega SST model and k-kl-omega model	52
46	Pressure field along the wingsail boundaries	53
47	Iteration history for the structural optimization	54
48	Mesh sensitivity analysis for S11 and S22	60
49	Mesh sensitivity analysis S12 and U	60
50	Deformed wingsail illustration	61
51	Mainsail with ribs and mast placed in the mainsail mould	63
52	Mainsail production - Air bubbles	64
53	Mainsail shell after demoulding	65
54	The CFRP mast with ends cutted	65
55	Scratches observed on mandrel	66
56	All six ribs trimmed and demoulded	67
57	Rib mould damage details	68
58	Final Electronics Box	69
59	Design suggestion for flap for controlling the sail orientation	71

60 Autonomous boat test-rig 72
61 Suggestion for a ball bearing mast foot which was used in a similar project 73

List of Tables

1	Pros and cons of both dry and pre-impregnated fibers.	11
2	Reynolds Number and the respective colours for the plots in Figure 15b, Figure 15a, Figure 17b and Figure 17a	17
3	CFD setup-properties for 6.5 m/s in Ansys Fluent.	23
4	CFD setup-properties for a wind speed of 20 m/s.	24
5	Summary of material constant for TeXtreme.	25
6	Input parameters and the respective bounds in the structural parameter study . . .	28
7	Properties for the materials used in the analysis	29
8	Properties for fail stress of the materials used in the analysis	30
9	Final layup for all the various components of the wingsail.	30
10	Overview of the different components and production methods used.	37
11	Winding parameters	42
12	Results for the three best candidate points after 200 iterations.	55
13	Main Geometric and Aerodynamic Properties of the Wing Sail for Candidate Point 1 with a figure describing the optimal rib placement in the wingsail to the right. . .	56
14	Results Ansys Mechanical including Failure criterions, with load case 1 as the pressure imported from CFD at 6.5 m/s and AOA of 11 °.	57
15	Summary of the design results for the total wing sail, the worst loaded rib, mast and glue for 6.5 m/s and 20 m/s loadcase	57
16	Results from buckling analysis for 6.5 m/s and 11 deg	58
17	Weight after production for each part.	62
18	Minimum requirements for the mast foot.	74
19	Test results from the tensile tests	112
20	Provided data from research group	113

Nomenclature

AOA Angle of Attack

ASV Autonomous Surface Vessel

CAD Computer Aided Design

CFD Computational Fluid Dynamics

CFRP Carbon Fiber Reinforced Plastic

FEA Finite Element Analysis

MDF Medium Density Fiberboard

NACA The National Advisory Committee for Aeronautics

SWASH Small-waterplane-area single hull

SWATH Small-waterplane-area twin hull

UD Unidirectional

VARI Vacuum-Assisted Resin Infusion

Symbols

Property	Unit	Description
V_w	$\frac{m}{s}$	Wind Velocity
V_v	$\frac{m}{s}$	Vessel Velocity
μ	$\frac{kg}{m \cdot s}$	Dynamic Viscosity
ν	$\frac{m^2}{s}$	Kinematic Viscosity
ρ	$\frac{kg}{m^3}$	Density
L	m	Length
L_{chord}	m	Chord Length
S	m^2	Span
Re	-	Reynolds Number
c_l	-	Lift Coefficient
c_d	-	Drag Coefficient
L_f	N	Lift Force
D_f	N	Drag Force
P	MPa	Pressure
t	s	Time
$\sigma_{t_{1-3}}$	MPa	Max Principle Stress in Tensile
$\sigma_{c_{1-3}}$	MPa	Max Principle Stress in Compression
$F_{R_{tot}}$	N	Total Reaction Force

1 Introduction

1.1 Background and motivation

The autonomous and sensor technology have taken significant steps in the last years, which have made Autonomous Unmanned Surface Vessels possible to develop without the need for large budgets. Several development teams have come up with different concepts for autonomous vessels, such as the Saildrone [1]. Autonomous vessels eliminate the need for personnel and can be on the ocean for many years by utilizing renewable energy resources. The autonomous vessel can carry instrumental equipment and map the oceans while being self-sufficient for energy.

1.2 Problem Description

The overall goal of the project is to develop a self-sufficient, autonomous surface vessel that will map the oceans. The multidisciplinary team from marine and mechanical technology started in august 2019 with relatively clean sheets and worked together to decide the overall concept for the autonomous surface vessel. After the start-up period, the project was divided into different areas of responsibility and this thesis focuses on the development and production of the vessel's sail. Further work on the autonomous vessel will be done by two master students from mechanical engineering at NTNU this fall. Since the project's continuation will include instrumentation the wingsail, it was decided that the author would not complete the assembly process of the wingsail components, but leave it for a later stage in the project. Nevertheless, plan and analysis of the assembly will be presented in this thesis. This decision also affects the testing of the wingsail, where a test rig has been produced and is ready when the team is ready for assembly.

The work presented in this thesis is a continuation of the work done in the specialisation project in the course TMM4560 in the fall of 2019 and some sections are therefore identical [2].

1.3 Project Scope

Development, design and manufacturing of a wingsail for an autonomous surface vessel.

1.4 Requirements for the autonomous surface vessel

Firstly, the overall requirements for the vessel are presented. It is desirable that the research vessel is robust and can be at the oceans without maintenance for several years. The vessel should be able to and shall:

- Have a length of approximately 2 meters
- Be able to resist high wind velocity and rough sea
- Cruise at a speed of 1.5 m/s
- Survive high waves of 10 m
- Be self-sufficient of energy
- Perform measurements at sea
- No need for maintenance so it can be out at seas from 1-20 years
- Minimize the numbers of moving parts
- Have a low center of gravity

Based on these overall requirements for the vessel, the following requirements are set for the design of the sail:

- Must survive high wind speeds up to 20 m/s
- Must house electronics, cables and sensors
- Must be able to change the angle of attack
- Must weight less than 20 kg
- Must be able to provide lift force higher than the hull resistance

1.5 Various Configurations of Sail

Rigid sails can be constructed by utilizing lightweight and robust composites and have several advantages compared to regular soft sails. For autonomous boats where no people are present, soft sails will be more unreliable due to problems with flapping and bluffing. With rigid sails, the only variable that needs to be controlled is the wingsail orientation. The drawback with rigid sails using composites is for now (2020) that they are more expensive than standard sail configurations.

1.5.1 Rigid Sail with Foam Core

The rigid sail with a foam core has a sandwich structure with a lightweight core material coated with fiber reinforced plastic, as seen in Figure 1. One advantage of this configuration is that the sandwich structure allows the shear stresses from external loads to be distributed over a wider area of the structure. Literature studies showed that a disadvantage of this configuration is that the core can get soaked in epoxy and the whole configuration can end up quite heavy as a result [3]. In the thesis "Design of a free-rotating wing sail for an autonomous sailboat" by Claes Tretow, the author suggested that a hollow wing would be a better option. However, the core material in a hollow configuration must be shaped or machined, which will raise the cost of manufacturing.

1.5.2 Rigid Sail with Ribs

Another possibility is to construct a wingsail with composites materials consisting of a wingsail skin with internal ribs [4] as seen in Figure 2. This concept is arranged the same way as a flight wing and has the advantage of having lightweight ribs where the placement of these can be optimized. The disadvantage



Figure 1: Wingsail produced as a sandwich structure with foam core [3].

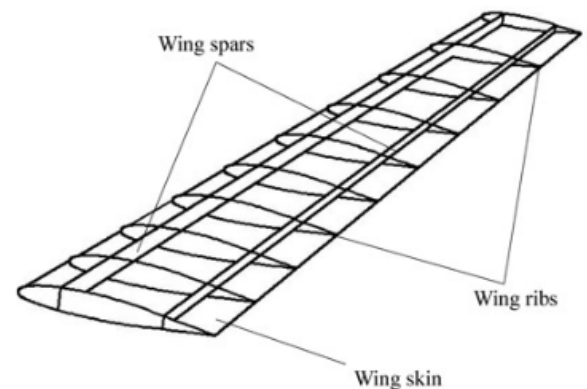


Figure 2: Wing with spars, ribs and wing skin [4].

of this configuration is that the ribs give less resistance against buckling than the foam core solution.

1.5.3 Symmetric Airfoil

The symmetric airfoil profile as seen in Figure 3 has a lower lift coefficient than an unsymmetrical airfoil, but a significant advantage for the symmetric airfoil is that the center of pressure and aerodynamic center will always be at 1/4 of the chord line from the leading edge [6], see

Figure 7. This placement will make the moments in this point zero and make the wingsail's orientation easy to control if the mast is placed at this point. Another advantage with the symmetric airfoil profile is that it will only require one negative mould which can be used twice for casting, and as a result the amount of work and the cost will be significantly reduced.

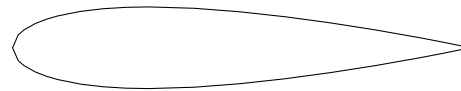


Figure 3: Symmetric airfoil profile [5].

1.5.4 Cambered Airfoil

The cambered wing profile, see Figure 4, provides a higher lift than the symmetric profile, but does not have the center of pressure and aerodynamic center at the same location. Additionally, the cambered airfoil will require two different mould parts.



Figure 4: Cambered airfoil profile [5].

1.5.5 Tapered Wing Profile

The most optimal wing shape for minimizing induced drag is the elliptical wing-shape, which can be seen in Figure 5. However, the tapered wing performs nearly as well as the elliptical wing while also having the benefit of being easier to manufacture than the elliptical wing. This is why one hardly sees elliptical wings on airplanes these days. The drawback of using tapered wing configuration on the wingsail is that it requires two moulds which will increase the cost of manufacturing.

1.5.6 Rectangular Wing Profile

As as seen in Figure 5, the rectangular wing has the advantage that it will only require one mould that will be used twice for casting. On the other hand, the disadvantage of rectangular wingsail compared to tapered, is that the induced drag is higher. For airplanes, this is an essential factor, but for wingsails where the wind speeds are far from as high as for airplanes, the induced drag increase would not be that high.

1.5.7 Chosen Concept: Symmetric, Rectangular Wingsail with Ribs

Due to the considerations discussed above, a configuration of composites skin and ribs with a rectangular, symmetric wing profile was chosen as the concept for this project.

1.6 Thesis structure

The thesis will first contain a chapter that includes relevant theory for FEA, CFD, composites, and the production methods used in this project. Some fundamental sail theory and airfoil theory is presented.

Chapter 3 contains the theoretical methods and procedures done in the development and design of the wingsail. The detailed setup for the software used is placed in the Appendices.

In Chapter 4, the production methods of all parts are presented.

Furthermore, Chapter 5 presents the results and discussion obtained from the design analysis. For CFD, the results obtained are validated by comparing different analysis methods. Discussion of the results is also provided where potential errors and uncertainties in the development and production of the wingsail will be assessed.

The results from the production are presented in Chapter 6 and a discussion around these is

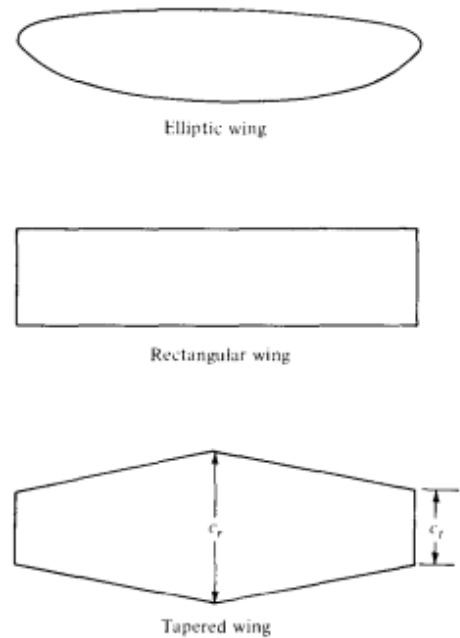


Figure 5: Various configurations of planform's for straight wings [6].

presented.

Chapter 7 includes some concluding remarks about the analysis and development before Chapter 8 presents a suggestion for further work that will be continued by the new students who are going to work on the project from August 2020.

In the end, the references cited through the work are listed, before the Appendices, with relevant information supplying the analysis, are presented in the thesis. The Appendices include datasheets, machine drawings, python scripts, test data and more detailed setup for the software and some additional results.

This thesis is written with the assumption that the reader already has a overview and basic understanding of:

- Finite Element Method (FEM)
- Computational Fluid Dynamics (CFD)
- Computer Aided Design (CAD)
- Application of FEA for orthotropic materials
- Carbon Fiber Reinforced Polymer (CFRP)

2 Theory

This section will describe some of the fundamental theory related to the project. Firstly, the external loads acting on the sail are presented before the term airfoil is described. After that, Computational Fluid Dynamics is briefly introduced, followed by an overview of the Classical Laminate Theory and the assumptions for modeling of composites. Composites are then introduced where various arrangements and definitions are presented. Lastly, a description of two of the manufacturing methods for composites that are utilized in this project are provided.

2.1 Loads on the Sail

The primary function of a sail is to create thrust force to the vessel. The different forces acting on a ship hull can be seen in Figure 6. As seen from this, V_B indicates the vessels heading direction, F_{Hx} the vessel's hull resistance in x-direction and F_{Hy} the heeling forces. The aerodynamic forces are seen with a resultant F_A and can be decomposed into a x-component F_{Ax} and a y-component F_{Ay} . α shows the angle of attack (AOA) for the sail with respect to the apparent wind, V_A , while β indicates the angle between the heading direction and the wind direction. Lastly, λ describes the angle between the midline of the vessel and the heading direction.

The forces seen in Figure 6, are all critical parameters for developing the sail. The hull resistance F_{Hx} needs to be less than the F_{Ax} .

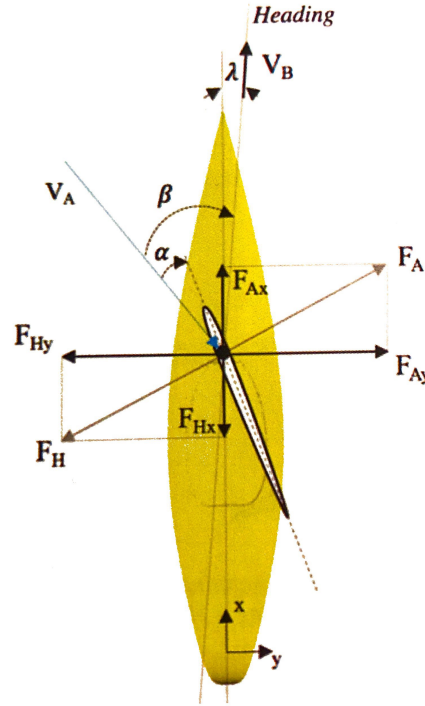


Figure 6: Forces acting on a wingsail [3].

2.2 Airfoil

The term airfoil is any section of the wing cut by the xz -plane, as seen in Figure 7.

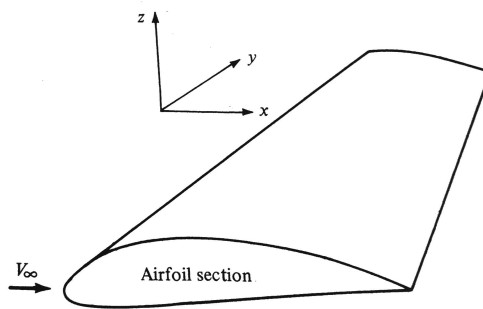


Figure 7: Definition of an airfoil [6].

The research for more efficient designs for wings has been studied extensively in the last century, where airplanes have become essential in many fields. Airfoils come in a variation of

shapes and it is crucial to choose the right profile where properties correspond to the use. In 1938, the National Advisory Committee for Aeronautics (NACA, now NASA), started to test and develop different shapes of airfoils where the results have been made available online. They identified different profiles as combinations of numbers, where the first edition of airfoils developed by NACA was a "four-digit"-series, e.g. NACA 2412. The first digit in the number represents the maximum camber as a percentage of the chord, the second digit describes the location distance of maximum camber along the chord from the leading edge in tens of percent of the chord. The last two digits describe the maximum thickness as a percentage of the chord where an illustration of some definitions as chord and camber can be seen in Figure 8.

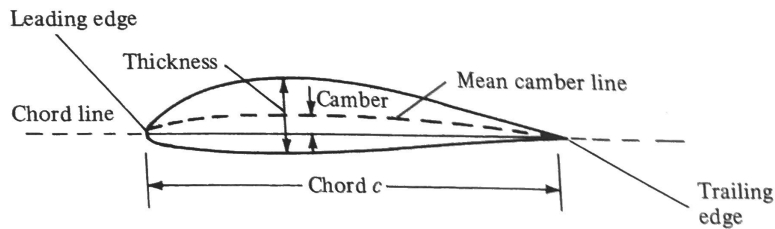


Figure 8: Airfoil nomenclature [6].

2.3 CFD

To simulate the flow around the wingsail, CFD can be used, which is, as H.Versteeg [7] stated, "CFD is the analysis of systems involving fluid flow, heat transfer and associated phenomena such as chemical reactions by means of computer-based simulation". The most well-established CFD software uses the finite volume method for the solver and includes a pre-processor for the input for the flow problem and a post-processor for visualization.

The flow case for the wingsail is turbulent which appears in the flow as eddies or swirling fluid flow. This flow requires a turbulence model which predicts the effects of turbulence. For the wingsail, the transition k-kl-omega model can be applicable since it has excellent performance for low Reynolds numbers ($Re \leq 500\,000$) [8]. The Reynolds Number is defined in Equation 4 [6], where ν is the kinematic viscosity, L_{chord} is the length of the chord and V is the windspeed.

$$Re = \frac{V \cdot L_{chord}}{\nu} \quad (1)$$

The airfoil performance is highly dependent on the boundary layer transition and this model solves this transition. The model resolves the boundary layer which is the area in the immediate vicinity of the wingsail surface where the effects of viscosity are significant, through three transport equations. One for the laminar fluctuations kinetic energy, k_l , one for the turbulent kinetic energy, κ , and the last one for the turbulent kinetic energy dissipation rate, ω [9]. The k-omega SST model can also be suitable since it has good accuracy for a wide class of low Reynolds number airfoil, where the model resolves the boundary layer with two transport equations, one for the turbulent kinetic energy, κ and one for the turbulent kinetic energy dissipation rate, ω [9]. XFOIL, which combines an integral boundary layer formulation and a panel method to analyze the potential flow which is present around airfoils [9], can be used to compare the results obtained through the two turbulence models, k- k_l -omega and k-omega SST. To read more about the theory around turbulence models and turbulent flows, read the Ansys manual [10] or for example the theory book "An Introduction to Computational Fluid Dynamics" [7].

2.4 Structural Analysis

To model a laminate, Classical Laminate Theory is used where the following assumptions are valid and will give an accurate representation when analyzing thin composite shells:

- Perfectly bonded layers
- Individual layers are treated as homogeneous
- Individual layers can either be orthotropic, transverse isotropic or isotropic
- Transverse shear is negligible (plane stress)
- Kirchoffs assumptions are valid for laminate deformation

2.5 Composites

A composite material is a material that consists of two or more materials. Carbon Fiber Reinforced Plastics is a type of composite material with high strength and moduli, excellent fatigue properties and does not corrode [11]. Carbon Fibers are usually arranged in unidirectional (UD) filaments

and can be woven into various patterns where some arrangement can be seen in Figure 9. UD weave has all of its fibers in one direction, providing high strength in that direction, while other arrangements such as plain weave usually have the same amount of fibers in both the principal directions, resulting in similar properties in both directions.

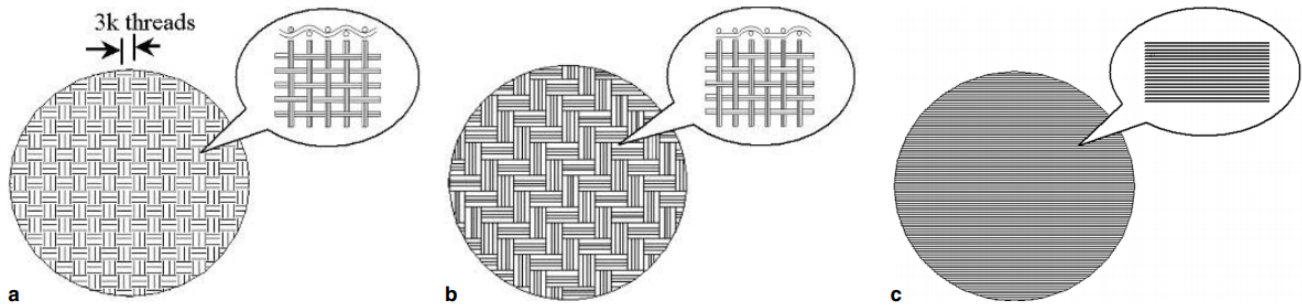


Figure 9: Different patterns of woven Carbon Fibers, (a) Plain weave, (b) balanced-twill weave, (c) UD [12].

When purchasing fibers there are usually two options: pre-impregnated fibers or dry-fabric which needs to be impregnated with resin. The advantages and disadvantages of both options are presented in Table 1.

Table 1: Pros and cons of both dry and pre-impregnated fibers.

Dry fibers	Pre-preg
+ Cost	+ Controlled fiber to matrix ratio
+ Expiring date	+ Easy to work with
+ Low curing temp available	+ High quality of the end product
+ Numerous combinations of matrix and reinforcement	- Often high cure temperatures
- More difficult to control orientations	- Cost
- Difficult to control fiber matrix ratio	- Outlife

Composites can be considered in-plane anisotropic which means that the strength varies by direction compared isotropic materials which have the same characteristics in each direction. This is one of the great advantages of using composites, since the strength can be designed to where it is needed which gives a high strength-to-weight ratio.

2.5.1 Typical Definitions for Composites

Sheets of fibers are called plies, while a stacking of plies is called a layer. Together they form a laminate, which is a layered structure of the stacked ply layers. To understand composites modeling, the orientation of the plies is essential. Figure 10 illustrates a laminate with red lines indicating the direction of each ply in the laminate.

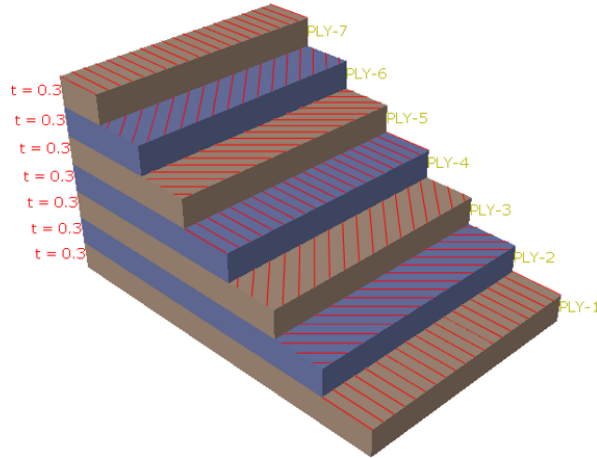


Figure 10: Overview of layers and the respective orientation for a laminate.

A composite layup and the respective orientation for each layer can be described by sequencing from the bottom of the laminate to the top, each orientation in square brackets. As an example, the stack up in Figure 10 would be described by $[0/45/-45/0/45/-45/0]$.

2.6 Manufacturing Methods

2.6.1 Filament Winding of Tubes

Filament winding is a production method in line impregnation process for continuous fibers and is commonly used to manufacture composites tubes and pressure vessels. Continuous rovings of dry fibers are placed in a tension system and passed through a resin bath before they are controlled in a pre-specified path onto a rotating mandrel which has been pre-treated with a release agent, as seen in Figure 11. The nip rollers control the amount of resin being transferred to the guiding eye which has a lateral movement for guiding the rovings onto the mandrel. If a low angle helical pattern is wanted, there is a possibility that the fibers will start sliding on each other on the mandrel. To reduce the amount of sliding, cones can be added to the ends, making the turning

process easier. Once the pre-defined program is finished and the desired amount of fibers and thickness are achieved, the tension is turned off, and rovings are cut. The mandrel is left on rotating mode until the resin has hardened. The mandrel is then placed in an oven with a rotating mechanism to cure according to the datasheet of the used epoxy. The finished tube can then be demoulded from the mandrel.

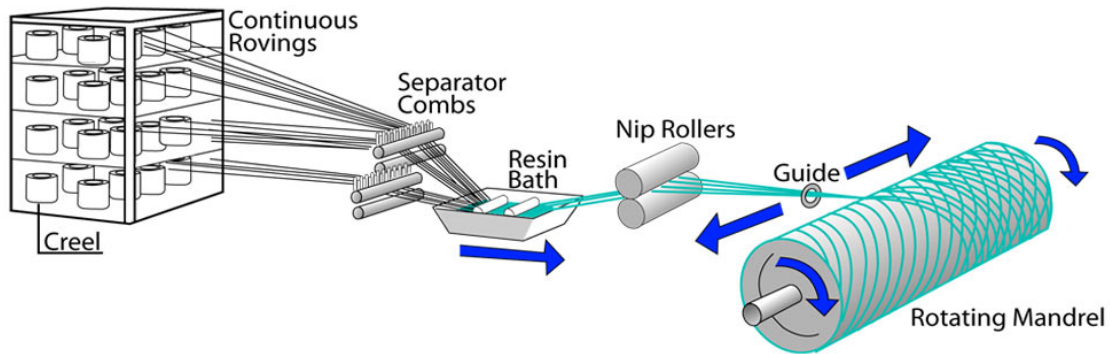


Figure 11: Overview of the filament winding process where continuous rovings are passed through a resin bath before wound onto a rotating mandrel [13].

With the use of filament winding, one can produce tubes and pressure vessels with high mechanical performance with excellent control of fiber orientations and controllable fiber content. Furthermore, since the fibers are impregnated right before its wound onto the mandrel, fibers and resin are used in the lowest cost form compared to pre-impregnated fibers. On the other hand, the filament winding process requires a high investment cost with the machine, mandrels, curing oven, and domes. The machine is also limited in the different shapes that it can produce which needs to be round, symmetric or convex, with convex shapes being more complicated to make.

2.6.2 Vacuum Assisted Resin Transfer

Vacuum-Assisted Resin Infusion is a well-established production method for producing high-quality composite components. After the mould has been cleaned and the release agent has been applied, the fiber reinforcement is placed in the desired position. Furthermore, peel ply and/or flow mesh is placed on top of the reinforcements, where the peel ply has the function of separating the vacuum bag and flow mesh from casting together and are often used when it is desired to end up with a rough surface suitable for gluing or further lamination. The flow mesh

is placed onto the mould to help the flow of resin pass through the laminate. Then, the vacuum bag is placed on top of the flow mesh and sealed with sealant tape, preventing air from entering bag. Lastly, a resin inlet and a vacuum outlet are placed going into the bag. The vacuum outlet tube is connected with a resin catch pot, avoiding resin to be transferred into the vacuum pump attached. An overview of the schematics for Vacuum Assisted Resin Transfer can be seen in Figure 12.

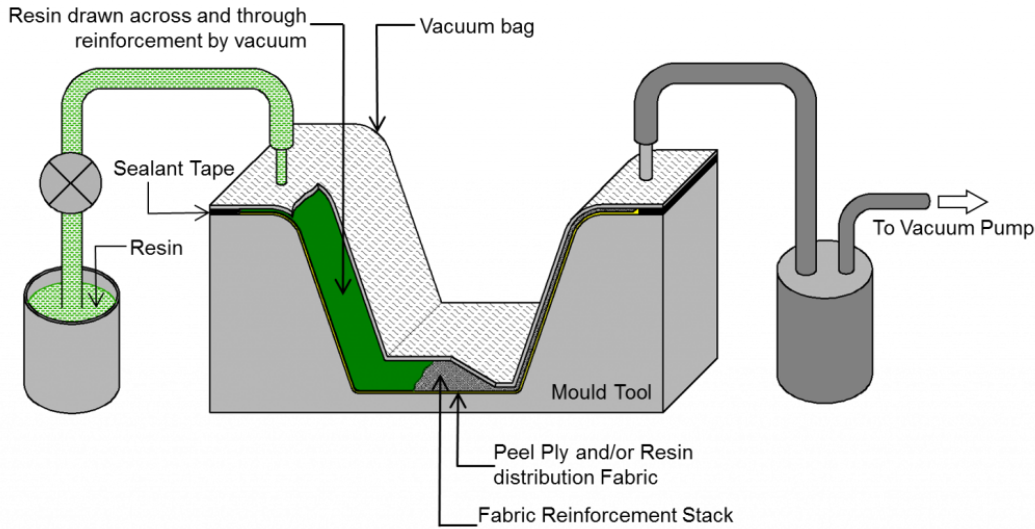


Figure 12: Schematics of Vacuum Assisted Resin Transfer (VART) where resin are drawn by vacuum through the reinforcement, peel ply and resin distribution fabric. A catch pot is placed at the vacuum inlet to avoid resin to be transferred into the vacuum pump [14].

Compared to traditional hand layup, where the resin is applied with a brush on each layer, vacuum infusion provides an improved fiber-to-weight ratio, is much cleaner and has an unlimited time frame since all of the work with preparing for VARI can be done before mixing epoxy and hardener. Disadvantages are that there is a somewhat complicated set-up where the resin inlets and flow mesh should be carefully considered before starting the process. Once the resin infusion has started, corrections of the set-up are challenging to perform. Also, if the vacuum bag has leaks, air will be drawn into the bag which could result in poor laminate with voids.

2.6.3 Pre-preg "Out-of-Autoclave"

Fibers and fabrics can be purchased as pre-impregnated from the producer which are called pre-pregs. Pre-pregs are hand layed onto the mould before vacuum bagged before cured, and a

illustration of the process can be seen in Figure 13. Often, pre-preg fibers have resin which needs to be cured in a pressurized oven named autoclave. A configuration of prepreg that can cure out-of-autoclave are made the same way as conventional prepreg, except of the resin chemistries which can cure at low temperatures (60 °-120°).

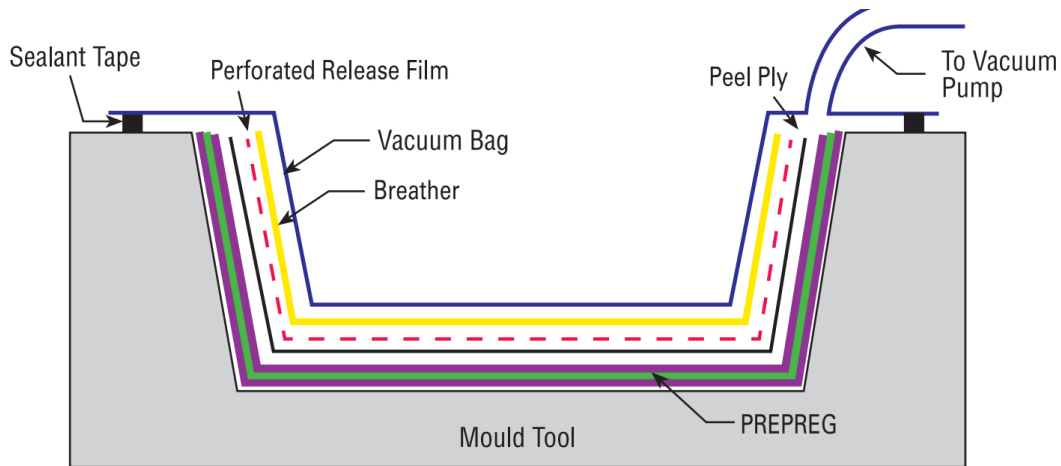


Figure 13: Overview of the production method for Out-of-Autoclave Prepreg [15].

The pre-pregs have a limited working life, often from a week to several months, while if kept in freezer the working life can be extended to up to a year. Since the fibers and fabrics are pre-impregnated by the manufacturer, a high fiber to matrix accuracy is obtained. The out-of-autoclave prepregs have the advantage that they can be used together with low temperature resistant moulds, as Medium-Density Fiberboard. However, a disadvantage with prepregs is that they are high in cost compared to dry fibers.

3 Methods and Procedure - Design

3.1 Overview

In this section, the method and procedures for the entire design process of the wingsail are described. Firstly, the wingsail area and shape are decided. Thereafter, CAD and CFD set-up are presented, before the structural optimization method with all the various parameters are described. The optimization then creates a base for further structural analysis which was executed in Abaqus and the set-up is described in Section 3.8.

3.2 Deciding Airfoil Profile

In the examination of selecting which type of airfoil section that will be used for the wingsail, a comparison between symmetric and asymmetric airfoil can be done. When NACA developed the different airfoils, they performed wind tunnel experiments on each airfoil. The experimental data can be used to compare the different airfoils sections and to find the most suitable alternative. This is done through examining the lift, drag and moment to the angle of attack of the wing. The lift coefficient, c_l , is given by the equation 2.

$$c_l = \frac{2 \cdot F_l}{S \cdot \rho \cdot V^2} \tag{2}$$

Furthermore, the drag coefficient, c_d , can be described by the equation 3.

$$c_d = \frac{2 \cdot F_d}{S \cdot \rho \cdot V^2} \tag{3}$$

A comparison between a symmetric airfoil, NACA0018, and a non-symmetric airfoil, NACA2412, is done and can be seen in Figure 14a and Figure 14b.

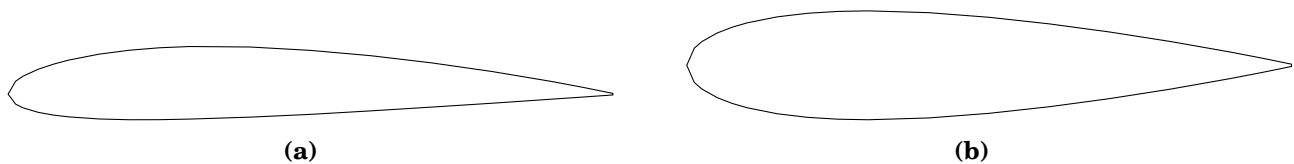


Figure 14: (a) Wingprofile for the non-symmetric profile NACA2412 [5], (b) Wingprofile for the symmetric profile NACA0018 [5].

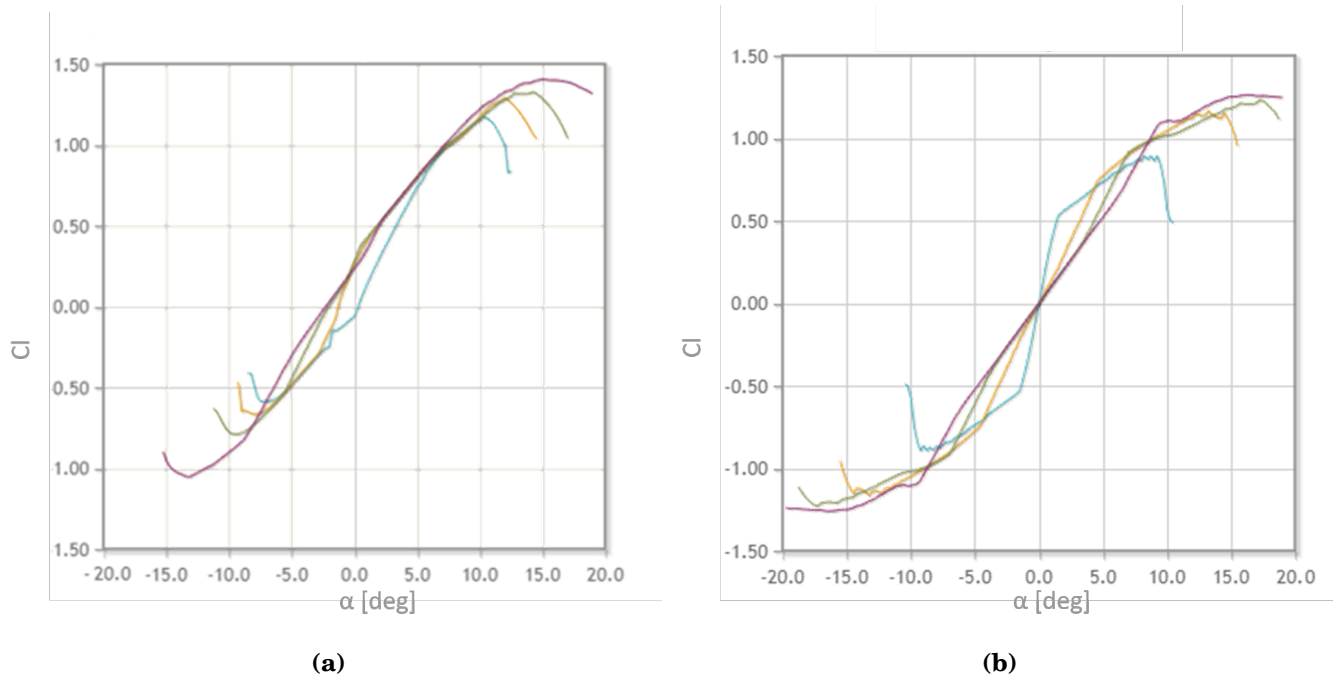


Figure 15: (a) NACA2412 Lift coefficient vs alpha from XFOIL [16], (b) NACA0018 Lift coefficient vs alpha from XFOIL [16].

Comparing the two airfoils, one can see that the symmetric airfoil provides lift over a larger span both in negative and positive angles, while the non-symmetric airfoil performs for a larger span of positive angles as seen in Figure 15a and Figure 15b. The different lines represents different Reynolds numbers, which is given by equation 4 and the lines is given in Table 2.

Table 2: Reynolds Number and the respective colours for the plots in Figure 15b, Figure 15a, Figure 17b and Figure 17a

Reynolds Number	Colour
50,000	Blue
100,000	Yellow
200,000	Green
500,000	Purple

Furthermore, to give an approximate value of which flow regime the wing experiences, equation 4 can be used with some initial guesses for the chord length and kinematic viscosity of air at 20°C in the following equation:

$$Re = \frac{6.5 \frac{m}{s} \cdot 1.2m}{1.516 \cdot 10^{-5} \frac{m^2}{s}} \approx 514512 \quad (4)$$

Additionally, from thin airfoil theory, one can state that the center of pressure is at a quarter of chord from the leading edge, while for cambered airfoils, the quarter chord is not the center of pressure and varies with different angles. This feature is an essential aspect because it is desirable to have the mast situated at the center of pressure and gravity. Therefore, the airfoil profile is chosen to be symmetrical.

When it comes to deciding which of the symmetrical airfoils is most suitable for the autonomous vessel, the wing section must provide sufficient space for the mast. The area of the airfoil that needs to be thick enough is the quarter of the chord from the leading edge since it is here the aerodynamic pressure is located. The most slender profiles such as NACA0006 and NACA008 will not be considered due to the low thickness and therefore not enough space for the mast. NACA0018 which can be seen from Figure 14b, have a maximum thickness of 18 % as the two last numbers in the name indicates and would have sufficient space for a mast. A comparison between NACA0018 and NACA0021 with 21 % thickness, see Figure 16, can provide more information before the choice of airfoil is made.

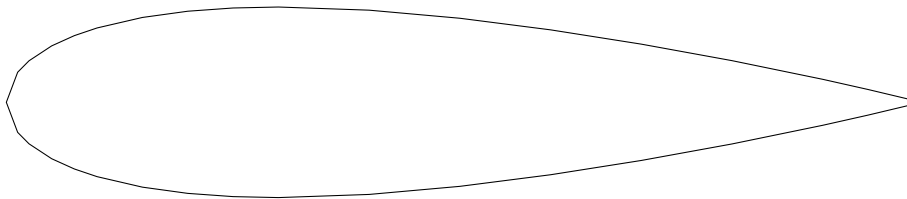


Figure 16: NACA0021 profile [5].

Plots of C_l/C_d v Alpha for NACA0018 and NACA0021 can be seen in Figure 17a and Figure 17b.

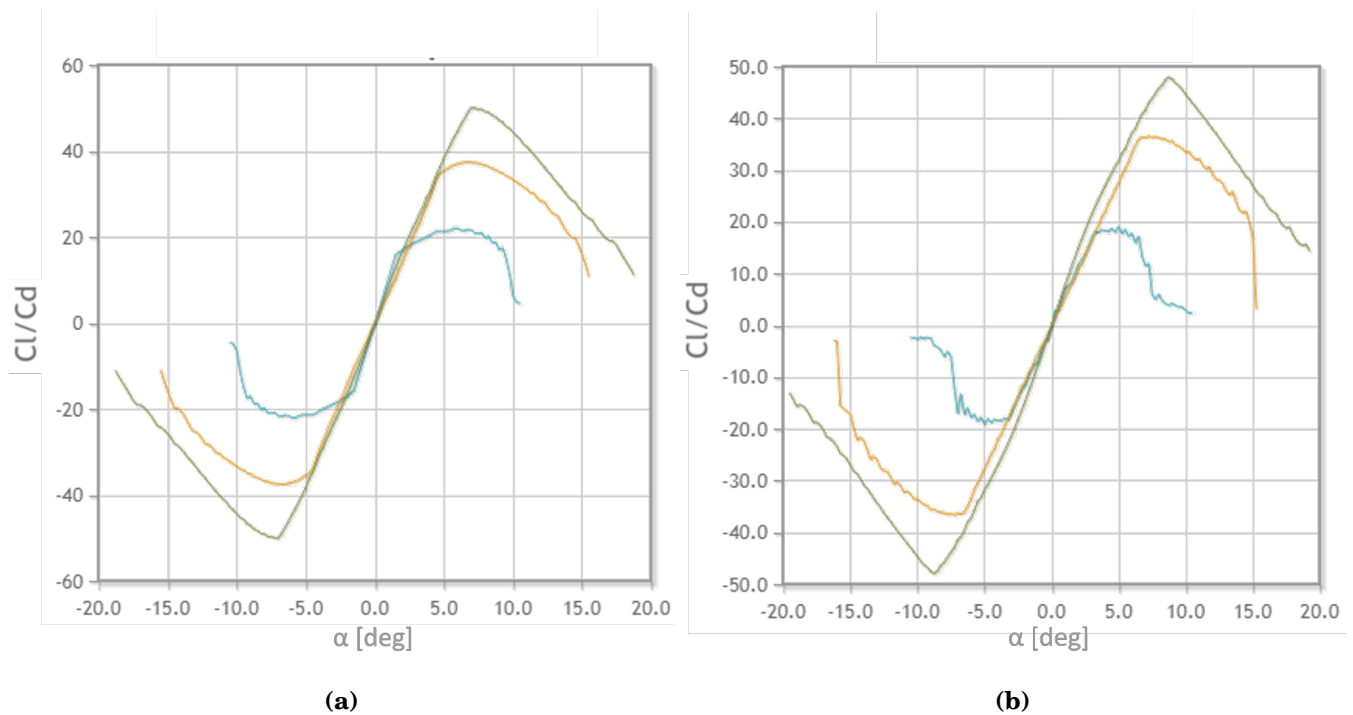


Figure 17: (a) NACA0018 Lift coefficient/ Drag coefficient vs alpha from XFOIL [16], (b) NACA0021 Lift coefficient/ Drag coefficient vs alpha from XFOIL [16].

From the plots in Figure 17a and Figure 17b, it is evident that a higher thickness airfoil gets wing stalling faster than a more slender profile, which is the condition where the flow gets separated at a specific alpha where lift decreases drastically while drag increases. This effect can be seen as a rapid drop in Cl/Cd and is a non-desirable effect if one wants to create thrust to a vessel. From the plots, one can also state that the NACA0018 provides more stable results than NACA0021 where Cl/Cd tends to oscillate in some regions. Based on this, a NACA0018 profile is chosen for the wingsail.

3.3 Deciding Wing Area

The wingsail area is dependent on how much power the wing sail must generate. In the research group, Hermann Brodin is responsible for determining the hull resistance. A resistance plot of his studies can be seen in Figure 18.

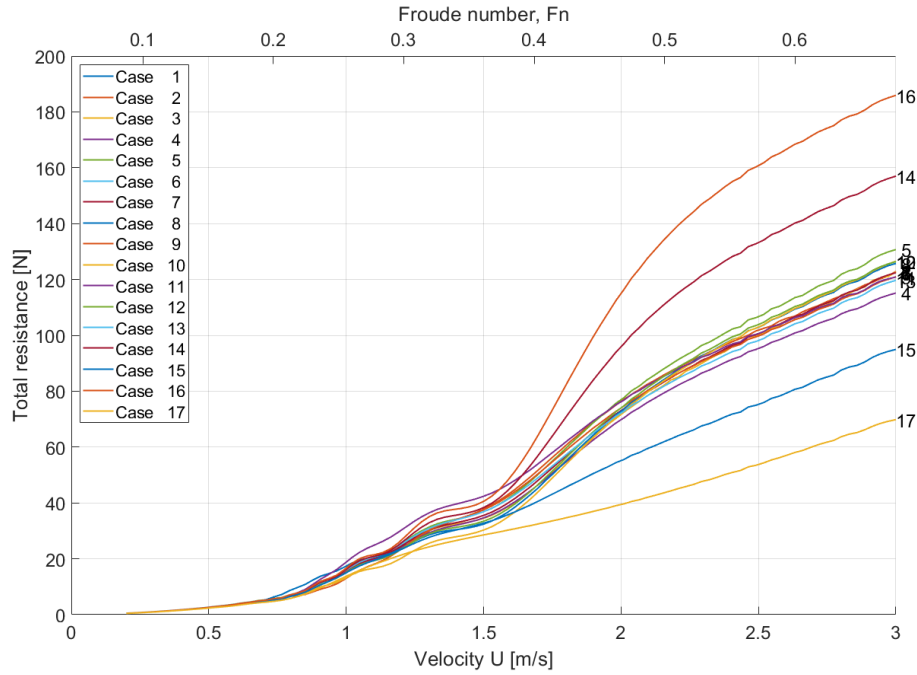


Figure 18: Hull resistance for different cases vs vessel velocity for the 2 meter long hull [by Hermann Brodin].

The plot in Figure 18 shows that the hull resistance for the vessel velocity goal of 1.5 m/s is for all the cases under approximately 42 N.

A simple estimation of the lift can be calculated by equation 5 [6]:

$$F_l = \frac{C_l \cdot S \cdot \rho \cdot V^2}{2} \quad (5)$$

This can be rearranged to calculate the required span of the sail:

$$S = \frac{2 \cdot F_l}{C_l \cdot \rho \cdot V^2} = \frac{2 \cdot 40N}{0.576 \cdot 1.225 \frac{kg}{m^3} \cdot ((6.64) \frac{m}{s})^2} \approx 2.88m^2 \quad (6)$$

Where C_l is the lift coefficient for NACA 0018 at 6 deg obtained from Ansys Fluent, ρ is the density of the air, F_l is the lift force and V is the wind speed. The value for velocity is used since the average wind speed at the oceans is approximately 6.64 m/s [17].

Hence, the area of the sail needs to be around $2.88 m^2$ which is going to be used as a value for the dimensions in the analysis. A chord length of 1200 mm and a height of 2400 mm is chosen, which gives the desired area.

3.4 Overview CFD and Structural Optimization

CFD-analysis was done to ensure that the sail can deliver its primary function, to provide thrust to the vessel, while FEA was performed so that the structural aspects are optimized. The forces acting on the sail which are obtained in the CFD analysis, are imported into the FEA which provides a realistic pressure field for the structural analysis. The results obtained from these computational software illustrate the performance of the wingsail.

First, a 2D-case of the airfoil profile is considered in Ansys Fluent which is done to ensure that the right meshing and turbulence models are used, by comparing the lift and drag coefficients against various angles of attack to XFOIL. Then, the 3D-case of the wing is considered where the pressure field is then imported into the structural analysis. Thereafter, structural optimization is done by varying the number of ribs, the distance between the ribs, the diameter of the mast, number of plies on all elements while aiming for as low a deflection and mass as possible together with high strength. This optimization will give a good overview of the trends and make a good base for the final design. It is essential to have in mind that the optimization provides just a base that needs further investigation, since it only considers the objectives that are being set, and are not a complete design tool where other design parameters are taken into account.

The wingsail has been designed by utilizing the software packages Ansys 2019 R3, Abaqus CAE and SolidWorks 2019, where the manual can be read in their official sites [18] [19] [20].

This setup provides a structural optimization setup that takes both aerodynamics and structural composites modeling of the wingsail into account. When the parametric analysis is initiated, the software changes the geometry of the wingsail in SolidWorks, runs the CFD analysis in Fluent, outputs the pressure field into the structural analysis, runs the structural analysis, before it outputs the values for each iteration in the parametric study window. An overview of the setup can be seen in Figure 19.

3.5 CAD Setup

The wing profile is created by importing the points for the NACA0018 airfoil from the source dat file at UIUC Airfoil Coordinates Database [5] into Solidworks. Furthermore, normal modelling tools are used and the parameters from the study are given the name *DS* and will automatically appear as a possible choice in Ansys.

3.6 CFD Setup

The CFD-analysis is executed in Ansys Fluent, where the geometry from SolidWorks is imported. The schematics of the setup can be seen in Figure 19.

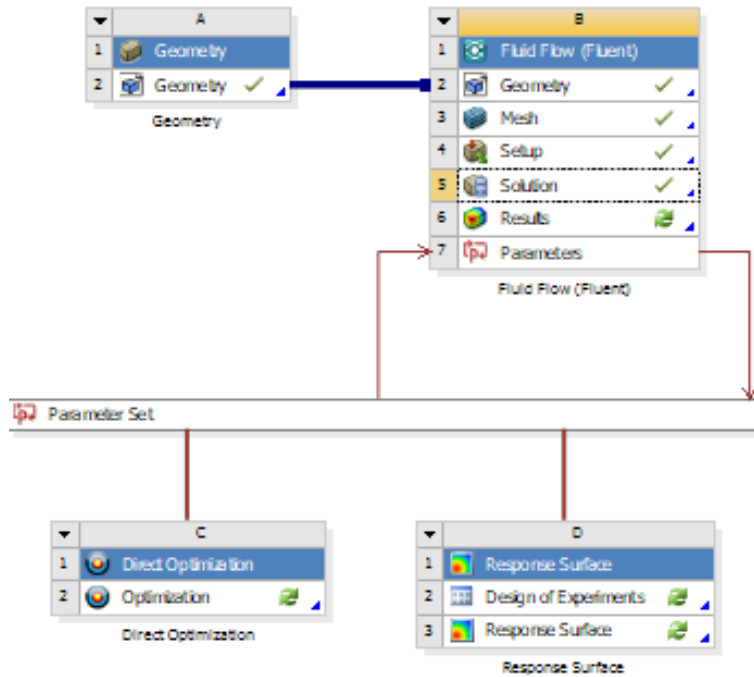


Figure 19: Design approach for the CFD-analysis.

3.6.1 CFD Mesh

A mesh with 66149 elements for the 2D-case and 6196183 elements for the 3D-case is created, see Appendix A.1.1 for detailed information.

3.6.2 Solver

3.6.2.1 6.5 m/s The most essential setup properties for the k-kl-omega model can be seen in Table 3, while more detailed information of the setup can be read in Appendix A.1.1. For external aerodynamics, the k-omega model is suitable since it captures the effect of separation on curved walls compared to k-epsilon model which performs poorly on such flows.

Table 3: CFD setup-properties for 6.5 m/s in Ansys Fluent.

Setup	Value
Solver	Pressure-Based, Steady, Absolute velocity
Model	Transition k-kl-omega (3-eqn)
Material	Air
Temperature	20°C
Inlet Velocity	6.5 $\frac{m}{s}$ normal to boundary
Pressure Outlet	0 Pa
Wing	Wall with no-slip
Solution Methods	Value
Scheme	SIMPLE
Gradient	Green-Gauss Cell Based
Pressure	PRESTO!
Momentum	Second Order Upwind
Laminar Kinetic Energy	First Order Upwind
Specific Dissipation Rate	Second Order Upwind
Initialization	Hybrid Initialization

3.6.2.2 20 m/s After the structural optimization, the extreme case for a wind load of 20 m/s was assessed, where the setup are listed in Table 4. In this setup, the k-omega model is chosen due to the higher airflow.

Table 4: CFD setup-properties for a wind speed of 20 m/s.

Setup	Value
Solver	Pressure-Based, Steady, Absolute velocity
Model	SST k-omega (2-eqn)
Material	Air
Temperature	20°C
Inlet Velocity	20 $\frac{m}{s}$ normal to boundary
Pressure Outlet	0 Pa
Wing	Wall with no-slip
Solution Methods	Value
Scheme	SIMPLE
Gradient	Green-Gauss Cell Based
Pressure	PRESTO!
Momentum	Second Order Upwind
Laminar Kinetic Energy	First Order Upwind
Specific Dissipation Rate	Second Order Upwind
Initialization	Hybrid Initialization

3.7 Structural Optimization Setup

3.7.1 Design Requirements

The goal for the structural optimization is to establish the main geometrical and composites layup characteristics for the given design space found in Section 3.2 and 3.3. Adjustments with respect to available production material and other characteristics will be done in the structural mechanical setup in Abaqus in Section 3.8.

3.7.2 Overview

An overview of the structural setup can be seen in Figure 20. The pressure field at an AOA of 11 ° for the 3-D wing is imported, where the 11° is chosen by examination of Cl/Cd vs Alpha plot in Figure 44a, where the optimal alpha is in the range 6-11° and the highest forces acting on the optimal operating range is 11°.

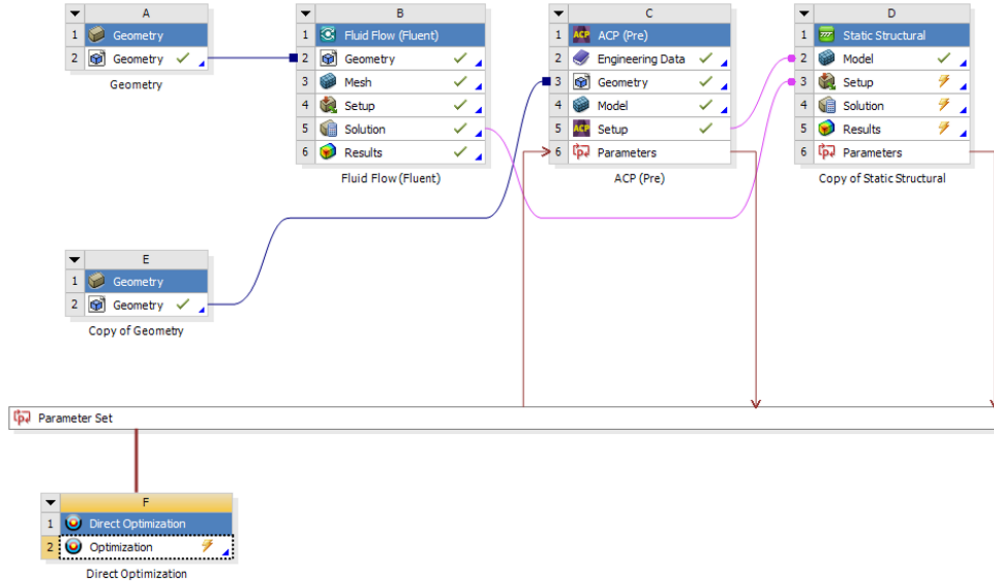


Figure 20: Overview of the structural setup.

3.7.3 Mesh

A mesh with 19729 quad shell elements is used, where the element type is SHELL181, which is a 4-node thin or thick shell with reduced integration, hourglass control and finite membrane strains, see Ansys manual for more details [18].

3.7.4 Material

The values for TeXtreme carbon fiber is chosen in the study with the properties shown in Table 5. Unfortunately, this was not the fiber which was used in the final production, but was considered to be used at the start of the project since other projects at the department have used this and had good testing results on the material. Regardless, as mentioned before, the optimization is just a design base for further analysis.

Table 5: Summary of material constant for TeXtreme [21].

Material	Ply thickness [mm]	E_1 [MPa]	E_2 [MPa]	ν_{12}	G_{12} [MPa]	G_{13} [MPa]	G_{23} [MPa]	X_t [MPa]	X_c [MPa]	Y_t [MPa]	Y_c [MPa]	S_{12} [MPa]
TeXtreme	0.15	67100	67100	0.04	3470	1388	1041	990	277	990	277	52

3.7.5 Boundary Conditions, Load and Interactions

A fixed support is applied to the mast. The pressure from CFD-analysis is imported and applies an external pressure on the sail, as seen in Figure 21. The ribs are assumed tied to the mast and the mainsail skin.

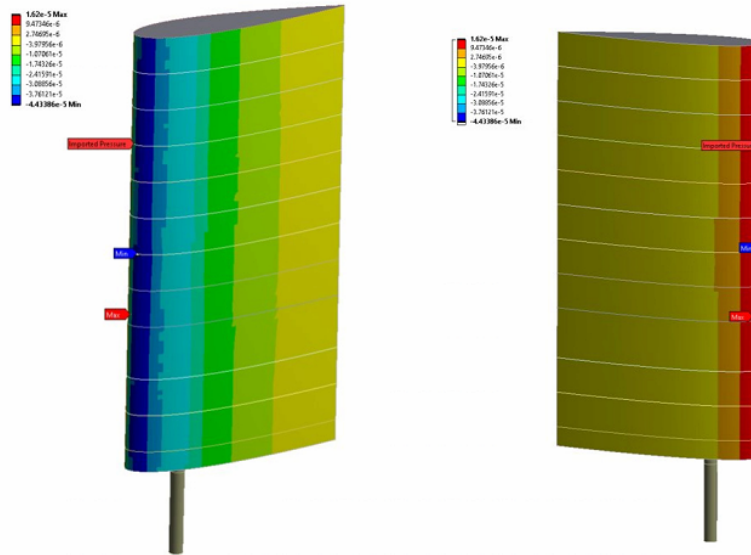


Figure 21: Overview of the imported pressure imported from CFD seen from both sides of the wingsail.

3.7.6 Regions

The different regions in the structural analysis can be seen in Figure 22.

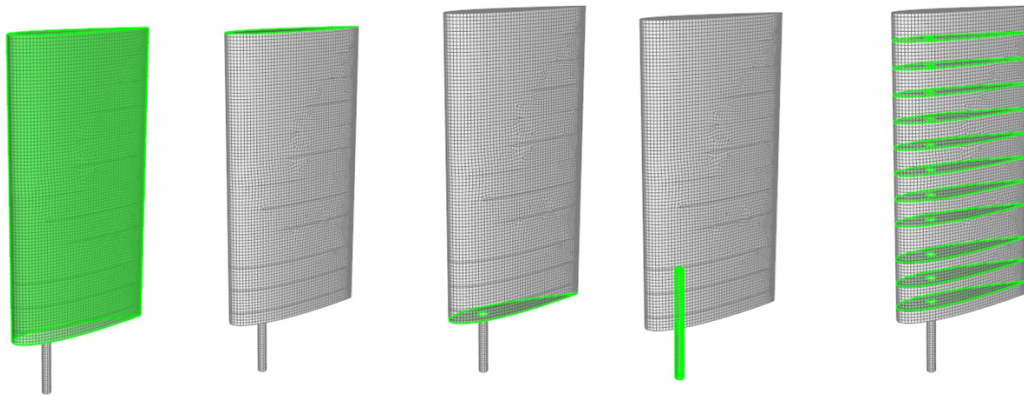


Figure 22: Overview regions, from left to right: main sail, top, bottom, mast, rib.

3.7.7 Composite Layup

A composite layup is done with a stack-up, rosettes and oriented selection set properties where the details can be seen in Appendix A.2.2.

3.7.8 Parameter Study Values

The parametric study objectives and constrains for the optimization are:

- Minimize strain energy average
- Minimize total weight
- Total deformation maximum under 2 mm

All the objectives above are essential for the design. It is desired to minimize the strain energy density since it will maximize the structure's total stiffness. Lastly, minimizing the total weight is also set as an objective since a the sail's weight will contribute to the placement of the boat's center of gravity, where a low value will contribute to higher stability. Low weight will also lower the hull resistance, which is ideally. All the design parameters used in the parameter study is found in Table 6.

Table 6: Input parameters and the respective bounds in the structural parameter study

Input Parameters	Lower Bound	Upper Bound
Mast height in sail [mm]	450	1000
Mast diameter [mm]	73.792	120
Spacing rib 1 [mm]	110	290
Spacing rib 2 [mm]	310	490
Spacing rib 3 [mm]	510	690
Spacing rib 4 [mm]	710	890
Spacing rib 5 [mm]	910	1090
Spacing rib 6 [mm]	1110	1290
Spacing rib 7 [mm]	1310	1490
Spacing rib 8 [mm]	1510	1690
Spacing rib 9 [mm]	1710	1890
Spacing rib 10 [mm]	1910	2090
Spacing rib 11 [mm]	2110	2290
Input Parameters	Numbers of layers	
Bottom number of layers	1	2 3 4
Top number of layers	1	2 3 4
MainSail number of layers	1	2 3 4
Rib number of layers	1	2 3 4 5 6
Mast number of layers	1	2 3 4 5 6 7
Input Parameters	Present(1) or not present(0)	
Rib 1	0-1	
Rib 2	0-1	
Rib 3	0-1	
Rib 4	0-1	
Rib 5	0-1	
Rib 6	0-1	
Rib 7	0-1	
Rib 8	0-1	
Rib 9	0-1	
Rib 10	0-1	
Rib 11	0-1	

3.8 Structural Mechanical Setup in Abaqus

3.8.1 Overview

The optimization provides a design base with information about the placement of the ribs, dimensions of the mast, number of plies for each part and the total number of ribs with the objectives and requirements to minimize strain energy density, minimize weight and total deformation maximum under 2 mm. In this section, further analysis based on the optimization results with adjustments to available production material, mandrel dimensions and assembly analysis with glue are presented.

First, all of the data from Ansys was imported into Abaqus which was done due to personal preference of the mechanical FEA setup in Abaqus compared to Ansys Mechanical. The composite shell parts were modeled as a conventional shell element with linear elastic properties. The layup properties was done in the Abaqus Composites modeling module, where orientations, plies and material can be assigned to each component.

3.8.2 Material

The composites modeling was done through defining a lamina with the constants E1, E2, Nu12, G12, G13 and G23 which was assigned to each composite part. The material data used for the different parts are listed in Table 7 and 8. See Section B.2.1 for detailed material setup.

Table 7: Properties for the materials used in the analysis

Composite type	E1 [MPa]	E2 [MPa]	Nu12	G12 [MPa]	G13 [MPa]	G23 [MPa]	ρ [$\frac{kg}{m^3}$]
XPREG XC110 416 g Prepreg *	55100 [I.6]	55100 [I.6]	0.05 [E.5]	3300 [20]	3300 [20]	3500 [20]	1540 [I.6]
GRAFIL 34-700 24K **	137000 [I.3]	9200 [I.3]	0.30 ***	4000 ***	4000 ***	2581 ***	1600 [I.3]
Pyrofil TR30S 3K **	52400 [I.5]	52400 [I.5]	0.04 [I.5]	2700 ***	2700 ***	3587 ***	1420 [I.4]
Epoxy Type	E [MPa]	ν	ρ [$\frac{kg}{m^3}$]				
RIMR 135/ RIMH 137	3000 [I.8]	0.3 [I.8]	1190 [I.8]				

* Properties for cured prepreg

** Properties for cured fiber and epoxy

*** Estimated

3.8.3 Properties and Composite Layup

From the results for the optimization, Table 9 shows the layup which were assigned to each part. For more detailed information about the composite layup and orientations, see Section B.2.2.

Table 8: Properties for fail stress of the materials used in the analysis

Composite type	Ten. Stress Fiber Direction [MPa]	Com. Stress Fiber Direction [MPa]	Ten. Stress Transv. Direction [MPa]	Com. stress Transv. Direction [MPa]	Shear Strength [MPa]
XPREG XC110 Prepreg	521 [I.6]	483 [I.6]	521 [I.6]	483 [I.6]	112 *
GRAFIL 34-700 24K	2572 [I.3]	1365 [I.3]	81 [I.3]	210 [I.3]	102 [I.3]
Pyrofil TR30S 3K	595 [I.5]	567 [I.5]	595 [I.5]	567 [I.5]	112 [I.5]

* *Estimated*

Table 9: Final layup for all the various components of the wingsail.

Part	Layup	Composite
Mainsail and Top	[0/±45/0]	Pyrofil TR30S 3K [I.4] [I.5]
Bottom	[0/±45/±45/0]	Pyrofil TR30S 3K [I.4] [I.5]
Rib 1	[0/±45/0/0/±45/0]	XPREG XC110 Prepreg [I.6]
Rib 2-6	[0/±45/0]	XPREG XC110 Prepreg [I.6]
Mast	[±15/±15/±15/±15/±15/±15]	GRAFIL 34-700 24K [I.3]
Glue	Isotropic	RIMR 135/ RIMH 137 [I.8]

3.8.4 Load and Interactions

3.8.4.1 Importing Loads From Ansys to Abaqus The pressure load from Ansys Fluent was imported into Abaqus through plotting pressure with respect to xy-values over the wingsail. Furthermore, a python script was made and used to estimate a polynomial regression function which was imported into Abaqus through analytical field. The python script can be seen in Appendix G.2.

3.8.4.2 Interactions The glued interfaces between mast, main sail and ribs were simplified to by a thin layer (0.15mm) between all connections. The glued regions were simplified by connecting these layers with a tie connector to the surrounding parts. Surface to surface contact was chosen and the coarser mesh as master (for most accurate result: Abaqus Documentation [19]). See section B.5 for more detailed information.

3.8.5 Boundary Conditions

The mast interface was simplified with a kinematic coupling connected to the reference point in the assumed center of the mast support interface.

3.8.6 Mesh

For the mesh, S4R elements were used which are linear quad elements with reduced integration. A global mesh size of 7 mm was selected, while a mesh refinement of the gluelines was applied. See Section B.7 for detailed information about the mesh.

3.8.7 Buckling Analysis Setup

For the buckling load case, a buckle step with linear perturbation with subspace eigensolver was used. The load case for the buckling was for the 6.5 m/s pressure field. See Section B.4 for more information.

4 Methods and Procedure - Production

4.1 Overview

This section describes the production process of the wingsail and starts with explaining how the moulds were made. Then, the production methods for the mainsail, ribs, mast and an electronics box are presented, followed by a description of the assembly plan and cable routing for the whole wingsail.

All the parts of the production were done by the author herself at the workshop at the Department of Mechanical and Industrial Engineering.

4.2 Mould Production

Three different moulds were needed to cast the mainsail, ribs and mast. The moulds for making the ribs and mainsail, were made in Medium-Density Fiberboard (MDF), while the mast which was wound on a stainless steel mandrel which is a steel tube designed with slip angle to ease demoulding of the wounded material. MDF was chosen since its relatively easy to form by milling machine available at the department and for large dimensions are quite cheap in material cost. On the other hand, there are several drawbacks of using MDF, which is going to be discussed further in the thesis. However, since the final casted product is highly dependent on the quality of the mould, excessive work was done to achieve the best possible surface finish on the moulds.

4.2.1 Mainsail Mould

An overview of the mainsail mould components before and after milling, can be seen in Figure 23a, 23b, while Figure 24 shows all of the components assembled. The mould is made as a negative mould, such that a nice surface finish can be obtained on the outer side of the mainsail. Guiding holes were drilled in the both upper and lower part by the CNC-machine, ensuring that the parts would assemble in the right place. These holes were then filled with filler material after assembly.

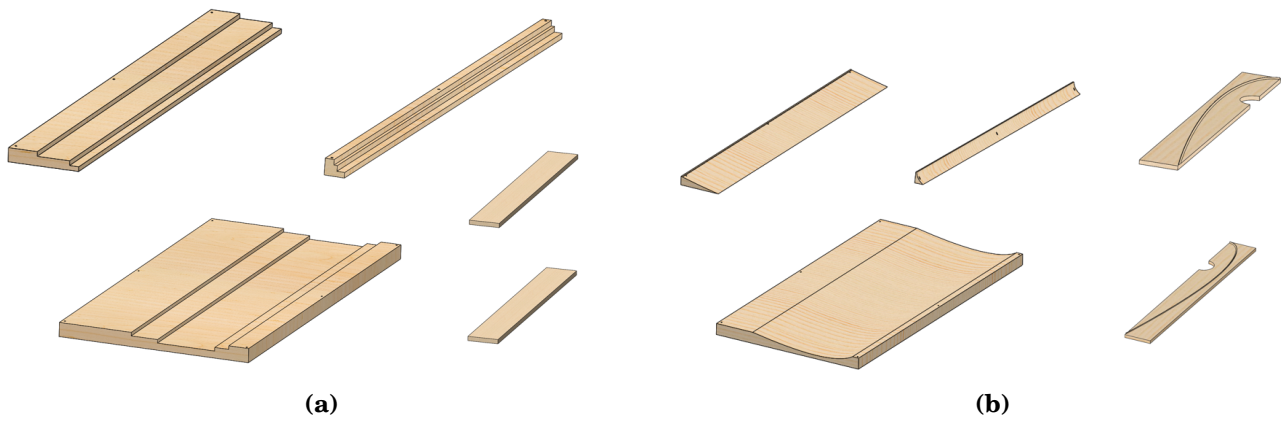


Figure 23: Mainsail mould components before (a) and after (b) milling.

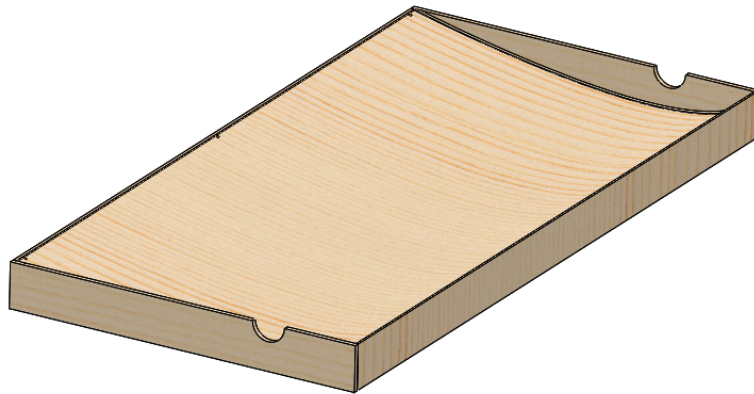


Figure 24: Milled mainsail mould components assembled together.

To reduce milling time from approximately 53 hours to 12 hours and optimize the use of material, the 3040x1220x22 mm MDF-plates [I.2] were cut into smaller pieces, as seen in the Figure 25a.



Figure 25: (a) Cutted MDF, (b) Gluing cutted MDF plates together with extra weights and clamps adding extra pressure.

After that, the pieces were glued together with Cascol Indoor glue from Casco [I.1] and to ensure proper bonding, clamps and extra weight was added in the process, as seen in Figure 25b. After the glue had cured, the glued plates were milled on an in-house milling machine and milled with the use of Autodesk Fusion 360 and the CNC motion control software Mach 4. Before (a) and after (b) milling can be seen in Figure 25. Due to height restrictions on the CNC-machine, the large mould was divided into three sections.



(a)

(b)

Figure 26: (a) Lower part of mainsail mould ready for milling, (b) Lower part of mainsail mould after milling.

The milled parts of the mould were then assembled and glued together. The joints and other imperfections were filled with fine filler material. Since the milling tool left some traces on the mould, it was sanded until a nice smooth surface was obtained. Then the milled end-plates were attached to each side of the mould with screws.



Figure 27: Mainsail Mould after assembly of milled components and filler applied.

Furthermore, a sealer, Teknoseal 4002-10 TS 0050 CLEAR [I.9], was applied all around of the surface which were wet sanded with 400 abrasive paper after curing which was done according to the datasheet. The sealer provides water resistance and ensures dimensional stability to the mould. 3 layers of Teknotherm 4350-00 TINTED Topcoat [I.10] was then applied and then sanded with 400-600 grit paper. Moreover, 3 layers of two-component clear coat from SprayMax [I.11] was applied on the area of casting and sanded with grit paper 800-1200. Then, the mould was polished to remove surface scratches, dirt and other imperfections before cleaned with isopropanol. As the last step, release agent [I.12] was applied to prevent the carbon fibers from bonding to the mould surface. Assembled Mainsail Mould can be seen in Figure 27.

4.2.2 Rib Mould

The moulds for the rib were also made of MDF and were made as a positive mould. A total of four rib moulds was made so that if some of the moulds was damaged during casting and demoulding, as well as the possibility to cast more than one rib at the time. CAD model of the MDF-stocks can be seen in Figure 28a while Figure 28b shows the rib mould after milling. The process of making the MDF-mould were the same for the rib mould as the mainsail mould.

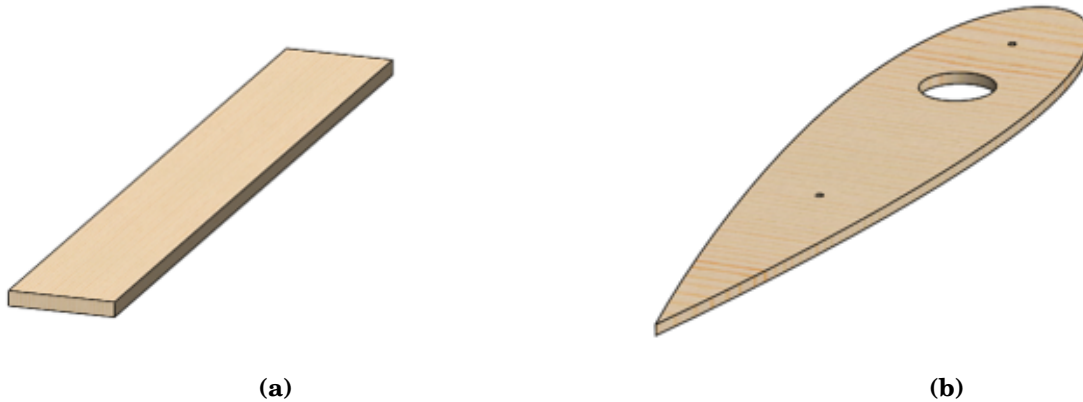


Figure 28: (a) Rib mould components before milling, (b) Rib mould after milling.

4.3 Carbon Fiber Reinforced Polymer Production

A total of three different types of CFRP parts was produced with three different methods and fibers, where an overview can be seen in Table 10.

Table 10: Overview of the different components and production methods used.

Part	Orientations [deg]	Production Method	Material
MainSail	0/90 and +-45	Vacuum Assisted Resin Infusion	Dry fibers
Rib	0/90 and +-45	Hand layup	Pre-impregnated fibers
Mast	15	Filament winding	Filament winding fiber

4.3.1 Mainsail CFRP Production

Since the wingsail was decided to be symmetric and straight, only one mould which was going to be casted on twice, was required. But since the mainsail shells needs to have the gluing surface for the mast on the same side, the shell needed to be mirrored for assembly. This required that both of the endplates had a hole for the mast included. For each cast, alternative endplate hole is applied fiber into. The fibers are placed around the edges and the top so that assembly process will be easier and ensuring that the fibers do not slip around during casting. These edges will be trimmed after assembly.

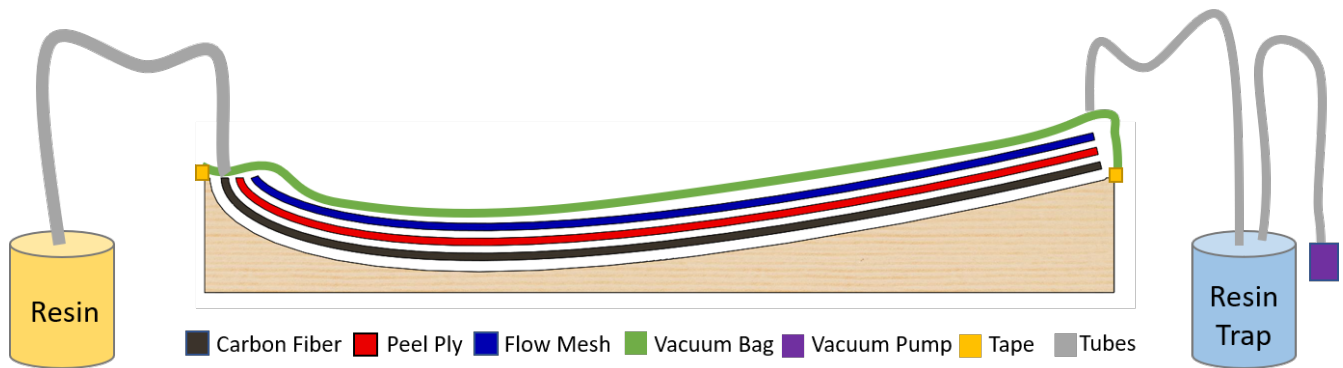


Figure 29: Illustration of the different elements involved in the casting process.

As seen in Table 10, the casting process for making the mainsail shells are Vacuum Assisted Resin Infusion. The process was described in Section 2.6.2 and an overview of the different elements can be seen in Figure 29.



(a)



(b)

Figure 30: (a) MainSail Production - Dry fibers placed onto the mould, (b) MainSail Production - Trimmed dry fibers and peelply placed onto the mould.

First, the cutted dry fiber mats was placed on the mould, as seen in Figure 30a before the ends

were trimmed. Then, peelply, as seen in Figure 30b, and flow mesh was applied onto the top of the fibers. Some additional flow mesh strips was placed on the edges and at the inlet spots for the four hoses which was placed in the mould, one on each endplate, and two on the length of the mould. Furthermore, the vacuum bag was applied onto the mould and sealed with sealant tape. Vacuum was then applied to the vacuum inlet while the resin inlet hoses was clamped. The bag was then checked for leaks. Hexion Epikote Resin RIMR 135 and Epikure Curing Agent 137, which has low viscosity and is therefore especially applicable for resin infusion, was mixed according to the datasheet [I.8]. To avoid heat ups of the resin, the resin was mixed up in batches throughout the infusion process. The resin was degassed in a degassing chamber until all small air bubbles from the mixing was removed, which took approximately 15 minutes. To initiate the resin infusion, three of the hoses were used as vacuum inlet while the last was used as a resin inlet with the hose placed in the resin bucket. When the resin started to near the next vacuum inlet, the vacuum in that hose was clamped off and used as a resin inlet for the rest of the infusion process. If some parts of the casting area did seem to not have been infused properly with resin, a syringe with vacuum applied was used to force the resin to these regions. After all parts seemed to have been infused with resin, the resin inlets were clamped while the vacuum pump with a resin catch pot applied, stayed attached for approximately 24 hours. After curing, vacuum bag, flow mesh and peel-ply was removed and the mainsail shell was detached from the mould. Then, the mould was cleaned and repaired for any damages, before the next shell was casted with the same process as described for the first one, except of alternating which endplate fiber was laid into.

4.3.2 Spars CFRP Production

Continuous plies of prepreg fiber was cutted with an overlap over the edges of the spar mould. Before laying the fibers onto the mould, the fiber backing was removed. The ply was then applied in the specified orientation from the analysis, see Table 9. To minimize bridging and proper placement of the plies, a debulk of 20 minutes was applied between each layer. After the last layer, the carbon fiber on the edges was trimmed with scalpel such that an even edge was obtained. Furthermore, release film was added around the whole mould which was applied tightly such that the fibers around the edges had no bridging or wrinkles (See Figure 32a). The release film has the function of isolating the breather and bag from the layup which is applied after release film. The vacuum bag was sealed with Vacuum Bag Sealent Tape, as seen in Figure 32b. A vacuum port was placed on the side of the mould, but connected to the mould with breather. A schematic

overview can be seen in Figure 31.

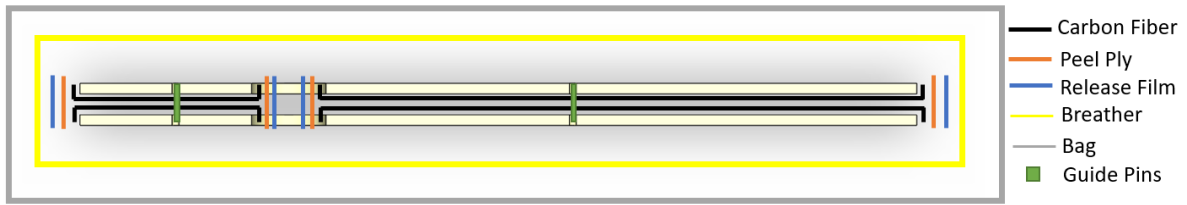


Figure 31: Illustration of the different elements involved in the casting process of the ribs.



(a)



(b)

Figure 32: (a) Rib production - prepreg and release film applied onto the mould, (b) Rib production - prepreg, release film, breather and vacuum bag applied onto the mould.

The bag was checked for any leaks by adding vacuum and monitor pressure drop by using a

pressure clock. During curing, a vacuum pump was attached to the vacuum port ensuring that pressure was obtained. Since the mould was made out of MDF and the maximum temperature was not tested, a low temperature curing cycle was chosen, which can be seen in Figure 33.

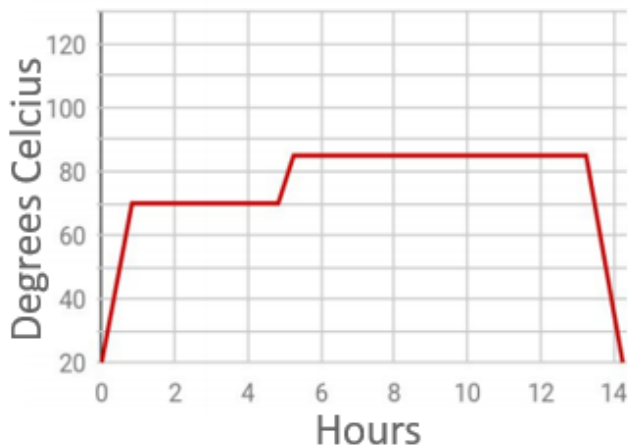


Figure 33: Low oven curing cycle was chosen for the ribs [I.7].

After curing, demoulding of the rib was done while trying to not damage the mould. Between every casting, any excessive resin was sanded and cleaned from the mould with mould cleaner, before release agent [I.12] was re-applied.

4.4 Mast CFPR Production

The mast was made utilizing filament winding production method, which was briefly introduced in Section 2.6.1. The mandrel, which are made with a slight slip in diameter over the length, was used as a mould where release wax was applied prior to casting. Cones were added to both sides to the 2000 mm long stainless steel mandrel, which can be seen in Figure 34. To ensure that no resin was able to enter into the mandrel, the joint between the mandrel and the cones was sealed with sealing tape with a strip of bag tape on top. The 4 axis controlled machine used was Mikrosam MAW 20 LS4/1, as seen in Figure 35, while the winding program was made through the software installed on the winding machine, Winding Expert and the parameters listed in Table 11 was set in the program.

Table 11: Winding parameters

Parameter	Value
Pre-tension	40 N
Fiber speed	20 m/min
Band width	5 mm
Vessel type	Helical
Pattern	No. 36, 16/1
Mandrel diameter	100 mm
Mandrel length with cones	2100 mm
Optimized pattern	On

After the parameters and mandrel was set in Winding Expert, the project file was uploaded into the execution program, Winding Commander, to start the winding process on the machine.

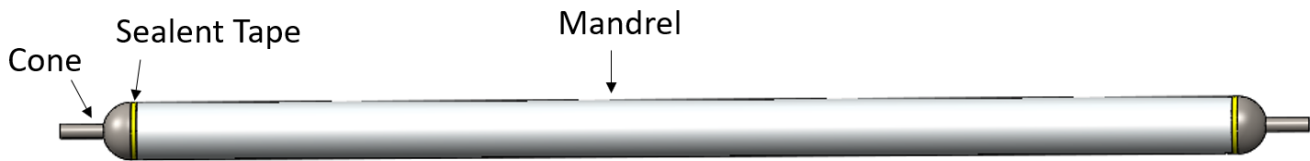


Figure 34: Stainless steel mandrel with cones attached to both ends.



Figure 35: Start of the first layer of PAN carbon fiber wound onto the mandrel.

The fiber used for the mast is GRAFIL 34-700 24K continuous, high strength, PAN based fiber where 24K means that the yarn consists of 24000 filament count tows [I.3]. The epoxy system used was EPIKOTE Resin MGS RIMR 135 with EPIKURE Curing Agent MGS RIMH 137 [I.8] was mixed in two batches to avoid high heat up's and were mixed according to the datasheet, before it was poured in the resin bath. The GRAFIL carbon fiber and Hexion epoxy system was chosen since they have been widely used at the NTNU composites lab for years with good results. The winding process lasted approximately 4 hours, with 6 layers of carbon fiber filaments. The machine speed was regulated during the winding session. After the machine was done with the lay-up, long strips of 5 mm strips of vacuum-bag was rapped around the fibers while the mandrel was slowly rotating and the filament at the ends of the mandrel were cut away to be able to get the mast detached from the mandrel, as seen in Figure 36. To ease the demoulding process, two profiles were added to the side of where the mast is going to be slided off the mandrel, as seen in Figure 37.



Figure 36: After the filament winding process was done with ends cut away and vacuum-bag strips attached.



Figure 37: Illustration of the profiles attached to ease demoulding.

Furthermore, the mast was left to pre-cure at rotating mode for 16 hours to prevent resin migration before the bag-tape was removed and the mast was post-cured at 60 degrees 16 hours in an curing oven with the possibility to rotate the mandrel ensuring uniform heat distribution.

4.4.1 Mast Extraction

Originally, the mast extraction method was done by thermal contracting the mandrel by pouring liquid nitrogen inside the mandrel, together with applying tension to the extraction "ears". The mast would not extract by this method and therefore, second method for extracting the mast was done by connecting a pipe with nuts on both ends which was placed inside the mandrel, while having an adapter plate connected to the pipe and mandrel, pushing on the mast. A nutrunner pistol together with a angular contact ball bearing was used in the extract. The principle of the extractor tool is similar to a "Jaw Puller" and the set-up can be seen in Figure 38.

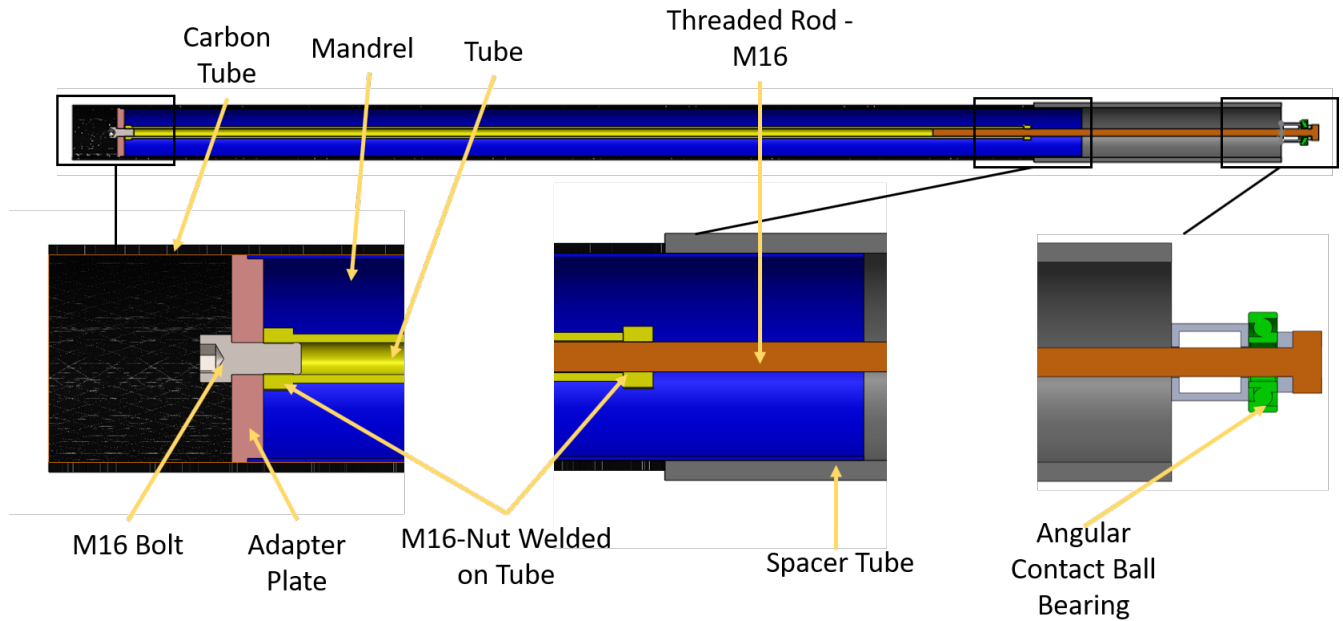


Figure 38: Overview of the mast extraction setup.

4.5 Electronics Box

Since the two parts of the mainsail are planned to bond permanently, it was decided that by including an electronics box at the top of the sail would be a good solution for having the ability to adjust electronic components after assembly. To mount the electronics box into the wingsail, the hole for the box in the CFRP needs to be trimmed. The design of the electronics box can be seen in Figure 39a, 39b, 40a and 40b, and was designed for the use of 3D-print in the production. To add strength to the electronics box top cover, a honeycomb structure was included in the design. The electronics box main room are designed with the ability to mount electronic components into the box so that no electronic components will move around freely in the box.

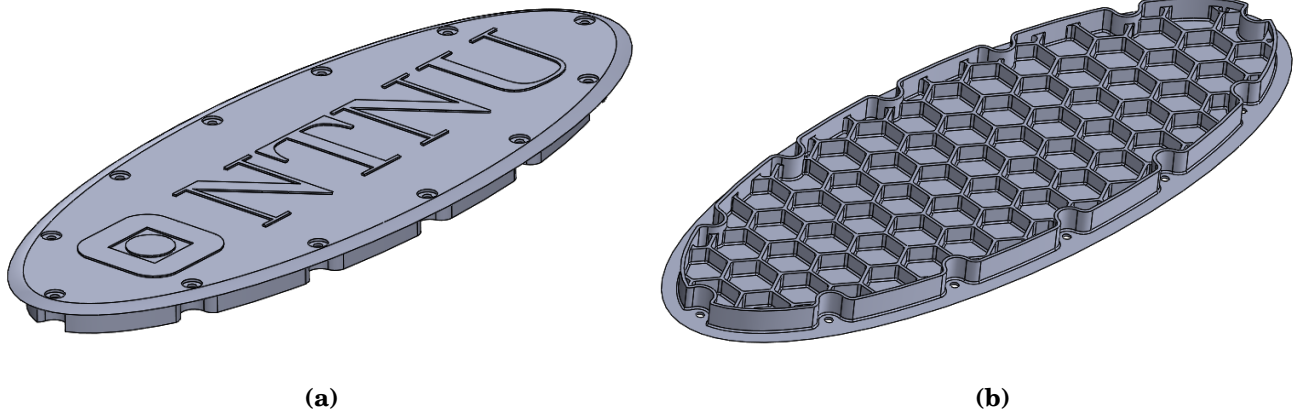


Figure 39: (a) Electronics box top cover seen from above, (b) Electronics box top cover seen from underneath.

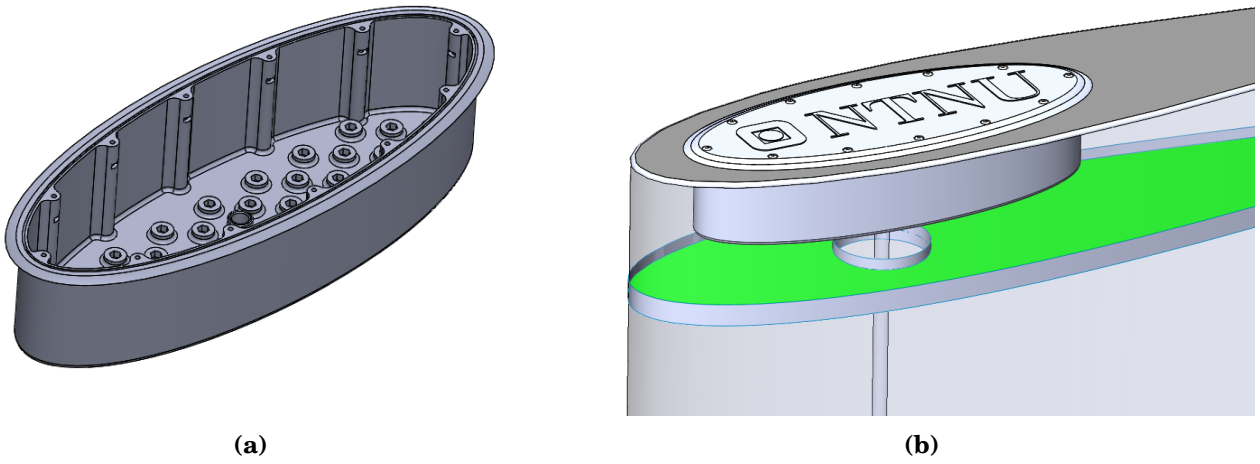


Figure 40: (a) Electronics box main room, (b) Electronics box placement in sail.

4.6 Electronics Routing

For internal routing of cables, a electrical pipe, where its possible to pull cables through after assembly, are going to be mounted going from the mast up to the electronics box, as seen in Figure 41.

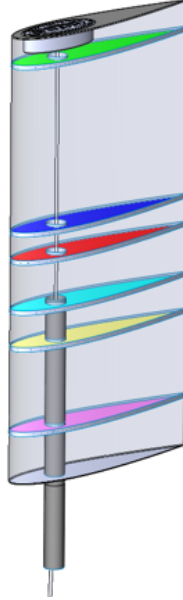


Figure 41: Internal routing of cables.

4.7 Assembly

The assembly process of the different elements are done after both mainsail shells, the mast and all the ribs have been produced, which can be seen in Figure 42 indicated by 1, 2 and 3, respectively. After that, the ribs is glued onto the mast according to the results from the analysis, as indicated by number 4 in Figure 42. Then, the mast and spars are glued into the inside of the first mainsail shell, before the other mainsail shell is glued onto the ribs, mast and the other mainsail shell, as seen in Figure 42 number 6.

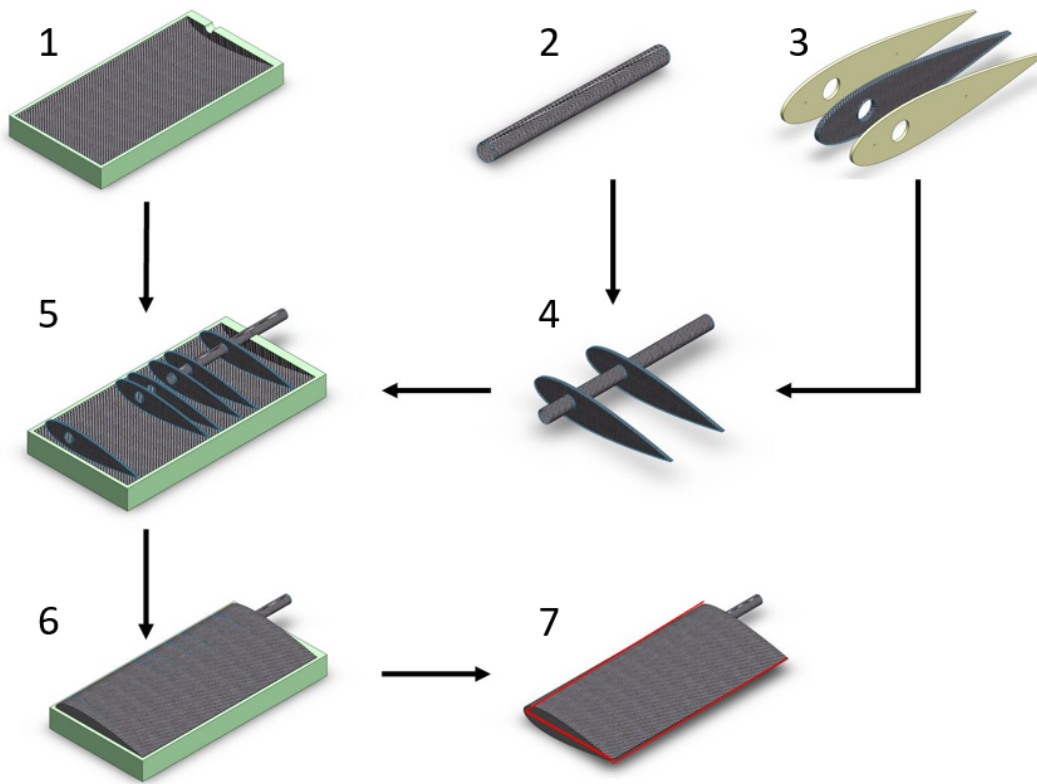


Figure 42: Schematics of the assembly process.

5 Results and Discussion - Design

In this section, the design results from CFD, the optimization and the structural analysis are presented and discussed.

5.1 CFD

The lift force obtained from the CFD-analysis, F_l , for angles of attack -20° to 20° and 6.5 m/s, can be seen in Figure 43.

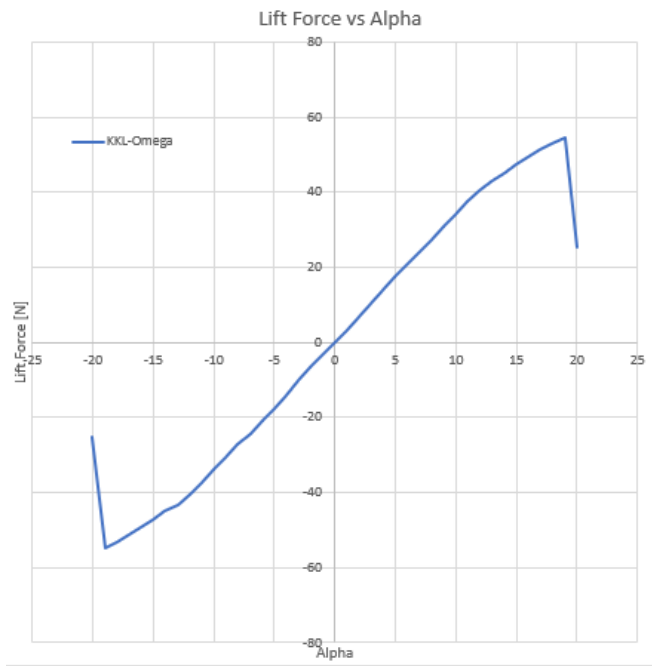


Figure 43: Lift force vs alpha for the wingsail of area 2.88 m^2 with K-KL-omega turbulence model.

From the plot in Figure 43, one can say that the numerical analysis done in Ansys Fluent shows that the wingsail can provide the desired amount of thrust to the vessel.

5.1.1 CFD Validation

Comparison of the analysis in Ansys Fluent 2D-case for NACA 0018 with the transition k-kl-omega turbulence model, the k-omega SST model and viscous analysis in XFOIL with Reynolds number 514512, can be seen in Figure 44a, Figure 44b, Figure 45 and Figure 46. The k-kl-omega

transition model is proven by literature to perform a good agreement with experimental data than SST k-omega [9] where the k-kl-omega is proven to predict a slightly higher drag coefficient, which seems to be the case here as well. For low angles of attack, all the models correspond well with each other, in the other hand, at higher angle of attacks, the results start to vary more with each other. This non-correlation at a high angle of attacks is most likely to be expected since the flow field at high AOA is getting more complex due to flow separation at the wing surface. However, initial attempts of the CFD analysis where the mesh was not refined, gave poor results, which verifies that the mesh play a major role in the study of fluid flows. Therefore, this non-correlation could have been that the mesh is not sufficient enough when the flow field becomes more complex to solve. By evaluating the lift coefficient vs alpha plot in Figure 44b, one can state that the trend is that the k-omega SST model gives a underestimation of the lift, which also can be read from literature [9].

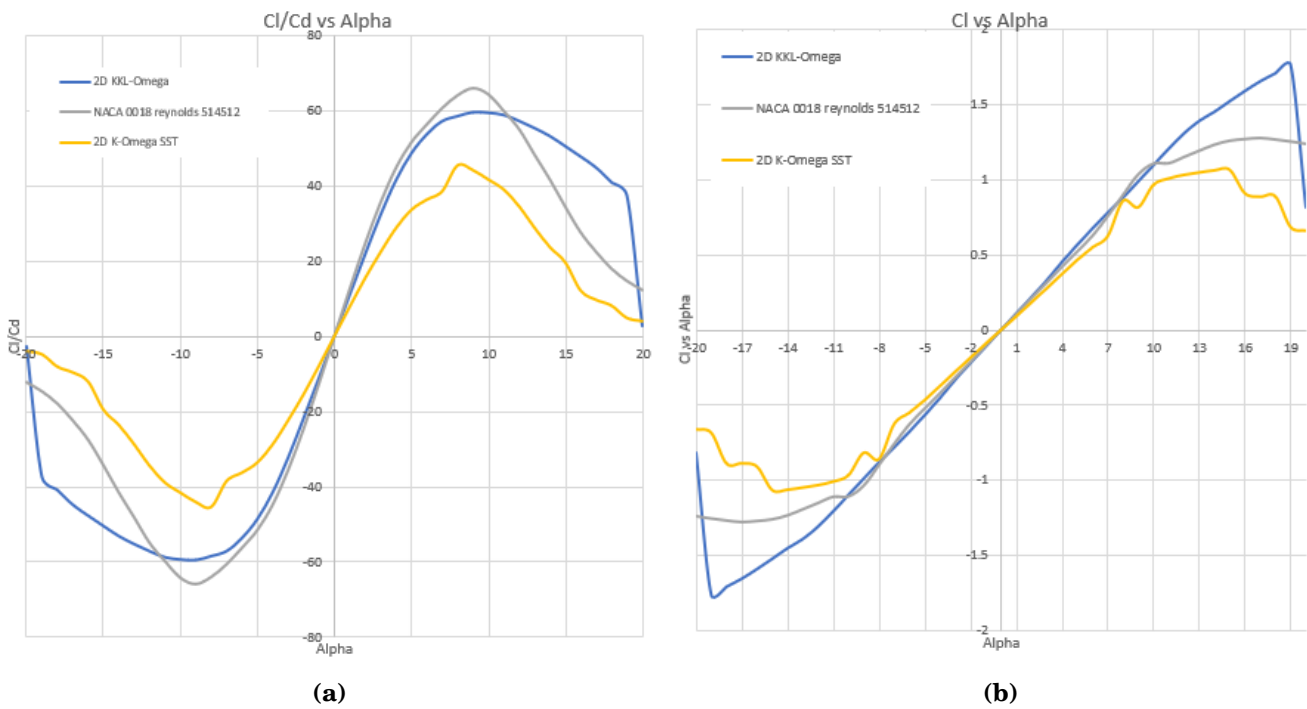


Figure 44: (a) Comparison of Cl/Cd vs alpha in Ansys Fluent 2D-model with k-kl-omega model (blue), k-omega SST (yellow) and XFOIL at Re 514511.87. Both cases are modelled for NACA 0018 airfoil., (b) Comparison of Cl vs alpha in Ansys Fluent 2D-model with k-kl-omega model (blue), k-omega SST (yellow) and XFOIL at Re 514511.87. All the cases are modelled for NACA 0018 airfoil.

The desired operating range, which can be seen from Figure 44a, is between 6-11 ° where the

optimal ratio between drag and lift is achieved. If more lift is being needed, a higher alpha will provide more lift and therefore more thrust to the vessel.

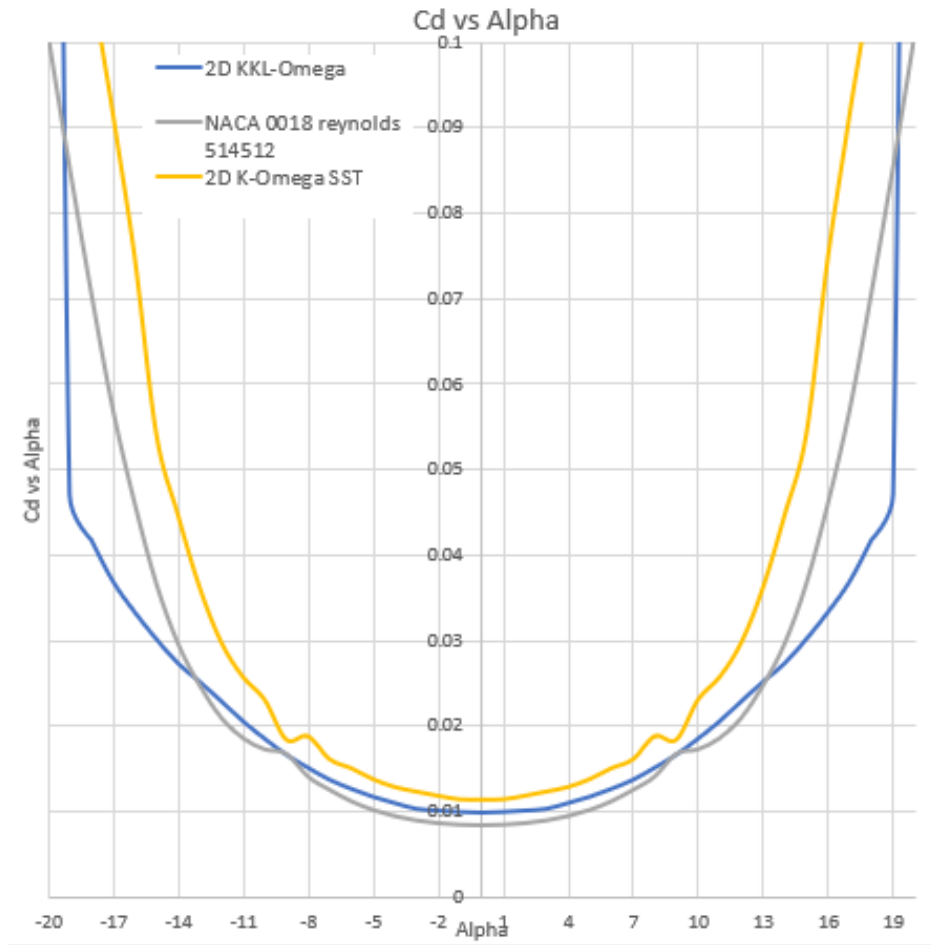


Figure 45: Comparison of Cd vs alpha for Ansys Fluent 2D-model with k-kl-omega model (blue), k-omega SST (yellow) and XFOIL at Re 514511.87 (grey). All the cases are modelled for NACA 0018 airfoil.

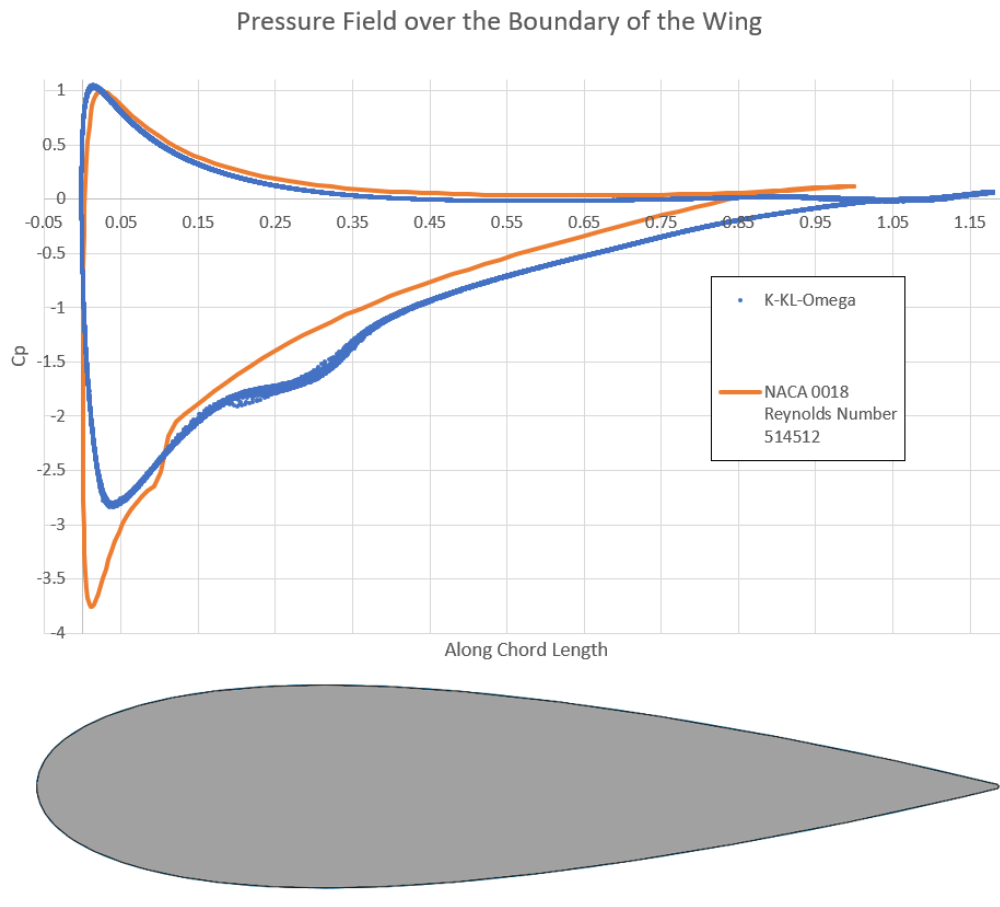


Figure 46: Pressure field along the wingsail boundaries where CFD-analysis (blue) are compared with XFOIL (orange). Calculated for a wing profile with AOA 11 and a wind velocity of 6.5 m/s.

Despite some uncorrelation of the different models at high AOA, the results show consistent values for low AOA. Even though it is numerically and theoretically proven that the wingsail will provide sufficient lift force, the ability to provide thrust at low wind speeds is limited which raises the question of adding a small electric motor to the vessel.

5.2 FEA

5.2.1 Structural Optimization

The structural optimization of 200 iterations can be seen in Figure 47 and the three best candidate points with regards to the objectives minimize total weight, minimize strain energy average and a maximum total deformation under 2 mm, as mentioned in Table 12. Starting with the first

iterations on the left, one can see that the weight is relatively high. The program then tries to find the pattern of which configuration of the different parameters gives minimized total weight, minimized strain energy average, while also obtaining an total deformation maximum of under 2 mm.

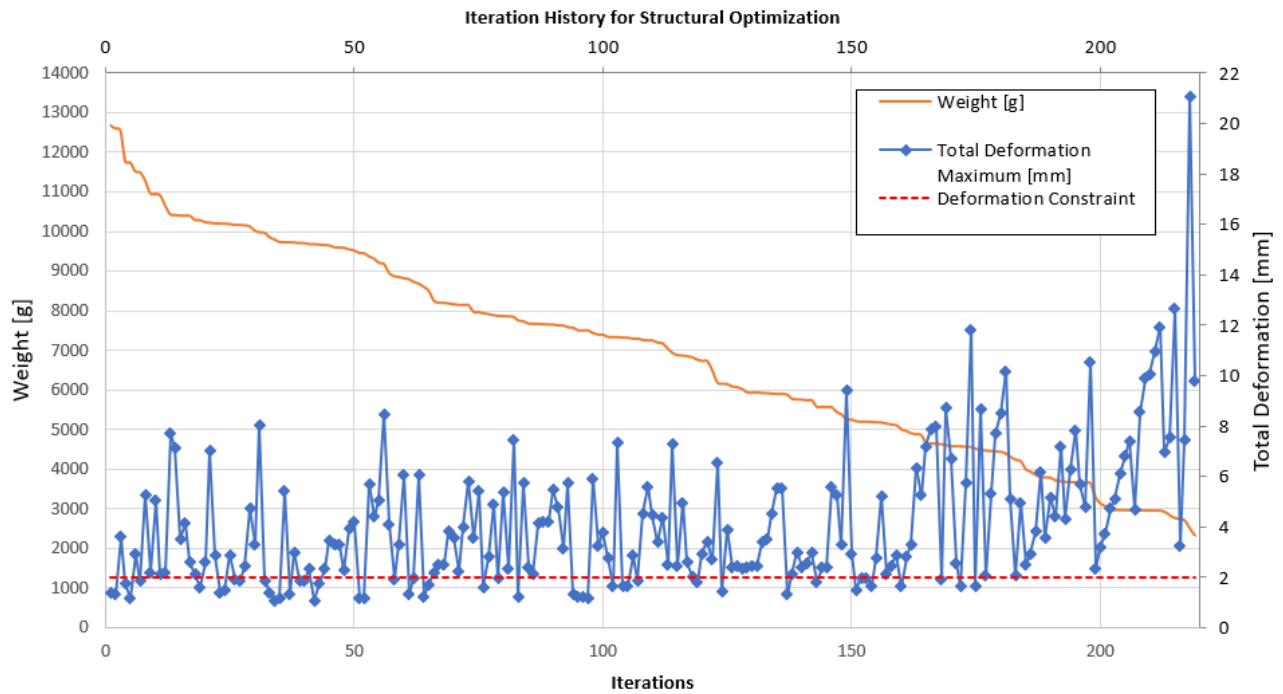


Figure 47: Iteration history for the structural optimization.

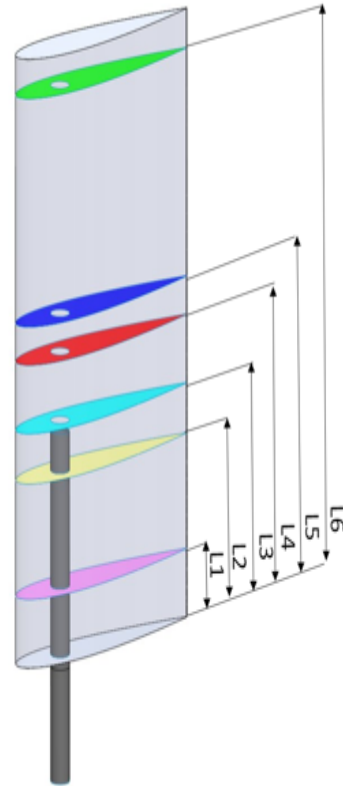
Table 12: Results for the three best candidate points after 200 iterations.

Property	Candidate Point 1	Candidate Point 2	Candidate Point 3
Mast height inside sail [mm]	880.19	667.95	791.18
Mast diameter [mm]	105.95	118.55	104.39
Spacing rib 1 [mm]	270.25	235.8	163.38
Spacing rib 2 [mm]	435.94	343.49	483.46
Spacing rib 3 [mm]	685.19	658.83	662.23
Spacing rib 4 [mm]	725.63	837.48	715.76
Spacing rib 5 [mm]	923.11	991.15	1056.3
Spacing rib 6 [mm]	1193.4	1245.5	1136.3
Spacing rib 7 [mm]	1344.4	1487.6	1398.5
Spacing rib 8 [mm]	1675.9	1548.2	1665.4
Spacing rib 9 [mm]	1728.4	1819.4	1853
Spacing rib 10 [mm]	2047.9	2018.2	2005.2
Spacing rib 11 [mm]	2244.2	2241.6	2211.7
Bottom number of layers	6	4	6
Top number of layers	4	2	4
MainSail number of layers	2	2	2
Rib number of layers	8	10	10
Mast number of layers	8	6	8
Rib 1	Present	Present	Present
Rib 2	Suppressed	Present	Present
Rib 3	Suppressed	Present	Present
Rib 4	Present	Present	Present
Rib 5	Present	Present	Suppressed
Rib 6	Present	Suppressed	Suppressed
Rib 7	Present	Suppressed	Suppressed
Rib 8	Suppressed	Suppressed	Suppressed
Rib 9	Suppressed	Suppressed	Present
Rib 10	Suppressed	Suppressed	Present
Rib 11	Present	Present	Present
Strain energy average [mJ]	16.972	16.417	16.953
Total deformation maximum [mm]	1.6641	1.6263	1.6633
Total weight [g]	4503.5	4566	5180.1

Candidate Point 1 was chosen, since it is the gives the most optimal design among the three candidates given by the objective and constrains, where the main properties of this Candidate Point can be seen in Table 13.

Table 13: Main Geometric and Aerodynamic Properties of the Wing Sail for Candidate Point 1 with a figure describing the optimal rib placement in the wingsail to the right.

Property	Value
Height main sail	2400 mm
Chord length main sail	1200 mm
Height mast	880.19 mm
Diameter mast	105.95 mm
Length to rib 1 (L1)	270.25 mm
Length to rib 2 (L2)	725.63 mm
Length to rib 3 (L3)	923.11 mm
Length to rib 4 (L4)	1193.4 mm
Length to rib 5 (L5)	1344.4 mm
Length to rib 6 (L6)	2244.2 mm
Number of ribs	6
Number of plies on mainsail	2
Number of plies top mainsail	4
Number of plies bottom mainsail	6
Number of plies ribs	8
Number of plies mast	8
Lift force	0-54 N
Drag force	0-1.4 N
Total weight	4503.5 g



Ideally, more calculations should have been done, since the optimization had not converged after solving for 230 different cases. Due to this, there may and most likely will be a structural design that is would have given even better result. However, the chosen design shows very promising results which is seen from Table 14, where a low maximum total deformation of 1.6641 mm has been achieved together with a low strain energy density of 16.972 mJ and a low weight of 4503.5 g and low value for both of the failure criterion's Tsai-Wu and Maximum-stress.

5.2.2 Results for Candidate 1

Further analysis was applied to the design of Candidate Point 1, where deformation, max stress and safety factors for the pressure field imported from Fluent for a windspeed of 6.5 m/s and AOA of 11 ° are presented in Table 14.

Table 14: Results Ansys Mechanical including Failure criterions, with load case 1 as the pressure imported from CFD at 6.5 m/s and AOA of 11 °.

Load Case	$F_{R_{tot}}$ [N]	Def. Total	Def. x [mm]	Def. y-dir.[mm]	σ_{t_1} [MPa]	σ_{c_1} [MPa]	σ_{t_2} [MPa]	σ_{c_2} [MPa]	σ_{t_3} [MPa]	σ_{c_3} [MPa]	Tsai-Wu Fail.Crit.	Max-Stress Fail.Crit.
1	43.76	1.6641	0.19343	0.085718	2.3347	2.3337	0.9482	0.9194	7.4196	7.2923	0.026771	0.02937

5.3 Validation - Mechanical Analysis Abaqus

The final results for the analysis in Abaqus are presented in Table 15. The Tsai-Wu and Max-stress failure criterion are well known criterions for assesment of failure of composites. Specific details can be read in any composites textbook [22]. Results plots can be seen in Section C.

Table 15: Summary of the design results for the total wing sail, the worst loaded rib, mast and glue for 6.5 m/s and 20 m/s loadcase

Part	Def. Total	$S_{11}(min/max)$ [MPa]	$S_{22}(min/max)$ [MPa]	$S_{12}(min/max)$ [MPa]	Tsai-Wu Fail.Crit.	Max-Stress Fail.Crit.
Load Case : Wind Speed 6.5 m/s						
Global	0.259	-1.644/1.393	-0.660/0.638	-0.062/0.042	0.00295	0.00128
Mast	-	-1.644/1.393	-0.064/0.064	-0.062/0.042	0.00295	0.00128
Rib 1	-	-0.326/0.270	-0.368/0.398	-0.029/0.036	0.00077	0.00067
Load Case : Wind Speed 20 m/s						
Global	3.371	-21.37/19.11	-8.586/8.299	-0.806/0.550	0.0383	0.0166
Mast	-	-21.37/18.11	-0.827/0.827	-0.805/0.550	0.0383	0.0166
Rib 1	-	-4.240/3.521	-4.777/5.174	-0.710/0.464	0.0099	0.0087
	$S_{11}(min/max)$ [MPa]	$S_{22}(min/max)$ [MPa]	$S_{33}(min/max)$ [MPa]	$S_{12}(min/max)$ [MPa]	$S_{13}(min/max)$ [MPa]	$S_{23}(min/max)$ [MPa]
Glue	-0.284/0.212	-0.153/0.163	-0.330/0.328	-0.172/0.145	-0.143/0.119	-0.220/0.158

Looking at the data presented in Table 15 we see that the highest stress occur on the mast. At 20 m/s the maximum values for Tsai-Wu and Max-Stress failure criterion are respectively

0.0383 and 0.0166, and are both significant lower than 1. The maximum stress and shear stress found in the glued interfaces are small and all under 0.4 MPa. Assuming a conservative shear strength of 5 MPa for the adhesive joints, we see that even if some local stress concentration is not captured, the stress would need to be more than 10 times higher to reach the assumed shear strength.

5.3.1 Buckling Results

Eigenvalue buckling prediction is a linear analysis which can be used to estimate critical buckling loads. Values in the range -1 to 1 indicates that the critical buckling load is reached. Negative eigenvalues does in most cases indicate that the structure will buckle if a load in the opposite direction was applied [19]. The eigenvalues from the buckling analysis at 6.5 m/s are presented in Table 16.

Table 16: Results from buckling analysis for 6.5 m/s and 11 deg

Eigenvalue mode	1	2	3	4	5	6
Eigenvalue	-73.781	-75.475	-83.324	-85.418	89.807	91.554

The total lift at 6.5 m/s is 43 N and the first eigenvalue is - 73.781, indicates that to reach the critical buckling load, a lift in the opposite direction of 3172 N would be needed. The lift at 20 m/s is 604 N which is 5.25 lower than the critical buckling load.

5.3.2 Material Data

The material properties for the materials used in the analysis was presented in Table 7 and Table 8. Since the material datasheets does not provide all of the necessary material properties, some of the values were tested and some was estimated. In this section, the choice of each material properties are described. The XPREG XC110 Prepreg used on the spars and the fiber used on the sail was tested, where set up and results from the tests can be seen in Appendices E.

5.3.2.1 XPREG XC110 410 g Prepreg For the XPREG XC110 Prepreg, the tested values was gave slightly higher values for E1 and E2 than the provided datasheet. The lowest value was chosen for the analysis. For Nu12, the mean value from the test data, seen in Table 19. G12, G13 and G23 was provided from another project in the composites research group at NTNU which can be seen in Table 20. The density was calculated from the provided datasheet [I.6]. The fail stress

values where all provided in the datasheet [I.6], except of the shear strength which was estimated as 112 MPa. The value for the shear strength was chosen to be the same as for Pyrofil TR30S 3K, since the XPREG XC110 uses Pyrofil TR50S 12k reinforcement and therefore should at least have the same value.

5.3.2.2 GRAFIL 34-700 24K For the GRAFIL 34-700 24K carbon fiber, E1, E2 and density was found from the provided datasheet from the manufacturer [I.3]. Nu12, G12, G13, G23 was not provided and was estimated by evaluating typical fiber properties for similar types fibers. The fail stress values was all provided in the datasheet as typical mechanical properties.

5.3.2.3 Pyrofil TR30S The Pyrofil TR30S 3K typical properties were not provided and needed to be estimated. A similar type of carbon fiber, Tencate 205 gsm 2x2 Twill with TR30S T 3k fibers, seen in datasheet [I.5] was used since it uses the same type of reinforcement. Two different values from E1 and E2 was listed in the datasheet [I.5], while in this analysis, both E1 and E2 was given the lowest value of those assuming symmetric weave. Nu12 was assumed same as Tencate TR30S T 3k, while G12, G13 and G23 was estimated based on typical values for CFPR twill weave. For the fail stresses, values for Tencate [I.5] was used for all values.

From testing the fiber 19, E1 and E2 had a mean value of 43622.5 MPa, which was slightly lower and the value used in the analysis. Yet, the laminate used making this test was made by hand-layup and the ply orientations was not that easily controlled. A test for Pyrofil TR30S HS Carbon in XPREG XC110 210 g prepreg with different matrix was also tested 20, stating a E1 and E2 of 53000 MPa. Therefore, it is likely that the values for E1 and E2 are somewhere in the range of 43642 MPa to 53000 MPa. Nevertheless, analysis with the lowest E1 and E2 gives minimal change of the global stresses since this fiber is not the most dimensioning related to stiffness and strength.

5.3.3 Mesh Sensitivity Analysis

To ensure that no high local stress concentrations are missed due to large mesh size, a mesh sensitivity analysis was conducted for the ribs, glue and mast, where a plot of S11, S22, S12 and U vs mesh size can be seen in Figure 48a, Figure 48b, Figure 49a and Figure 49b, respectively. The mesh sensitivity study have small changes from between each mesh size increment, yet there are some tendencies that the values have not converged when decreasing mesh size. Despite this,

the stresses are relatively low, and for the mesh size to be critical, a big jump in stress must take place and are probably well beyond the acceptable level.

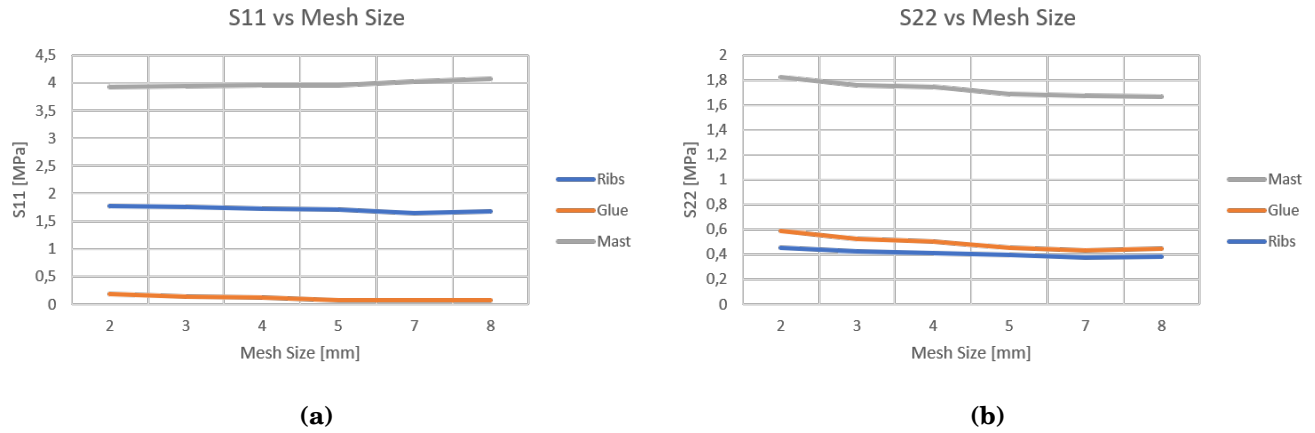


Figure 48: Mesh sensitivity analysis for (a) S11 and (b) S22 for mast glue and ribs.

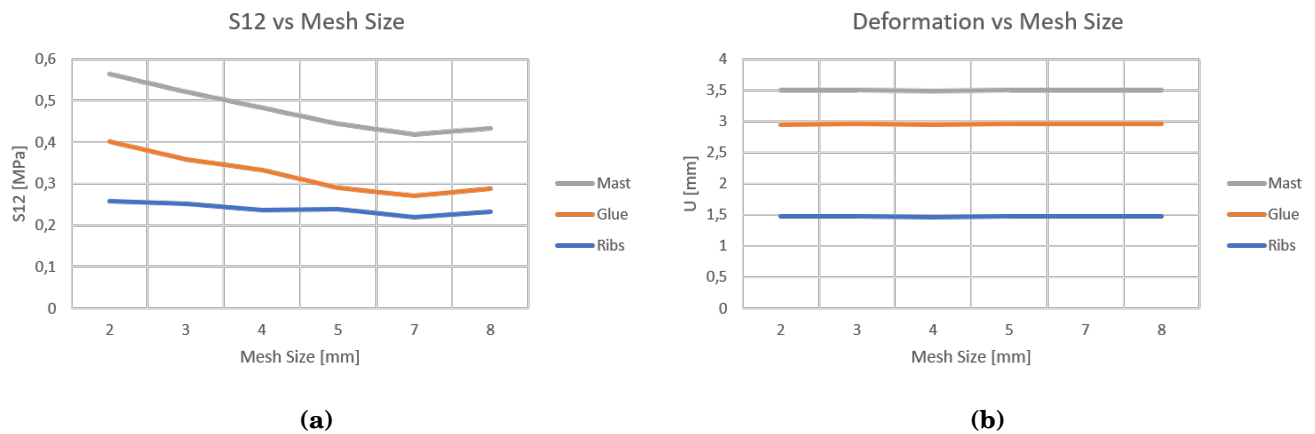
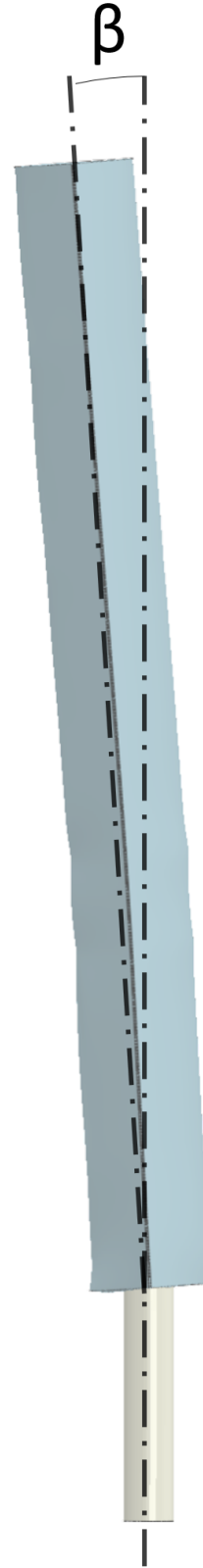


Figure 49: Mesh sensitivity analysis for (a) S12 and (b) deformation, U, for mast, glue and ribs.

5.4 Summary of Results

In Section 1, a list of requirements for the wingsail was presented. One of the requirements was that the wingsail must hold its shape. The wingsail design provides a stiffness high enough that the change in shape can be negligible since the maximum angular deflection of 0.08° at 20 m/s, illustrated as β in Figure 50. The first buckling mode has a critical buckling load that is 5.25 higher than the maximum wind load at 20 m/s. The wingsail was required to handle high wind speeds up to 20 m/s which the design have proven that it can based on the relatively high margins against failure for characteristic strength for both 6.5 m/s and 20 m/s.

In this thesis, only static strength have been investigated and not fatigue of stress rupture. However, fatigue properties of carbon composites are generally excellent and design is typically driven by static strength.



6 Results and Discussion - Production

In this section, the results from the production are presented and discussed. Two CFRP wingsail shells, CFRP six ribs and a CFRP mast have successfully been produced where multiple different production methods have been utilized and the weights of each individual part are presented in Table 17.

Table 17: Weight after production for each part.

Part	Weight
Mainsail shell 1	5778 g
Mainsail shell 2 *	6579 g
Rib 1 **	692 g
Rib 2	460 g
Rib 3	402.6 g
Rib 4	429.1 g
Rib 5	350.2 g
Rib 6	435 g
Mast	3956 g
Total	19081 g

* *Some peelply wasn't removed before weighing*

** *6 layers while the other ribs had only 3 layers*

As presented in Table 17, the final total weight for the wingsail ended up being approximately 19 kg which is around 4.24 times higher than the total weight for candidate point 1 in Table 12. This increase was mainly due to the change of fibers and an increase of number of plies on the mainsail. Additionally, the weight listed in Table 12 are theoretically and would probably been higher after production. On the other hand, the total deformation at 6.5 m/s have decreased 6.43 times, indicating an great increase in stiffness. In Figure 51, a test-assembly of the produced parts are checked.



Figure 51: Mainsail with ribs and mast placed in the mainsail mould.

6.1 Mainsail

In both of the vacuum assisted resin infusion processes, air bubbles were detected inside the bag, as seen in Figure 52. This is not optimal and can cause wrong volume fraction and less good mechanical properties for the end product. The air bubbles originated mainly from the joints between the MDF plates, even though the mould had been coated and glue was applied onto the joints. A solution for this had been to wrap the vacuum bag all around the whole mould, yet there would be problematic with the handling of the mould due to the dimensions.



Figure 52: From the Mainsail production, air bubbles was observed in the infusion process.

Some dryspots were detected on the first cast, but its not obvious what they came from. Possible reasons could be that the vacuum pump was turned off too early, or the resin in the vacuum hose cured faster than the resin in the main part. By inspection, one can see that there was some bridging in the curvature going from top, bottom and mainsail, as seen in Figure 53. This was due to the air leaking in especially in that area, and therefore less vacuum was applied at that point. But this is not critical and can be fixed with applying epoxy with fillers at those places.



Figure 53: Mainsail shell after demoulding.

6.2 Mast

A in-house produced, lightweight mast with a final dimension of 1820 mm long, outer diameter of approximately 110 mm and weighing 3956 g was successfully produced. The long strips of vacuum bag applied left a high quality surface finish of the final product, despite some grooves with excessive epoxy from the overlaps of the strips. These minor imperfections can be fixed by sanding and clear coat, but are only required if surface finish plays a major role. Finished and trimmed mast is shown in Figure 54.



Figure 54: The CFRP mast with ends cutted.

As seen in Figure 55, the mandrel used had some scratches and imperfections from earlier use which made the mast difficult to demould, even though release wax was applied into the scratches and over the whole surface beforehand. This could have been solved by lathe down all the scratches and polishing it, but will require a large lathe machine. A demoulding tool was made, which made the mast demould after a long time struggling to get it off.

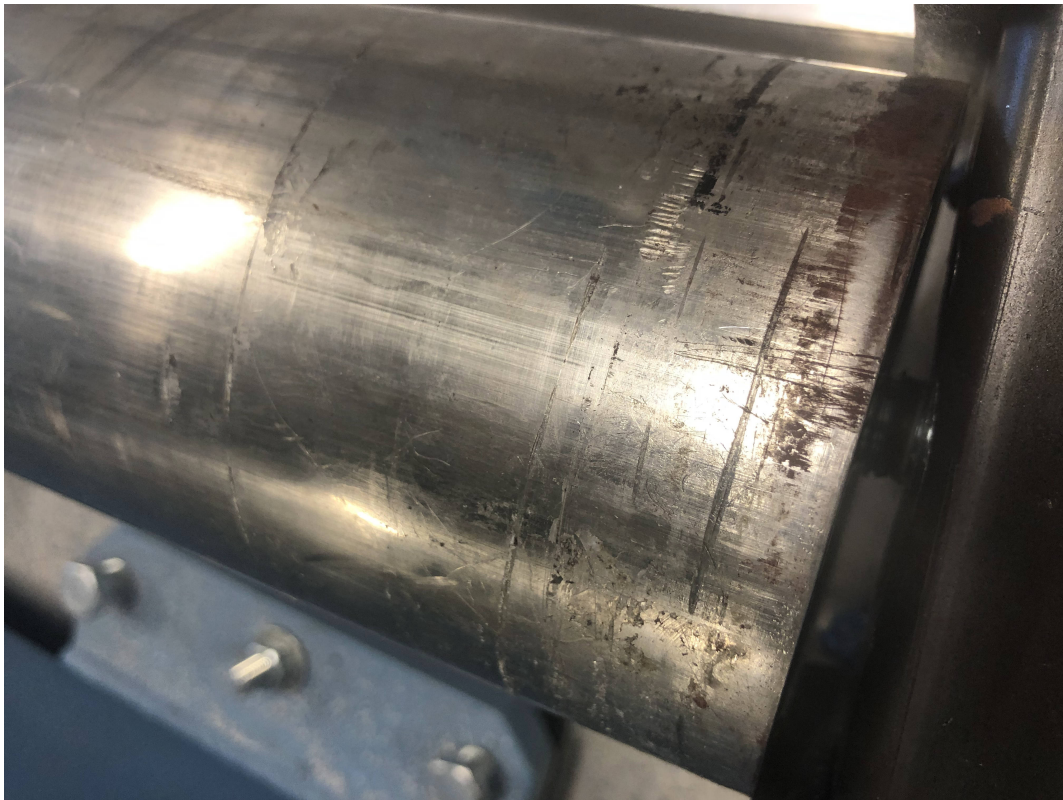


Figure 55: A few of the many scratches present on the mandrel surface.

6.3 Ribs



Figure 56: All six ribs trimmed and demoulded.

With the initial set-up method, the ribs were quite difficult to demould and it was difficult to obtain enough pressure inside the mast ring. As a result, it was decided to only use one mould and decrease the number of layers in the casting process since analysis showed that there was not large differences in strength and deformation with this change. After this change, the ribs demoulded quite easily compared to the first rib made. But as seen in Figure 57a and Figure 57b, there was still some damage on the moulds after all the ribs was made. Therefore, it may could been a good idea to have waterjetted the ribs mould in aluminium which also requires less

work on getting the mould surface nice and the standard curing cycle which uses 120 °C could have been used. On the other hand, waterjetting does not cut completely straight cuts and would require machining afterwards. Nevertheless, the ribs turned out good with nice surface finish and without visual any visual defects, except the first one casted. The first rib was sanded on the regions which low pressure had occurred. In Figure 56 all the ribs after production is shown.



Figure 57: Some damage on the rib mould after demoulding was detected.

6.4 Electronics Box

In Figure 58 one can see the finished 3D-printed electronic box. The electronic box was printed successfully and the top and bottom fitted perfectly.

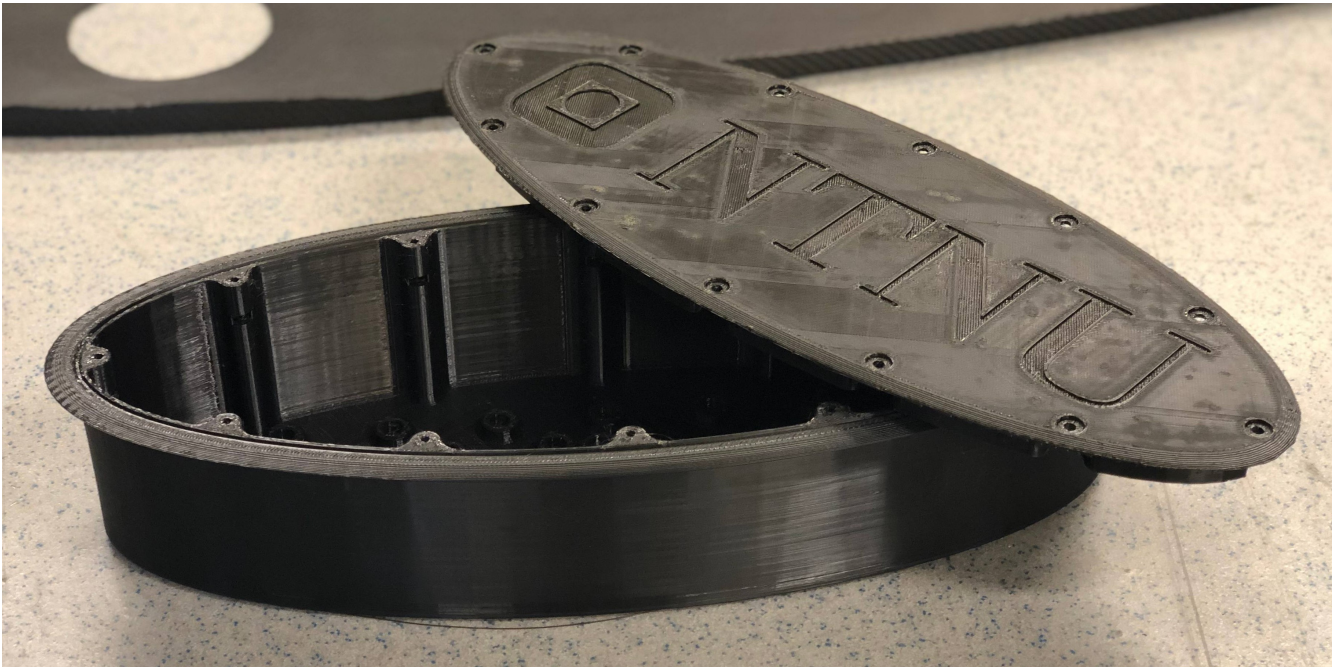


Figure 58: 3D-printed Electronics Box.

7 Conclusion

This report presents the full development process of a Carbon Fibre Reinforced Plastic, CFRP, wingsail for an autonomous boat, starting from deciding concepts and dimensions, to analysing the wingsail in CFD and FEA, structural optimization and production of all parts and moulds. The production process utilized various types of manufacturing methods for CFRP with: VARI, Filament winding and standard casting for pre-preg. The moulds were made in Medium-Density Fiberboard and the complete process for designing and production of the moulds is presented.

The wingsail with an area of 2.88 m^2 can theoretically provide a maximum lift force of 54 N at a wind speed of 6.5 m/s, which is higher than the hull resistance. This was further evaluated through CFD analysis in both 2D and 3D, and the results were compared to XFOIL. The structural optimization executed in Ansys Workbench, provided the optimal placement of internal ribs, the dimensions of the mast, the number of plies in each section of the wingsail with the objective of minimizing strain energy density and weight. At the maximum design wind speed of 20 m/s acting on the sail, the maximum stress in fiber direction, S11, is 21.37 MPa. The maximum stress, occurs in the mast and is 1.66 % of the strength. The weight target was met with the wingsail weighing 19 kg. The maximum deformation of 3.371 mm at the maximum design wind speed was low, which makes the aerodynamics behaviour related to geometrical changes of the wingsail negligible.

8 Further work

8.1 Controlling Sail Orientation

A conventional sailboat would regulate the sailing efficiency by trimming the sails. For rigid sails, the sail efficiency often controlled with a tail flap. This tail flap provides control of the orientation of the wing sail and therefore gives control of the vessels speed and heel [1]. This way of controlling the rigid sails requires less power consumption than by using by instance a step motor in the root of the mast. The pitch of the flap is controlled by a small servomotor placed in the wing, and an illustration a flap configuration on the wingsail can be seen in Figure 59.

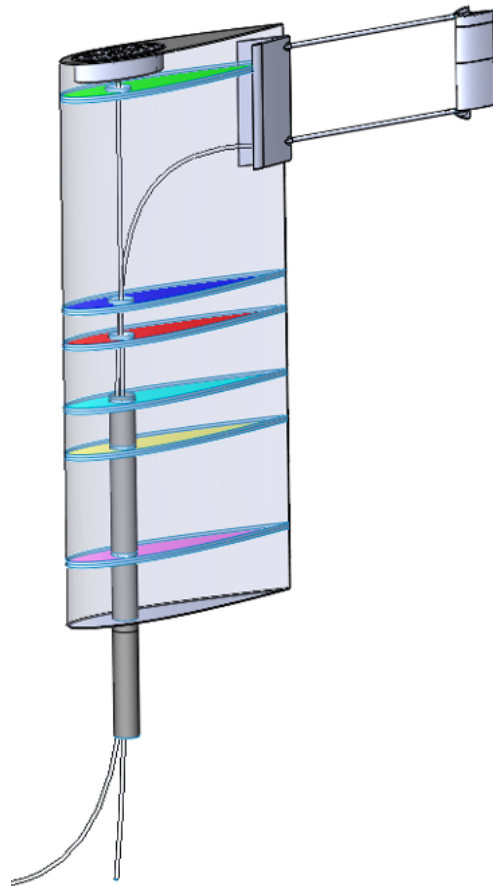


Figure 59: Design suggestion for a flap for controlling the sail orientation.

8.2 Assembly

The plan for assembly is presented in Section 4.7.

8.3 Testing

A test-rig is already made by waterjetting two 30 mm steel plates with room for the mast, as seen in Figure 60. Machine drawings can be seen in Appendix H. The mast is placed inside the mast hole and tightened with the clamps made which can be seen in Appendix H. Strain gauges can be attached while external loads are applied.

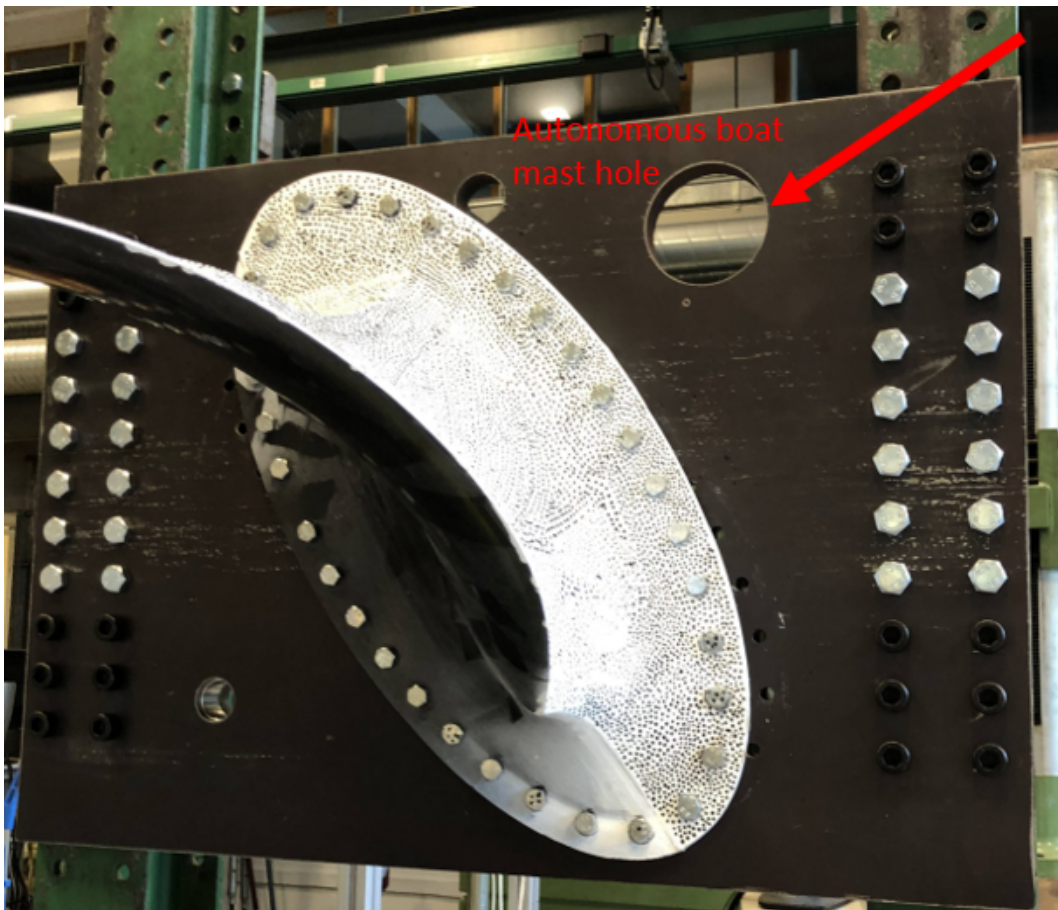


Figure 60: Test-rig autonomous boat where the 30 mm thick steel-plates was made in cooperation with another project. The mast hole is indicated by the red arrow.

8.4 Sensors and Electronics

Wind velocity and direction sensors must be mounted onto the wingsail, since this information is crucial for adjusting the angle of attack.

8.5 Mast Foot

A mast foot to hold the sail must be designed to handle the forces from the sail. If the flap configuration is going to be used, a free rotating mast foot should be used, and an alternative of a ball bearing mast foot can be seen in Figure 61.

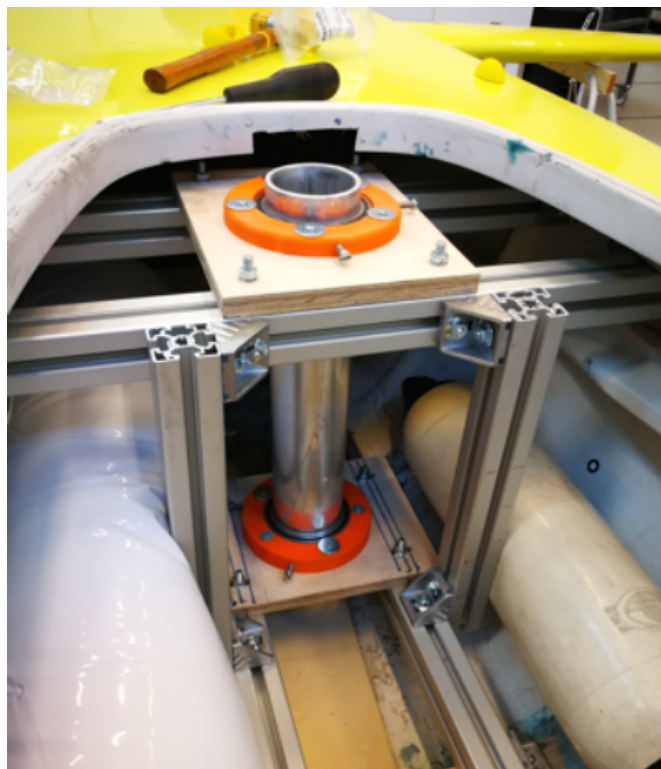


Figure 61: Suggestion for a ball bearing mast foot which was used in a similar project at the university KTH in Sweden [3].

The minimum requirements that needs to be set for the mast foot for a wind load of 20 m/s are shown in Table 18. These requirements were obtained through analysing reaction forces in Abaqus and through hand calculations. Torsional loads not applicable if a tail flap is used for controlling angle of attack.

Table 18: Minimum requirements for the mast foot.

Parameter	Value
F_{axial}	197 N
F_{radial}	603 N
M_{axial}	1327 Nm
T	23 Nm

8.6 UV-coating

Since epoxy which are exposed to UV-rays can degrade over time, the outer surfaces should be considered coated with a protective coating [23].

References

- [1] C. Meinig, N. Lawrence-Slavas, R. Jenkins, and H. Tabisola, “The use of saildrones to examine spring conditions in the bering sea: Vehicle specification and mission performance,” 10 2015, pp. 1–6.
- [2] M. Dyrseth, “Development and design of a wingsail for an autonomous surface vessel,” 2019, project work.
- [3] C. Tretow, “Design of a free-rotating wing sail for an autonomous sailboat,” Master’s thesis, 2017.
- [4] Y. Hailian and Y. Xiongqing, “Integration of manufacturing cost into structural optimization of composite wings,” *Chinese Journal of Aeronautics*, vol. 23, no. 6, pp. 670 – 676, 2010. [Online]. Available: <http://www.sciencedirect.com/science/article/pii/S1000936109602697>
- [5] U. A. A. G. D. of Aerospace Engineering. Uiuc airfoil coordinates database. Last accessed: 2020-07-24. [Online]. Available: https://m-selig.ae.illinois.edu/ads/coord_database.html
- [6] J. Anderson, *Fundamentals of Aerodynamics*. New York, NY 20121: McGraw-Hill Education, 2017.
- [7] W. M. H K Versteeg, *An Introduction to Computational Fluid Dynamics - The finite volume method*. Noida 201309, India: Pearson Education, Ltd., 2007.
- [8] H. Shah, S. Mathew, and C. Lim, “A novel low reynolds number airfoil design for small horizontal axis wind turbines,” *Wind Engineering*, vol. 38, pp. 377–392, 08 2014.
- [9] J. Morgado, R. Vizinho, M. Silvestre, and J. Páscoa, “Xfoil vs cfd performance predictions for high lift low reynolds number airfoils,” *Aerospace Science and Technology*, vol. 52, pp. 207 – 214, 2016. [Online]. Available: <http://www.sciencedirect.com/science/article/pii/S1270963816300839>
- [10] Ansys. Ansys fluent user’s guide. Last accessed: 2020-07-23. [Online]. Available: https://ansyshelp.ansys.com/account/secured?returnurl=/Views/Secured/corp/v195/flu_ug/flu_ug.html%23flu_ug

- [11] N. P. Vedvik. Tmm4175 polymer composites. Last accessed: 2019-12-17. [Online]. Available: <http://folk.ntnu.no/nilspv/TMM4175/Fibers.html>
- [12] W. Jou, “A novel structure of woven continuous-carbon fiber composites with high electromagnetic shielding,” *Journal of Electronic Materials*, vol. 33, pp. 162–170, 03 2004.
- [13] T. C. Hub. Filament winding: A cost-effective composites process. Last accessed: 2020-07-15. [Online]. Available: <https://www.thecompositeshub-india.com/filament-winding--a-cost-effective-composites-process>
- [14] K. K. Verma, B. L. Dinesh, K. Singh, K. M. Gaddikeri, V. Srinivasa, R. Kumar, and R. M. Sundaram, “Development of vacuum enhanced resin infusion technology (verity) process for manufacturing of primary aircraft structures,” *Journal of the Indian Institute of Science*, vol. 93, pp. 621–634, 2013.
- [15] G. to composites. Gurit. Last accessed: 2020-07-26. [Online]. Available: www.gurit.com
- [16] M. Drela. Xfoil. Last accessed: 2020-07-27. [Online]. Available: <http://web.mit.edu/drela/Public/web/xfoil/>
- [17] C. L. Archer and M. Z. Jacobson, “Evaluation of global wind power.”
- [18] Ansys. Ansys workbench user’s guide. Last accessed: 2019-12-14. [Online]. Available: https://ansyshelp.ansys.com/account/secured?returnurl=/Views/Secured/corp/v195/wb2_help/wb2_help.html%23wb2_help
- [19] Dassault Systèmes, *Abaqus documentation*. ©Dassault Systèmes, 2006.
- [20] D. Systèmes. Solidworks online help. Last accessed: 2019-12-14. [Online]. Available: http://help.solidworks.com/2019/english/SolidWorks/sldworks/r_welcome_sw_online_help.htm?id=84cd60fe8a8549d5a4eeb1db5b77548b#Pg0
- [21] E. V. Olsen, “Stress analysis, lay-up and production process for the tail section of a composite glider used for energy generation.” Master’s thesis, 2017, last accessed: 2020-07-23. [Online]. Available: <https://ntnuopen.ntnu.no/ntnu-xmlui/handle/11250/2464343?fbclid=IwAR1MOhhtkcjpO4q8Nqow577-p5hv5HLc2hoivQveIMa9tDvrOLkX92WNw7E>

- [22] C. H. Wang and C. N. Duong, "Chapter 2 - failure criteria," in *Bonded Joints and Repairs to Composite Airframe Structures*, C. H. Wang and C. N. Duong, Eds. Oxford: Academic Press, 2016, pp. 21 – 45. [Online]. Available: <http://www.sciencedirect.com/science/article/pii/B9780124171534000025>
- [23] A. Ghasemi-Kahrizsangi, J. Neshati, H. Shariatpanahi, and E. Akbarinezhad, "Improving the uv degradation resistance of epoxy coatings using modified carbon black nanoparticles," *Progress in Organic Coatings*, vol. 85, pp. 199 – 207, 2015. [Online]. Available: <http://www.sciencedirect.com/science/article/pii/S0300944015001265>

Appendices

A Modeling, Setup, Procedures and Results

A.1 CFD Setup

This section will present all the steps done in Ansys Workbench Fluent to set up the CFD-model for the wingsail. It will be structured as the work sequence that Fluent follows, which is mesh, setup and then solver.

A.1.1 2D-analysis

Mesh For the mesh, a big area which is going to be the fluid area is made around the airfoil and the wingsail is suppressed, as seen in Figure 62a. A refinement area can be made, as seen as the green area in Figure 62b.

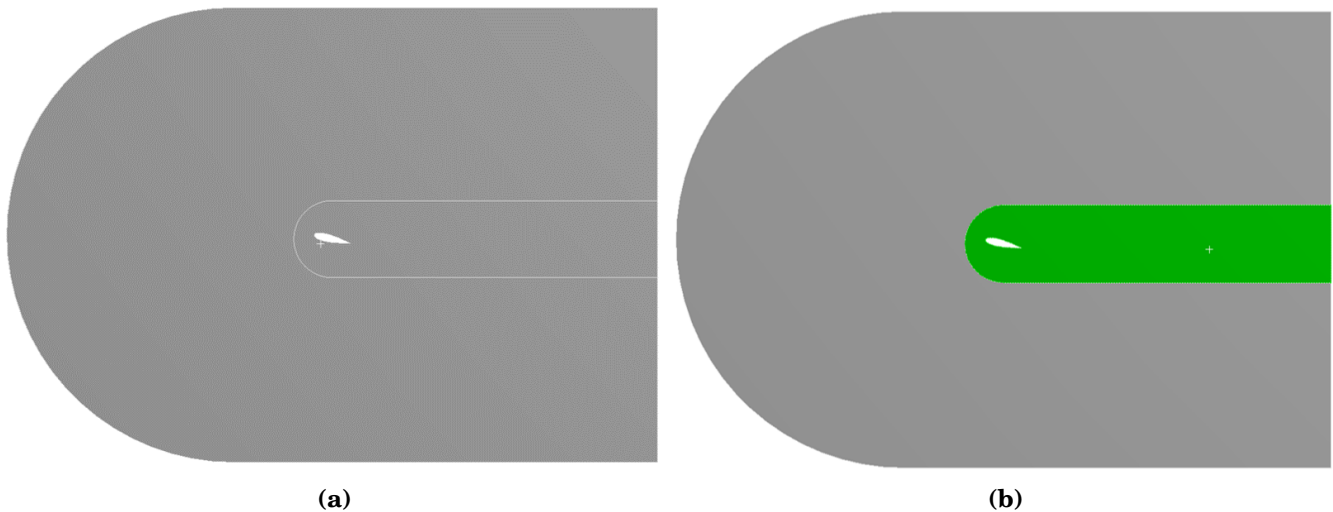


Figure 62: (a) Overview of the geometry of the model, (b) Refinement area highlighted in green.

Then the boundaries is defined, where the velocity-inlet is seen in Figure 63a, the named selection, wall, can be seen in Figure 63b where the opposite side is named the same. The Pressure-Outlet can be defined as seen in Figure 64a, while the wing is defined as a wall as well as the two sides, as seen in Figure 64b.

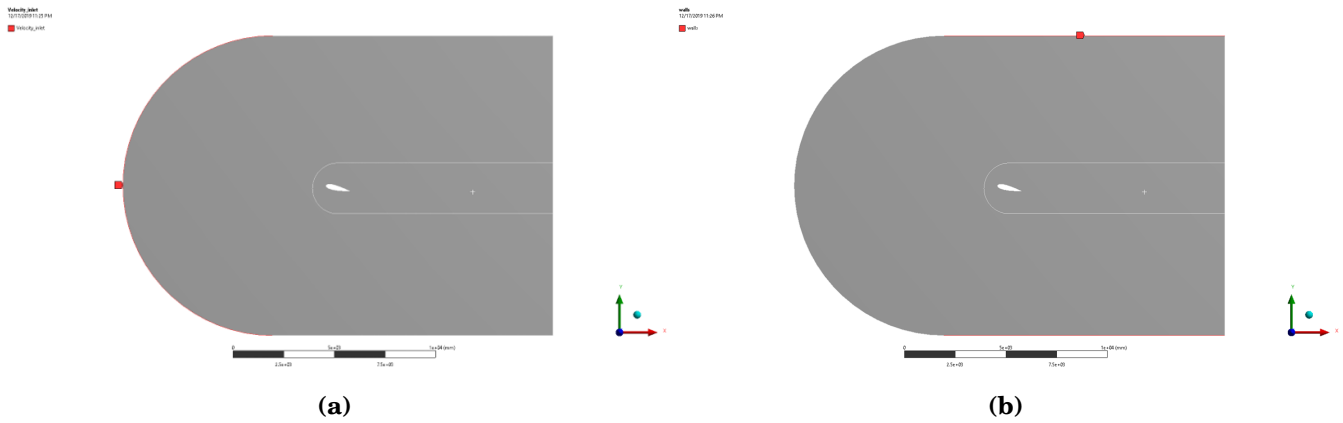


Figure 63: (a) Named region Velocity-Inlet, (b) Named region walls.

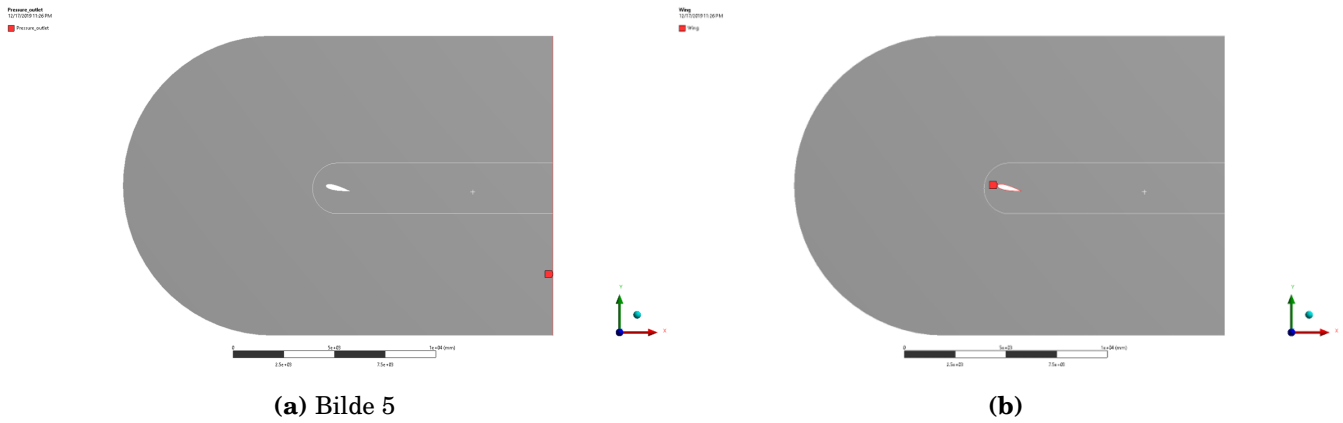
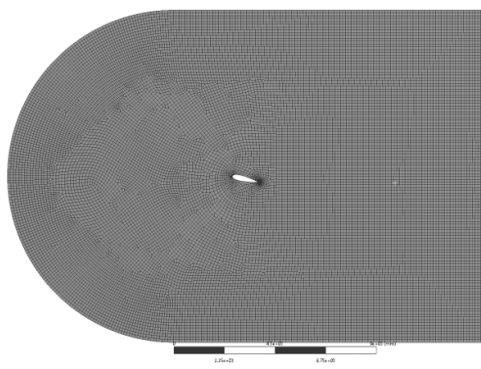
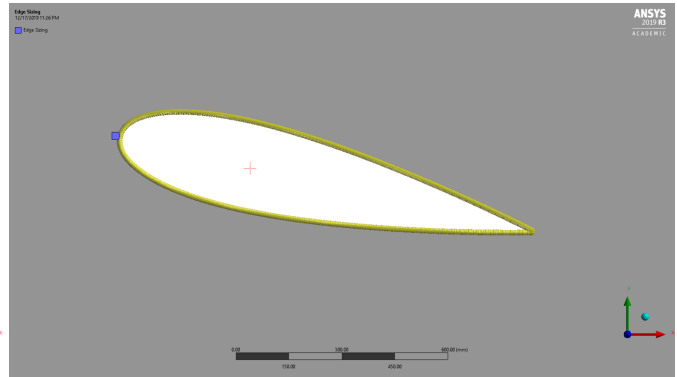


Figure 64: (a) Named region Pressure-outlet, (b) Named region wing.

Applying only a global element size of 125 mm, as the Figure 72 shows, the obtained mesh can be seen in Figure 65a. To improve the mesh, a edge seeding on the wing edges can be done, this is shown in Figure 65b and the improved mesh can be seen in Figure 66a. Values for the edge sizing can be seen in Figure 69.



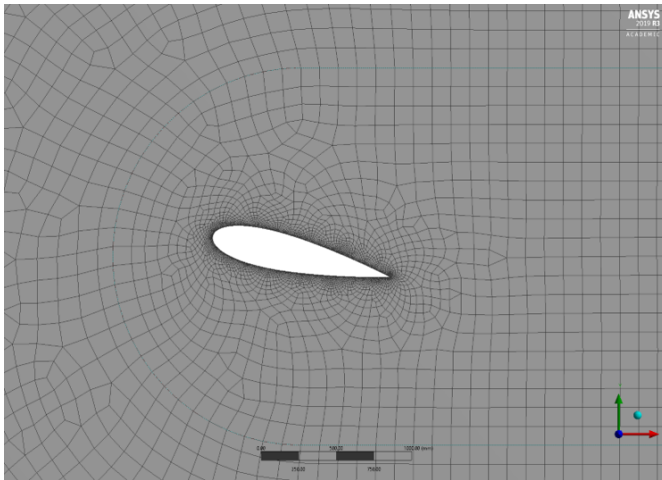
(a)



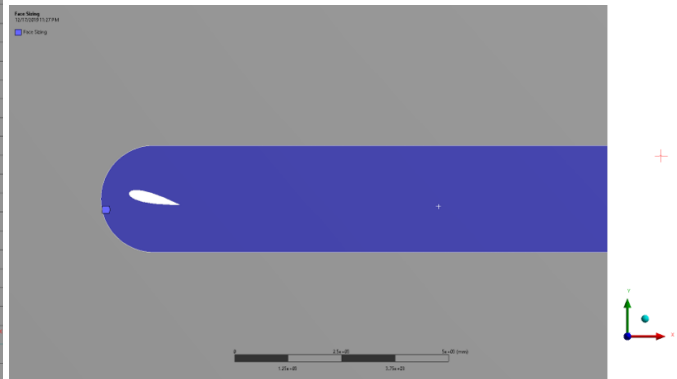
(b)

Figure 65: (a) Mesh with a global element size of 125 mm, (b) Edge seeding applied to the wing profile geometry.

Further improvements of the mesh can be provided by defining a refinement area, as seen in Figure 66b and the improved mesh after adding both edge seeding and refinement can be seen in Figure 67a and Figure 67b. The values for the refinement can be seen in Figure 70.



(a)



(b)

Figure 66: (a) Improved mesh after edge seeding of the wings boundary, (b) A refined area can be created, illustrated in purple.

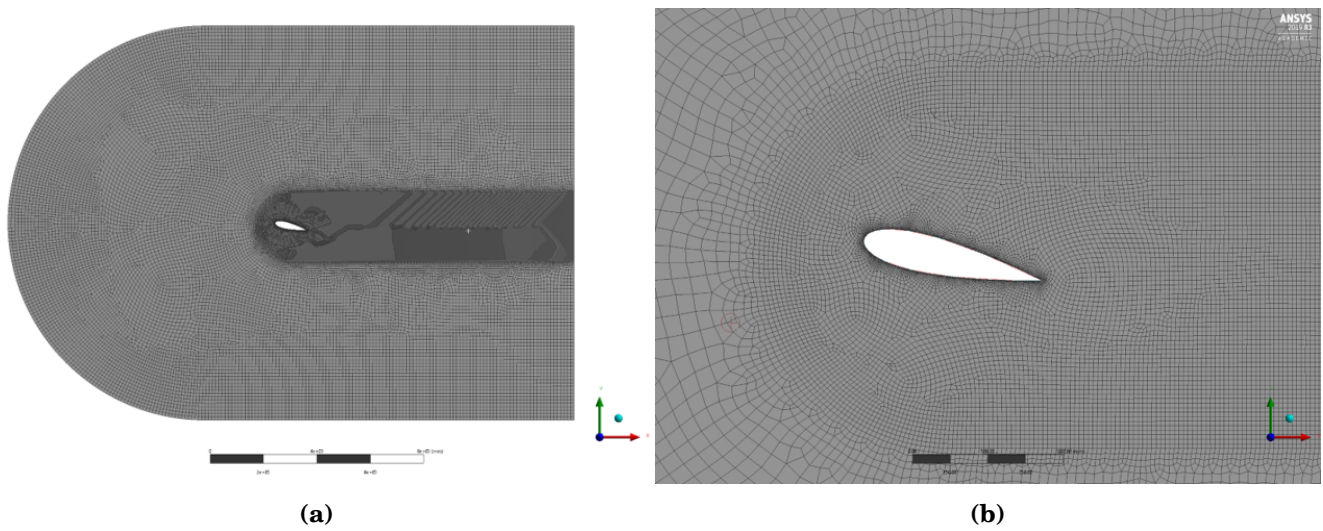


Figure 67: (a) Mesh after refinement area is described, (b) Closeup of the mesh after a refinement area is described

Further improvements that is done is to add a inflation near the boundary of the wing, seen in Figure 68a and Figure 68b.

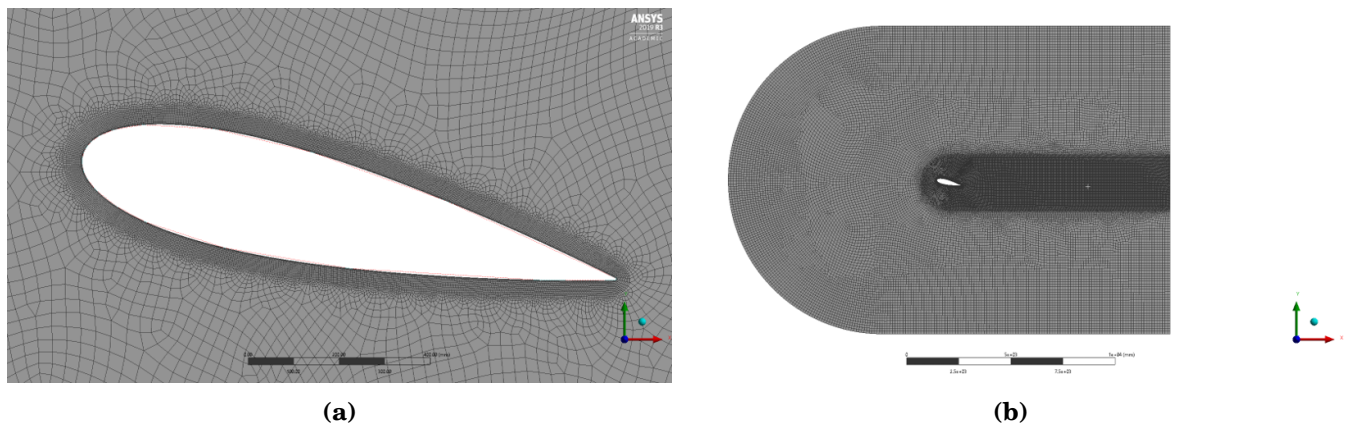


Figure 68: (a) Closeup of the mesh near the wing after edge seeding, inflation and refinement area is defined, (b) Mesh after edge seeding, inflation and refinement area is defined

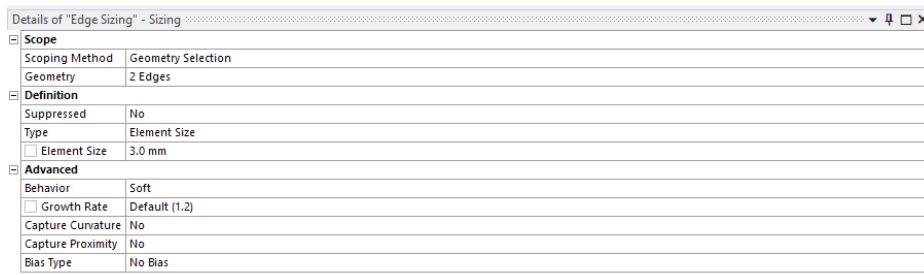


Figure 69: Details of edge sizing

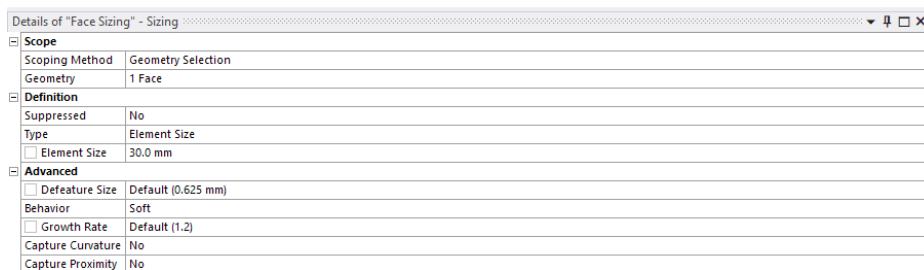


Figure 70: Details of face sizing



Figure 71: Details of inflation



Figure 72: Details of the global mesh.

It is in the mesh module, as shown under CAD parameters in Figure 73 the parameters for the optimization algorithms can be added.

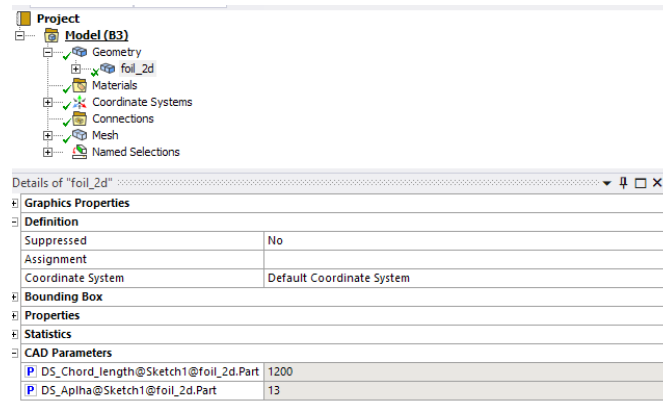
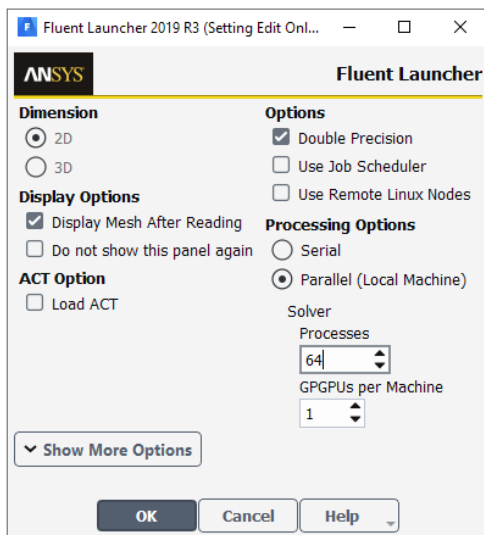
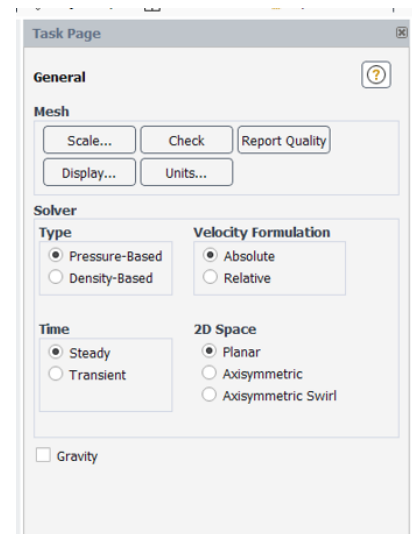


Figure 73: Mesh module overview.

Fluent In the Fluent Launcher, different analysis settings is chosen as 2D and processing options, as seen in Figure 74a. Furthermore, the mesh is checked through the general window and solver types is selected as Pressure-Based and Steady-state, seen in Figure 74b.



(a)



(b)

Figure 74: (a) CFD solver setup, (b) General window where different solver types can be selected.

The material for the flow is set as air with the given properties from the fluent database, as

seen in Figure 75a. The various boundary conditions are then checked, where a overview of the different boundary conditions can be seen in Figure 75b. These have been automatically detected and assigned from the named selections assigned in the mesh module.

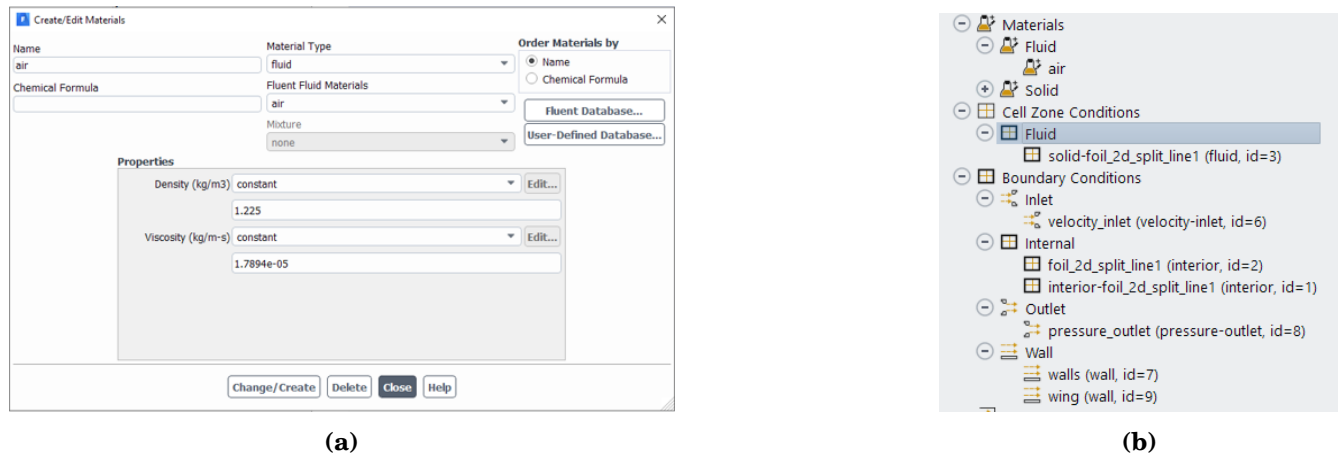


Figure 75: (a) Fluid properties of air, (b) Materials and boundary conditions in the analysis. The name set in mesh is automatically detected and assigned by the software.

The boundary conditions for the velocity inlet can be seen in Figure 76a where a velocity of 6.5 m/s is used. The pressure outlet is set to 0 Pa, as seen in Figure 76b.

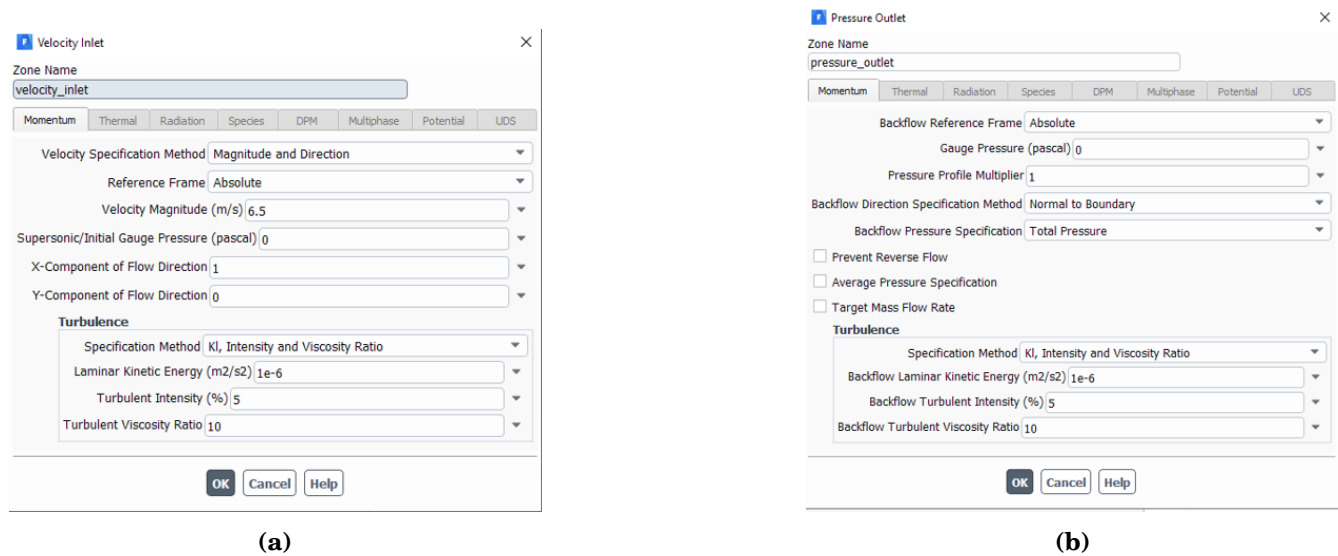
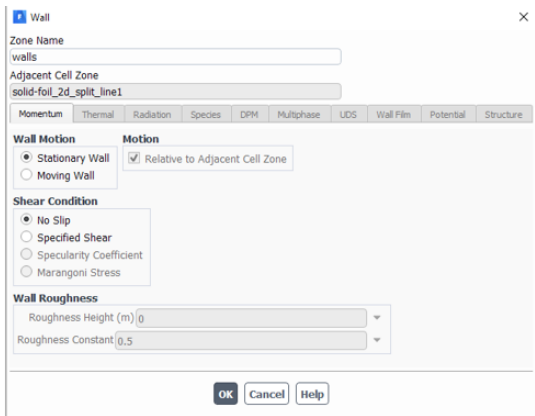
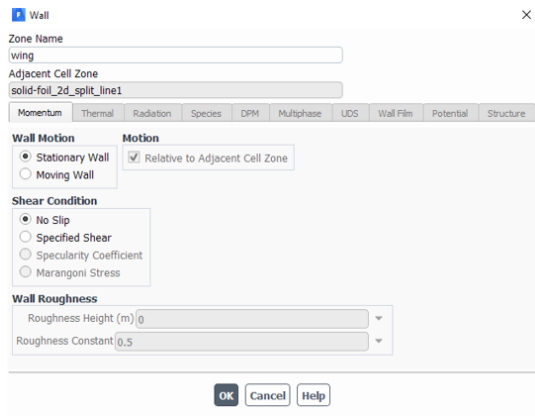


Figure 76: (a) Defining the properties for the velocity inlet, (b) Defining the properties for the pressure-outlet.

The wall is modeled as a stationary wall with no-slip condition as seen in Figure 77a. The wing is modeled the same way, as seen in Figure 77b.



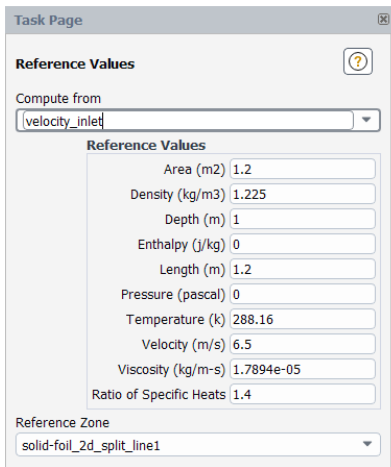
(a)



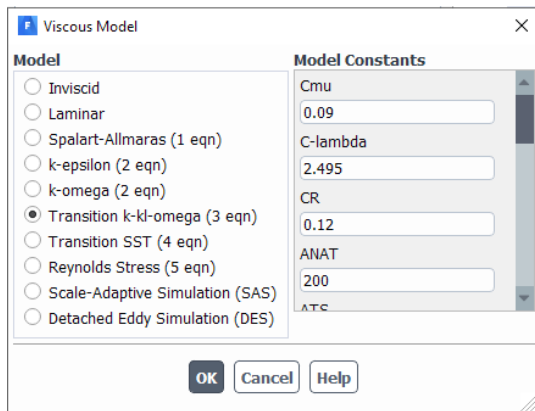
(b)

Figure 77: (a) Defining the property of the walls, (b) Defining the properties for the wing.

The reference values is computed from the velocity-inlet and the area is set as the chord length, as seen in Figure 78a. The visous model chosen for the first analysis is k-kl-omega, as seen in Figure 78b.



(a)



(b)

Figure 78: (a) CFD reference values computed from velocity inlet, (b) Viscous model chosen with Transition k-kl-omega chosen.

A hybrid initialization is chosen, as seen in Figure 79.

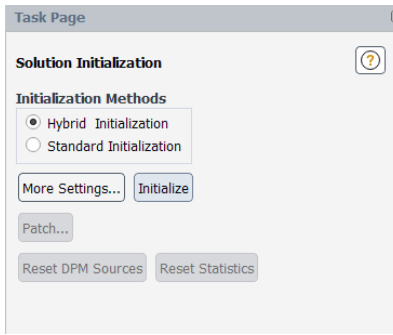
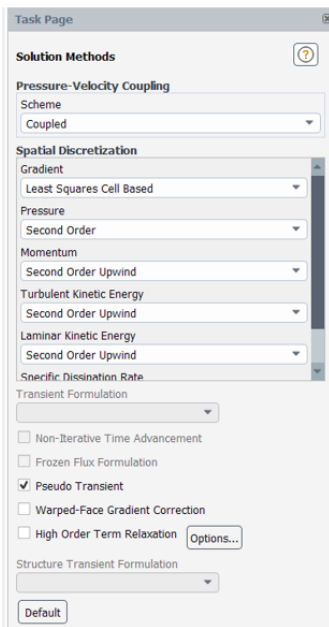
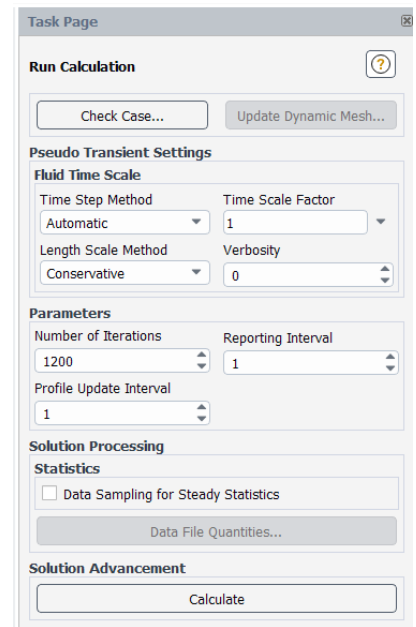


Figure 79: A hybrid initialization is chosen.

The solutions method is shown in Figure 80a where a coupled scheme is chosen together with least squares cell based with second order upwind for the rest of the parameters. The numbers of iteration is initially chosen to 1200 iterations, as seen in Figure 80b.



(a)



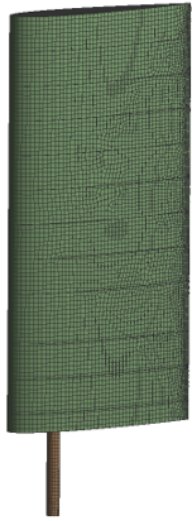
(b)

Figure 80: (a) Solution Method chosen for the analysis, (b) Run calculation window where number of iterations is chosen initially to 1200.

A.1.2 3-D In the 3-D case, many of the same procedures is done as in 2D.

A.2 Structural analysis

A.2.1 Mesh The mesh for the structural analysis can be seen in Figure 81a and Figure 81b, while the properties can be seen in Figure 82.



(a)



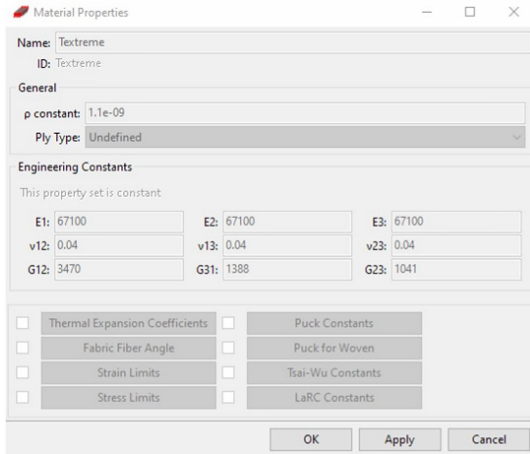
(b)

Figure 81: (a) Mesh sail and mast, (b) Mesh of ribs.

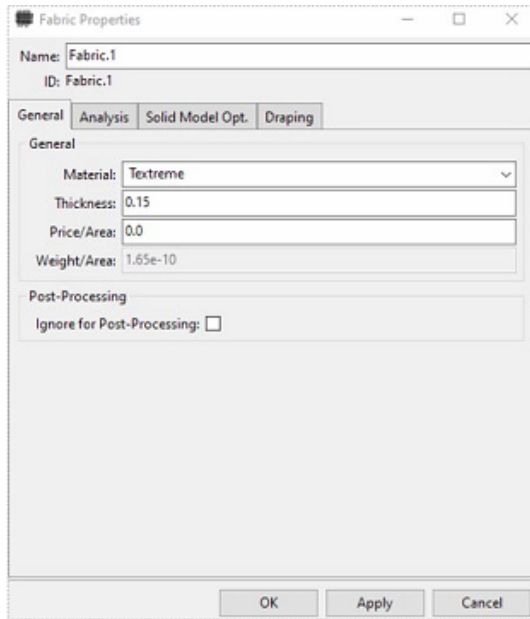
<input type="checkbox"/> Display	
Display Style	Use Geometry Setting
<input type="checkbox"/> Defaults	
Physics Preference	Mechanical
Element Order	Program Controlled
<input type="checkbox"/> Element Size	25.0 mm
<input checked="" type="checkbox"/> Sizing	
Use Adaptive Sizi...	No
<input type="checkbox"/> Growth Rate	Default (1.2)
Mesh Defeaturing	Yes
<input type="checkbox"/> Defeature Size	5. mm
Capture Curvature	Yes
<input type="checkbox"/> Curvature Mi...	6.0 mm
<input type="checkbox"/> Curvature Nor...	Default (30.0°)
Capture Proximity	No
Bounding Box Di...	3148.9 mm
Average Surface ...	5.2431e+005 mm ²
Minimum Edge L...	7.2792 mm
<input type="checkbox"/> Quality	
<input type="checkbox"/> Inflation	
<input type="checkbox"/> Batch Connections	
<input type="checkbox"/> Advanced	
<input type="checkbox"/> Statistics	
<input type="checkbox"/> Nodes	20103
<input type="checkbox"/> Elements	19729

Figure 82: Overview of the properties of the structural mesh.

A.2.2 Setup composite layup The setup for the composites modelling can be seen in the following figures:

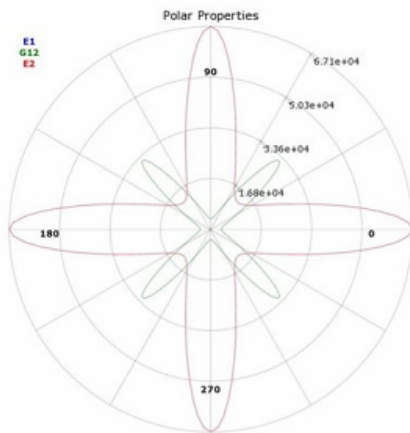


(a)

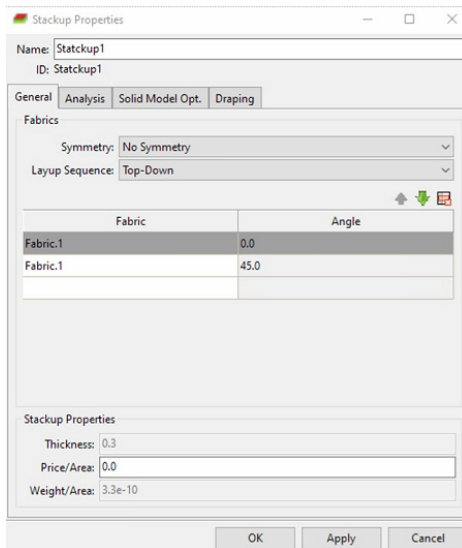


(b)

Figure 83: (a) Polar properties for the material, (b) Stackup properties defined.



(a)

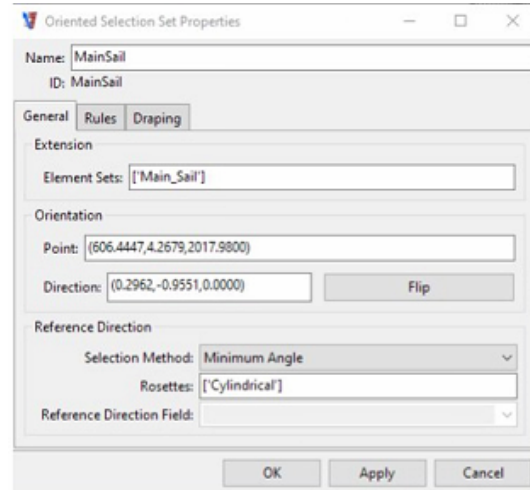


(b)

Figure 84: (a) Material properties defined, (b) Fabric properties defined.



(a)

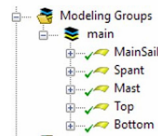


(b)

Figure 85: (a) Rosette definition, (b) Oriented Selection Set Properties.



(a)



(b)

Figure 86: (a) Material ply Properties, (b) Modeling groups.

B FEM Validation Setup in Abaqus

This section will follow all the steps necessary to set up the final FEA validation in Abaqus to validate the final sail assembly. The structure of this section will follow the work-tree in Abaqus, with the following points:

- Part
- Properties
 - Materials
 - Ribs
 - Mast
 - Main Sail
 - Glue
- Assembly
- Step
 - Static
 - Buckling
- Interactions
- Loads
 - Pressure loads @ 6.5 ms Wind Speed
 - Pressure loads @ 20 ms Wind Speed
- Mesh
 - Materials
 - Ribs
 - Mast
 - Main Sail
 - Glue

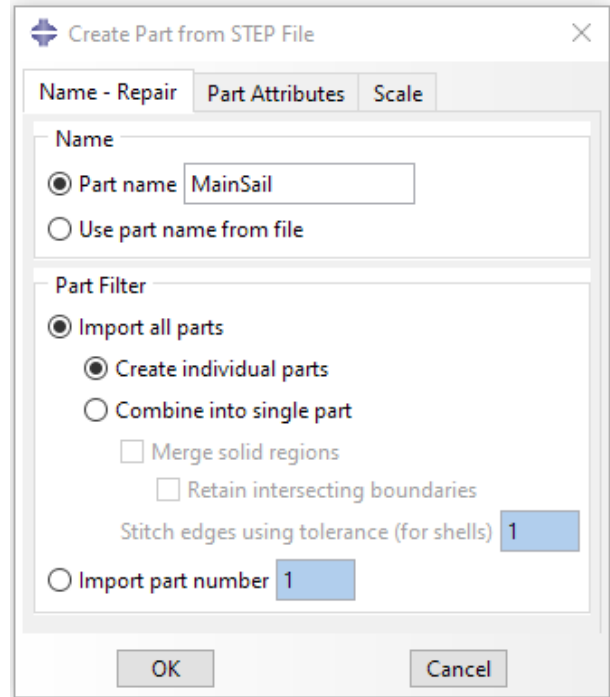


Figure 87

B.1 Part

All 3D modeling was done in SolidWorks and part geometry was imported (Figure 87 to Abaqus with Step file format. Part geometries is found in Figure 88.

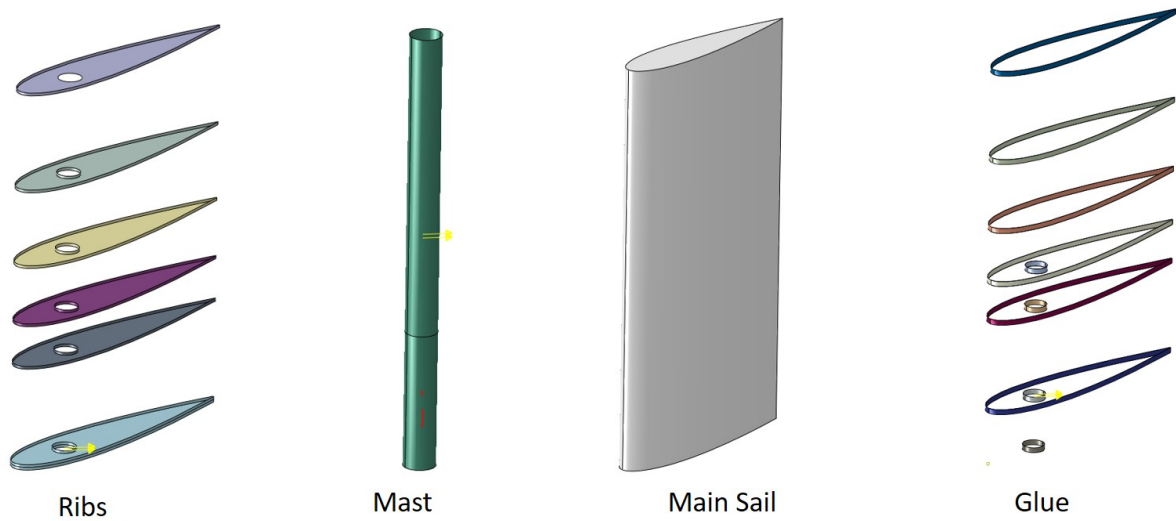
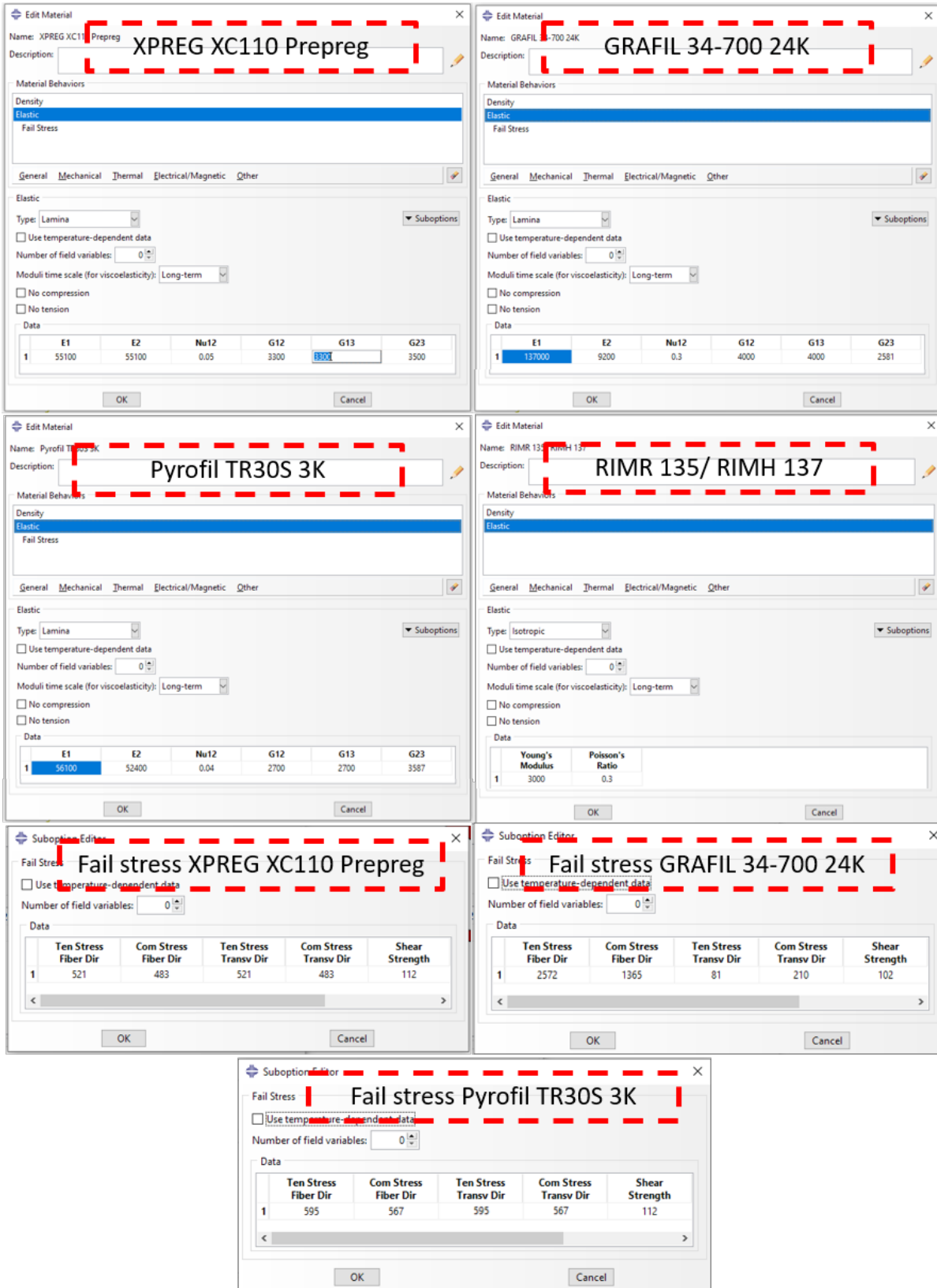


Figure 88

B.2 Properties

B.2.1 Materials Four materials were used in the validation: XPREG XC110 Prepreg, GRAFIL 34-700 24K , Pyrofil TR30S 3K and RIMR 135/ RIMH 137. All the materials were modeled as linear elastic, the epoxy as isotropic and the composites as lamina. The composites were defined with failure stress, to calculate Max Stress and Tsai Wu failure criterion. For material data see material data in Appendix I.3 - I.8. 89



92
Figure 89

B.2.2 Ribs, Mast and Main Sail Conventional shell were used to model composite ribs. The composite was modeled as a "Composite Layup" in Abaqus. Layup orientation was defined such that Z-direction is always normal to the surface. The main reference was set the X-axis defined by the local coordinate system illustrated in Figure 90. Layup for rib 1 is shown in Figure 91. The part global system is oriented 11 degree from the center line of the ribs, this is the reason way rotation angle is -11 and 34, and not 0 and 45. All ribs, main sail and mast were modeled with the same procedure as rib 1 explained above. For the mast, the reference direction will be along the axial direction of the tube.

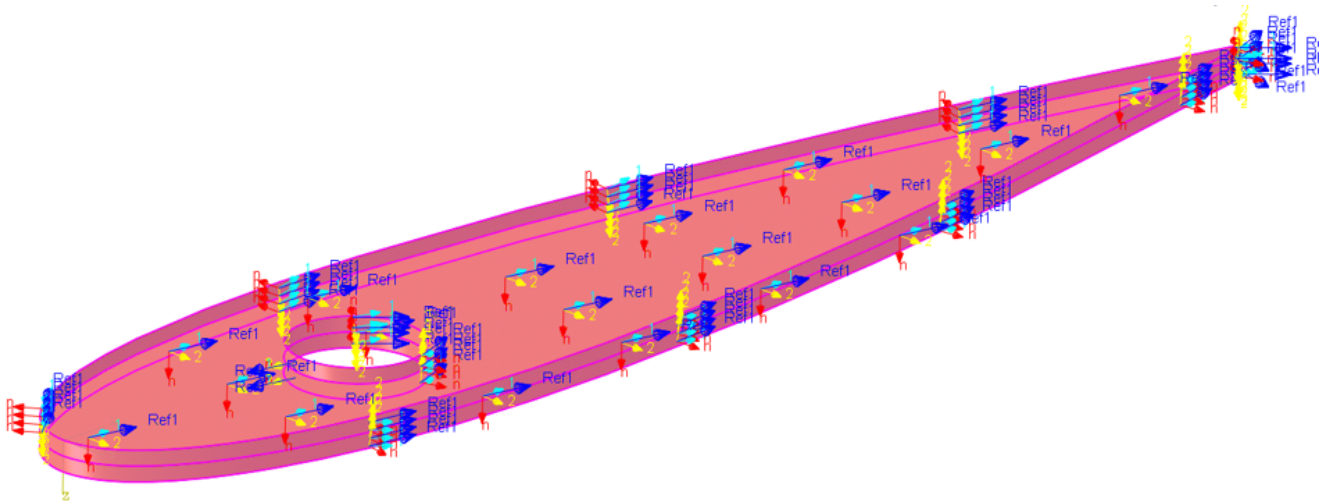


Figure 90

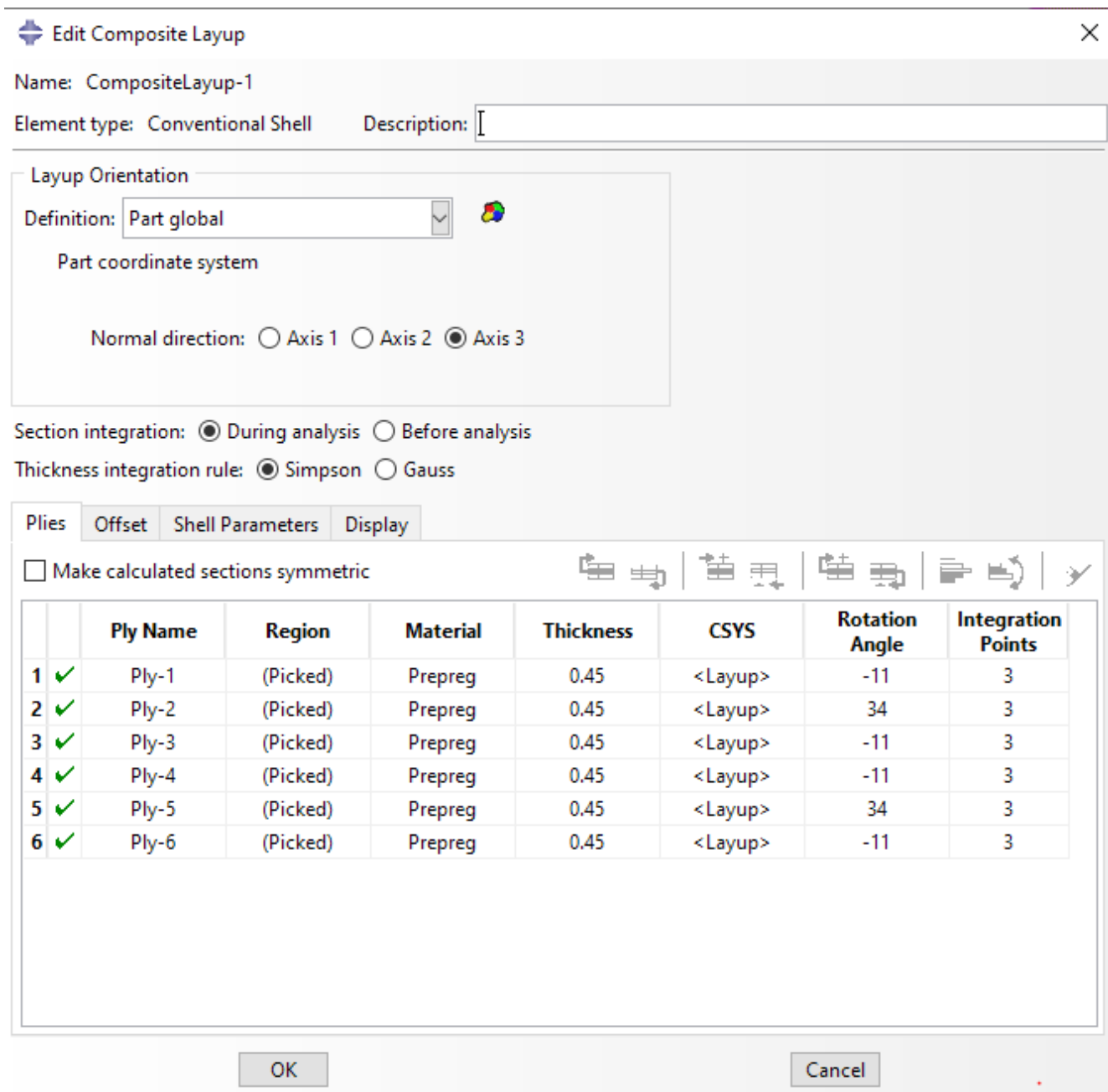


Figure 91

B.2.3 Glue The glue was modeled with a solid homogeneous section with RIMR 135/ RIMH 137 Epoxy as material. This is illustrated in Figure 92.

B.3 Assembly

All parts were imported with coordinate system according to the main assembly in SolidWorks. Importing parts including part coordinate system according to assembly eliminate the need for using assembly constraint in Abaqus. All parts were imported with dependent mesh (mesh on part). See Figure 93.

B.4 Step

B.4.1 Static For both of the wind load cases a static general step with default values were used.

B.4.2 Buckling For the buckling load case a buckle load step with the subspace solver was used. Abaqus have two solver for buckling; Subspace and Lanczos. Usually the Subspace solver is faster if number of requested eigenvalues is less than 20. For this analyse 6 eigenvalues were requested.

B.5 Interactions

B.5.1 Glued Connections The glued interfaces between mast, main sail and ribs were simplified to by a thin layer (0.15mm) between

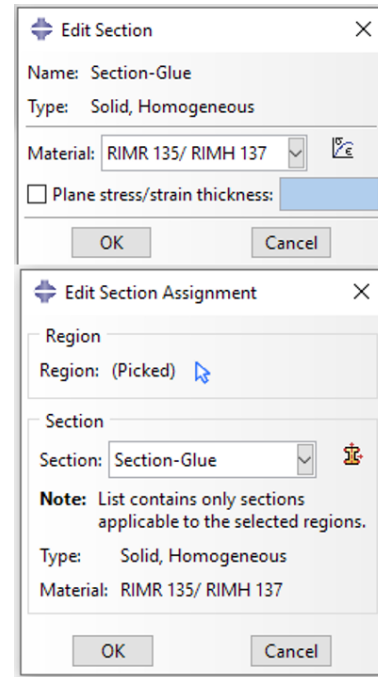


Figure 92

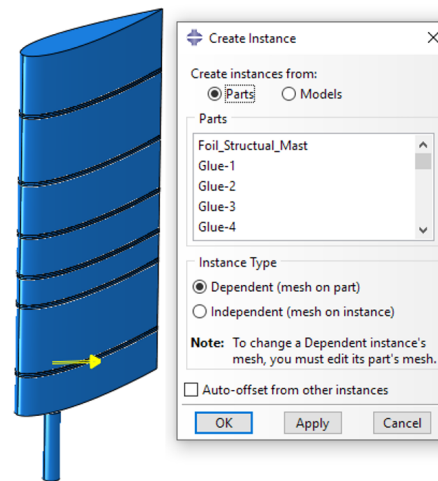


Figure 93

all connections. The glued regions were simplified by connecting these layers with a tie connector to the surrounding parts. Surface to surface contact was chosen and the coarser mesh as master (for most accurate result: Abaqus Documentation [19])

B.5.2 Mast Interface The mast interface was simplified with a kinematic coupling connected to reference point in the assumed center of the mast support interface. This was also used to retrieve the reaction forces and moments for mast support.

B.6 Loads

The pressure load from Ansys Fluent was imported into Abaqus through plotting pressure with respect to xy-values over the wingsail. Furthermore, a python script was made and used to estimate a polynomial regression function which was imported into Abaqus through analytical field (Figure 94. The python script can be seen in Appendix G.2. This process was used for both load cases:

- Pressure loads @ 6.5 ms Wind Speed
- Pressure loads @ 20 ms Wind Speed

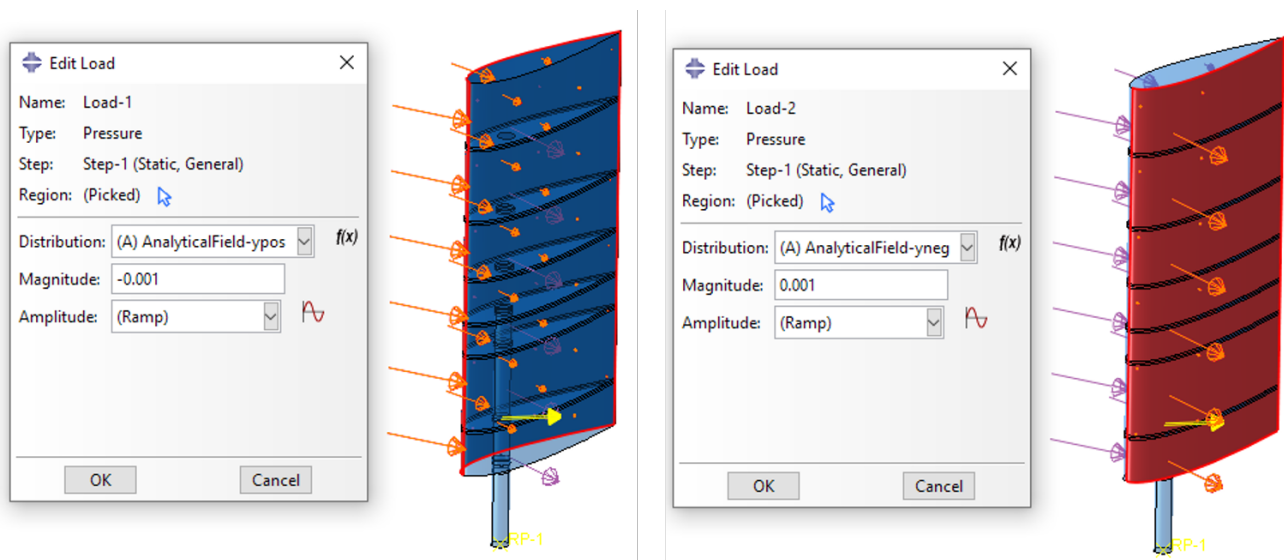


Figure 94

B.7 Mesh

B.7.1 Ribs The mesh for the ribs were made of 4-nodes doubly curved thin shell elements with reduces integration, hourglass control and finite membrane strains. The element shape is quad where mesh technique are partly Free and partly Sweep. For the Free technique Advancing front is used as algorithm. See Figure 95.

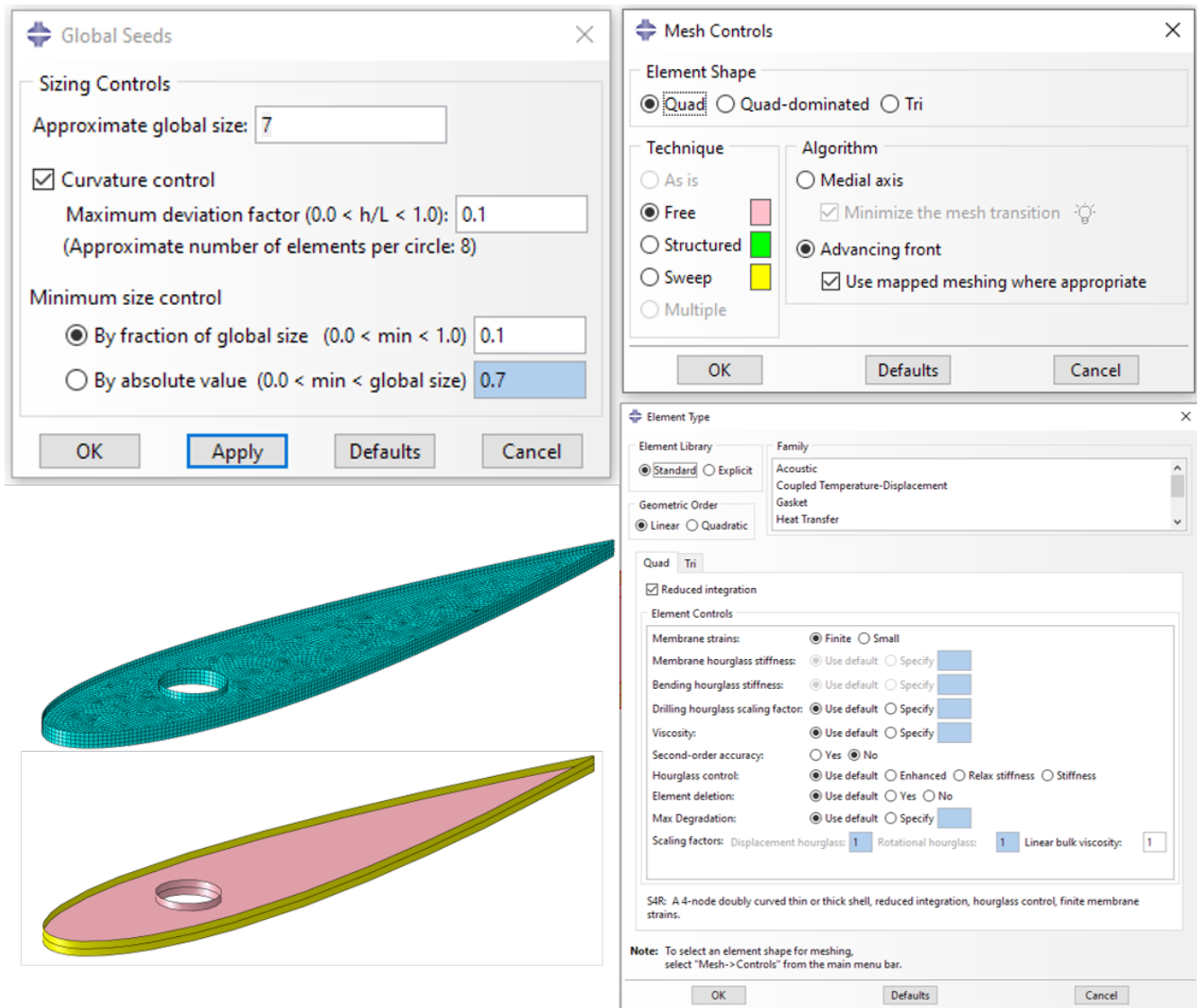


Figure 95

B.7.2 Mast Same mesh settings as used on ribs were applied on the mast except that the mesh technique was set to purely Structured. See Figure 96 for all settings.

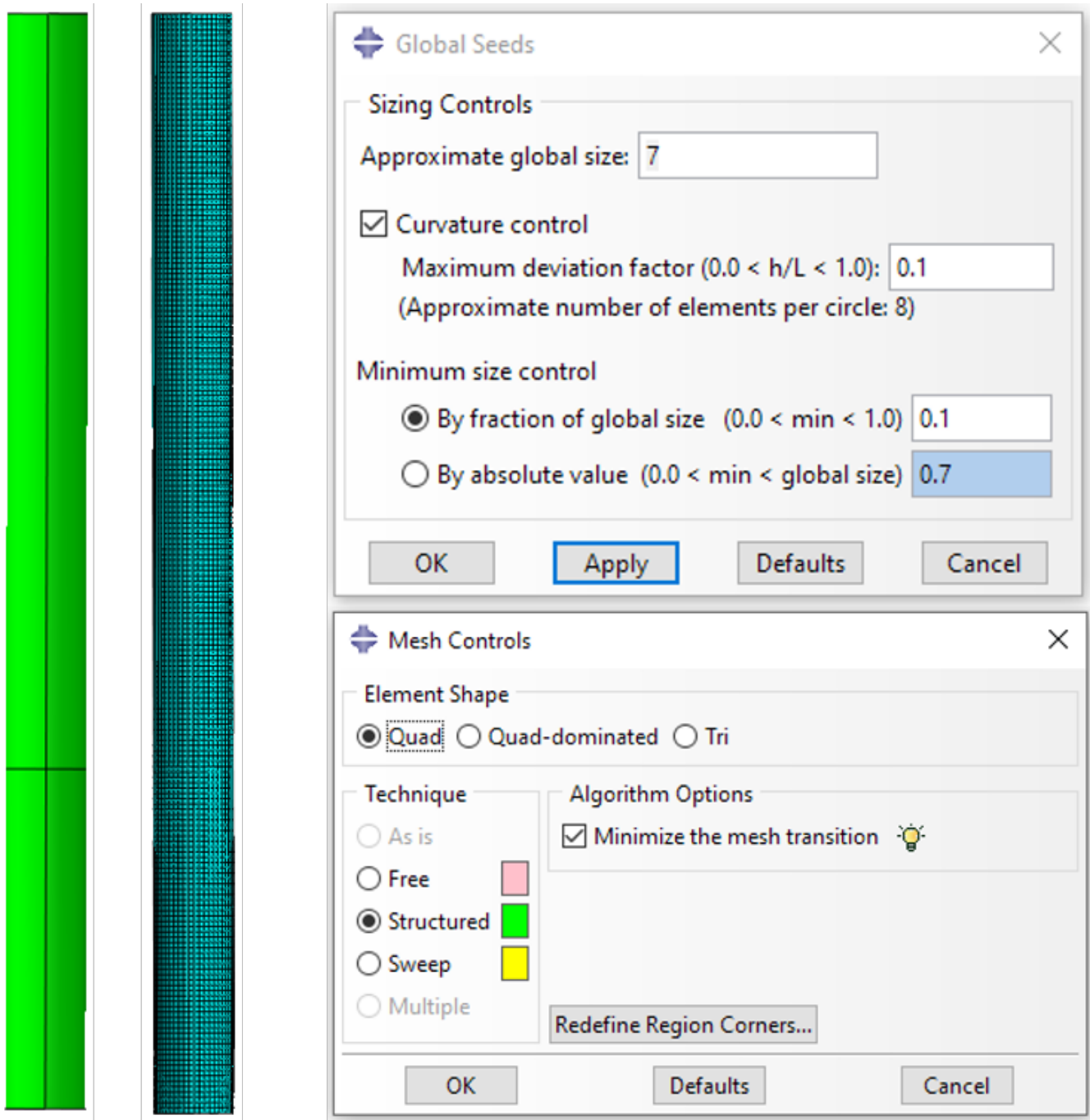


Figure 96

B.7.3 Main Sail Same mesh settings as used on ribs were applied on the mast except that the mesh technique was set to free with advancing front as algorithm. See Figure 97 for complete settings.

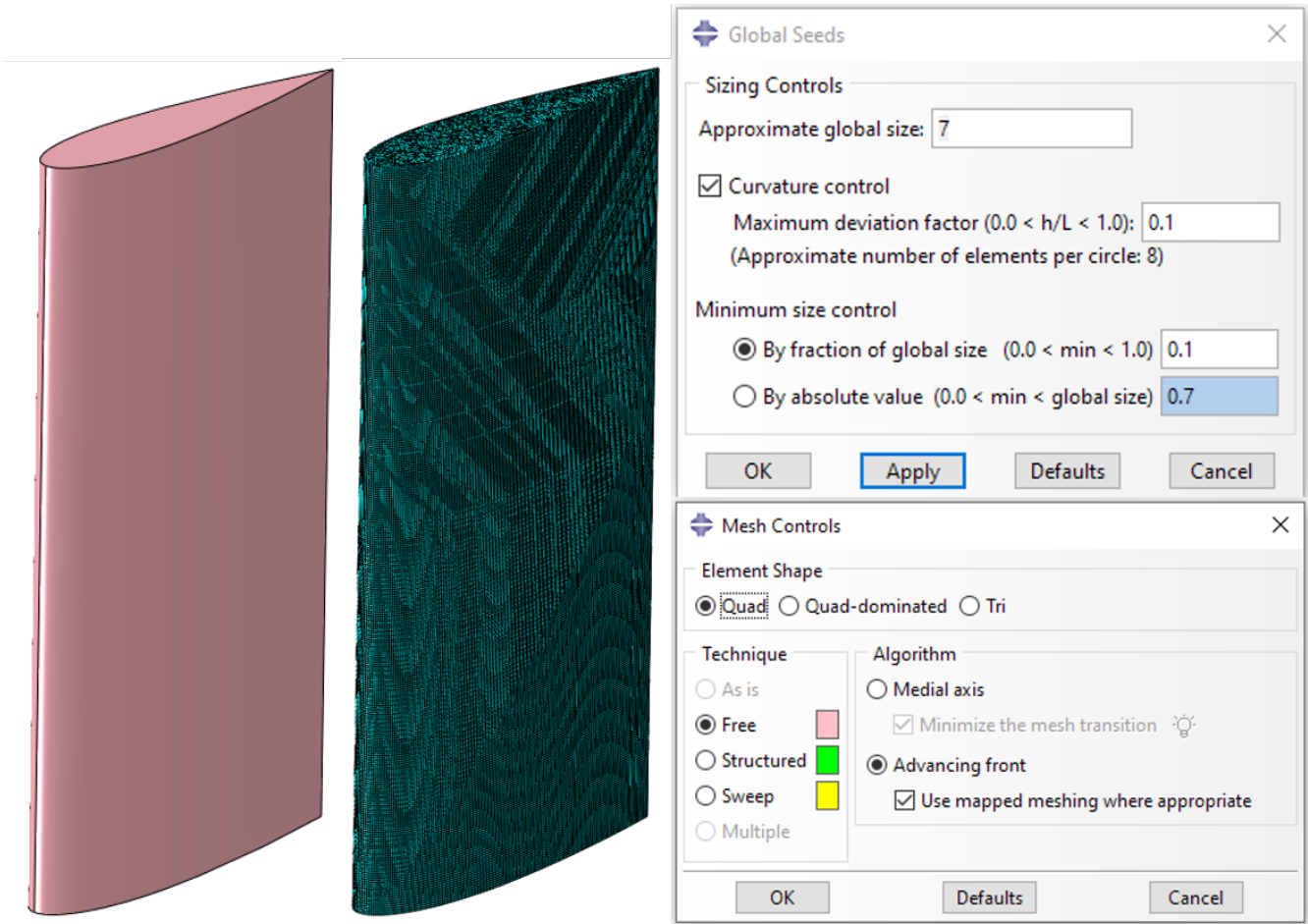


Figure 97

B.7.4 Glue Same mesh settings as used on ribs were applied on the glued connections except that the mesh technique was set to purely Structured.

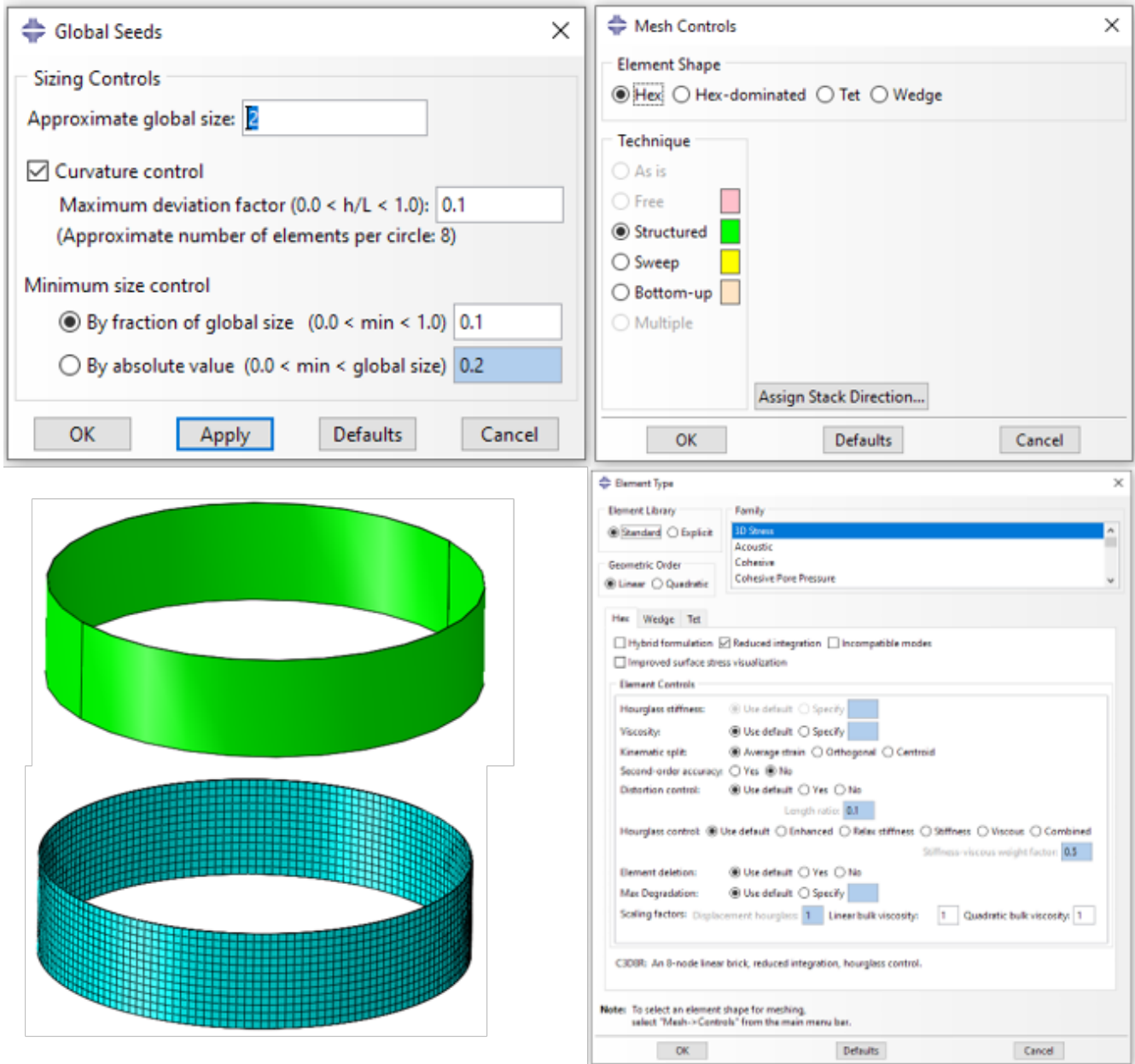
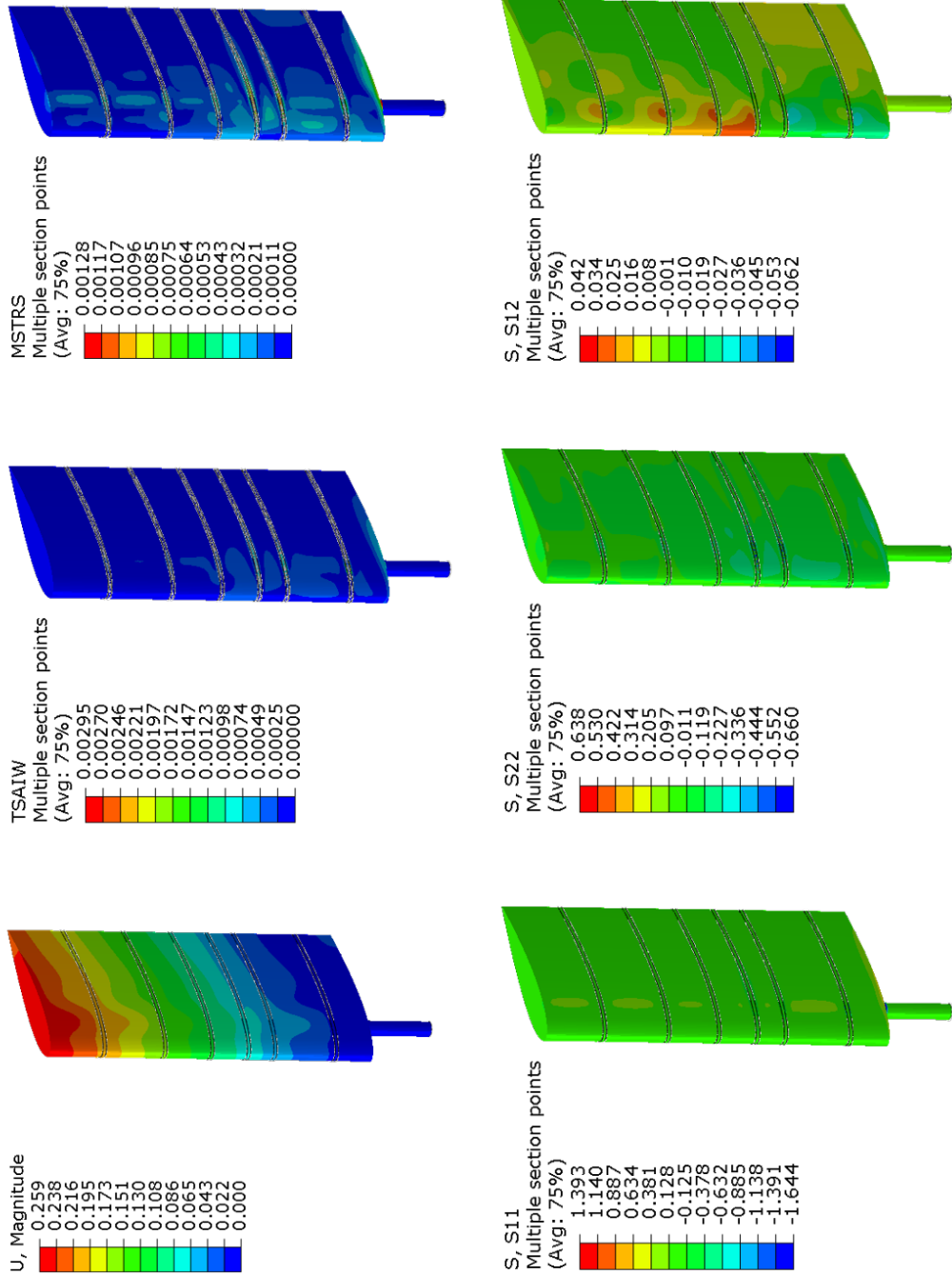


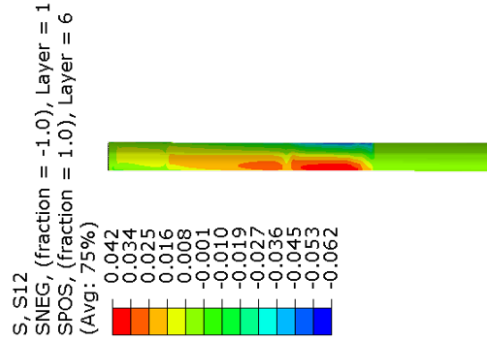
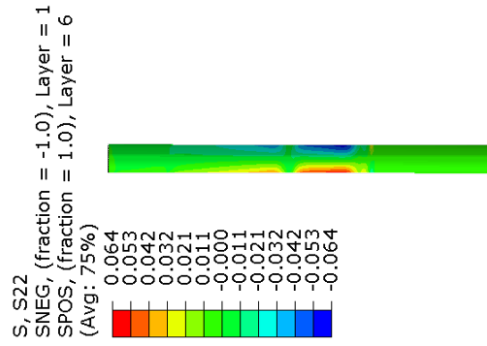
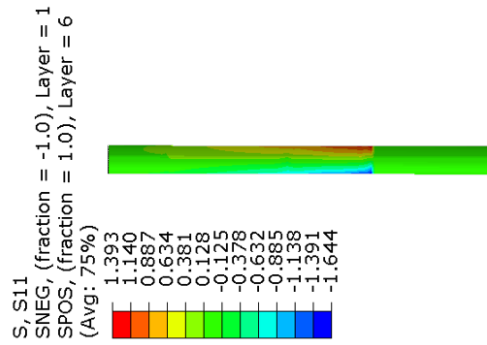
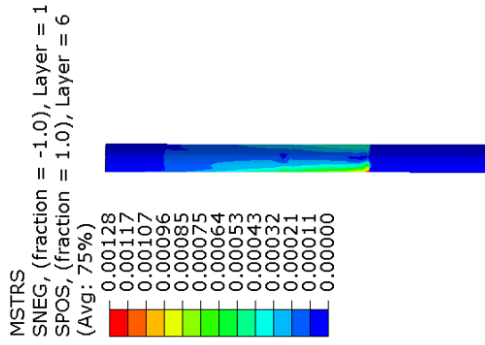
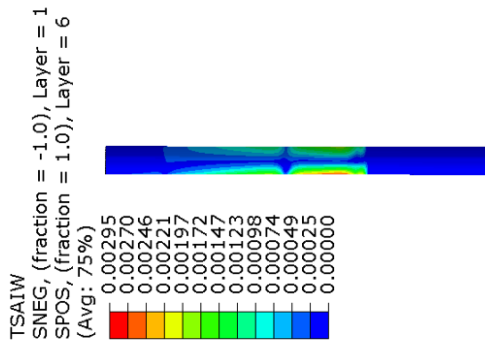
Figure 98

C FEM Validation Results from Abaqus

C.1 Global Result @ 6.5m/s Wind Speed

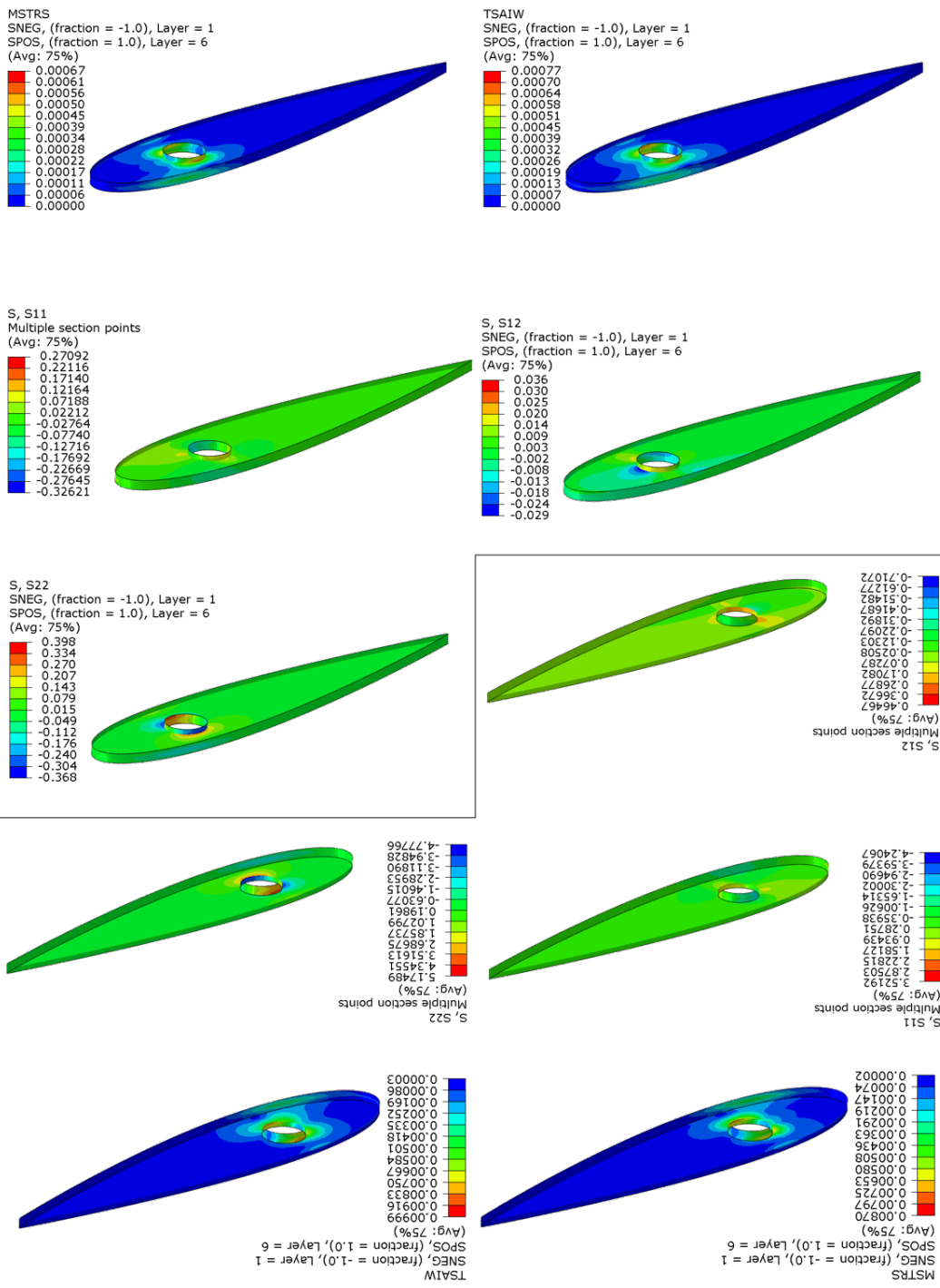


C.2 Mast Result @ 6.5m/s Wind Speed



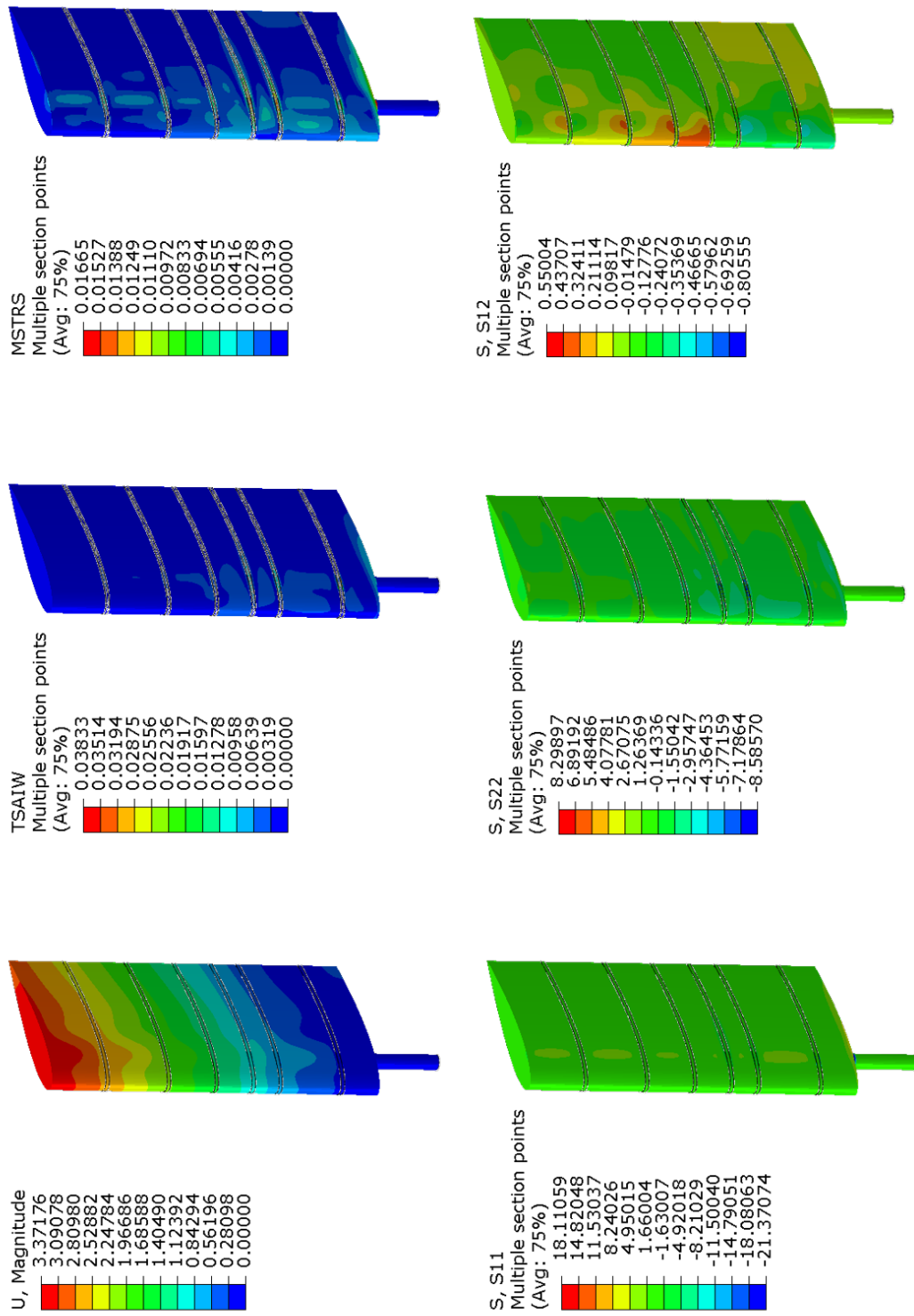
C.3 Spant Result @ 6.5m/s and 20m/s Wind Speed

6.5 m/s

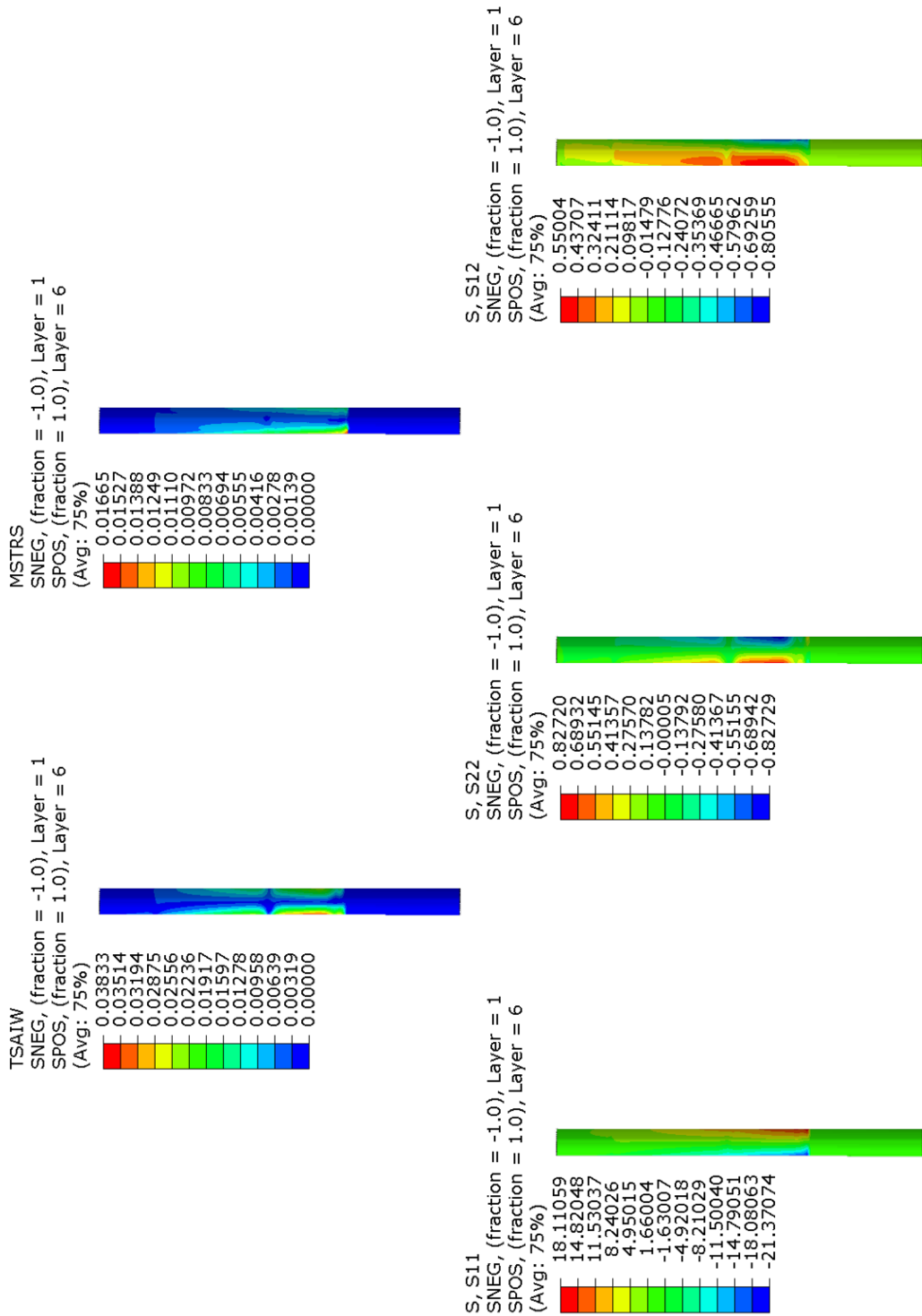


20 m/s

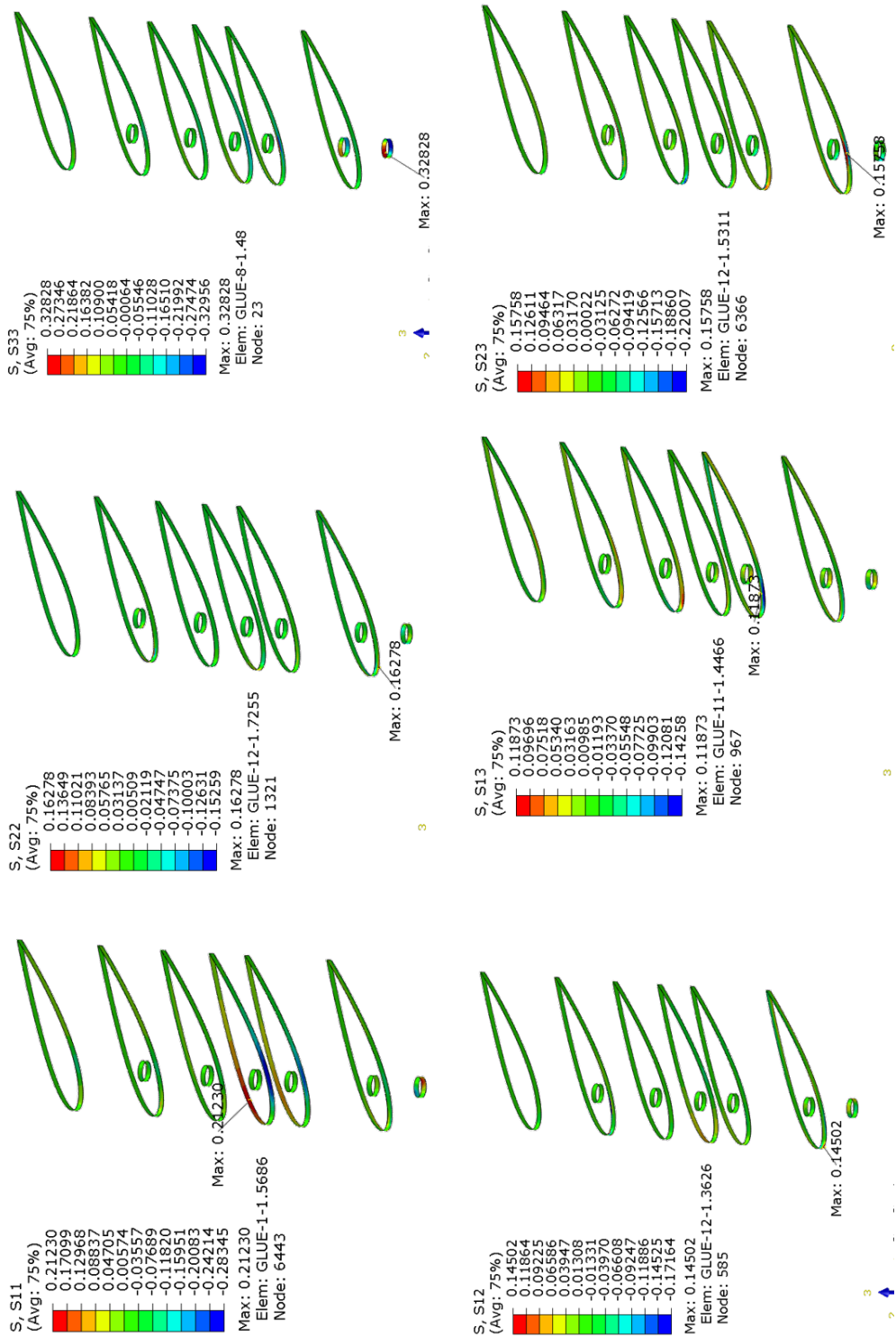
C.4 Global Result @ 20m/s Wind Speed



C.5 Mast Result @ 20m/s Wind Speed



C.6 Glue Result @ 20m/s Wind Speed



D Ansys Mechanical Additional Results

All the plots in this section are modeled at 6.5 m/s loadcase and AOA 11 °.

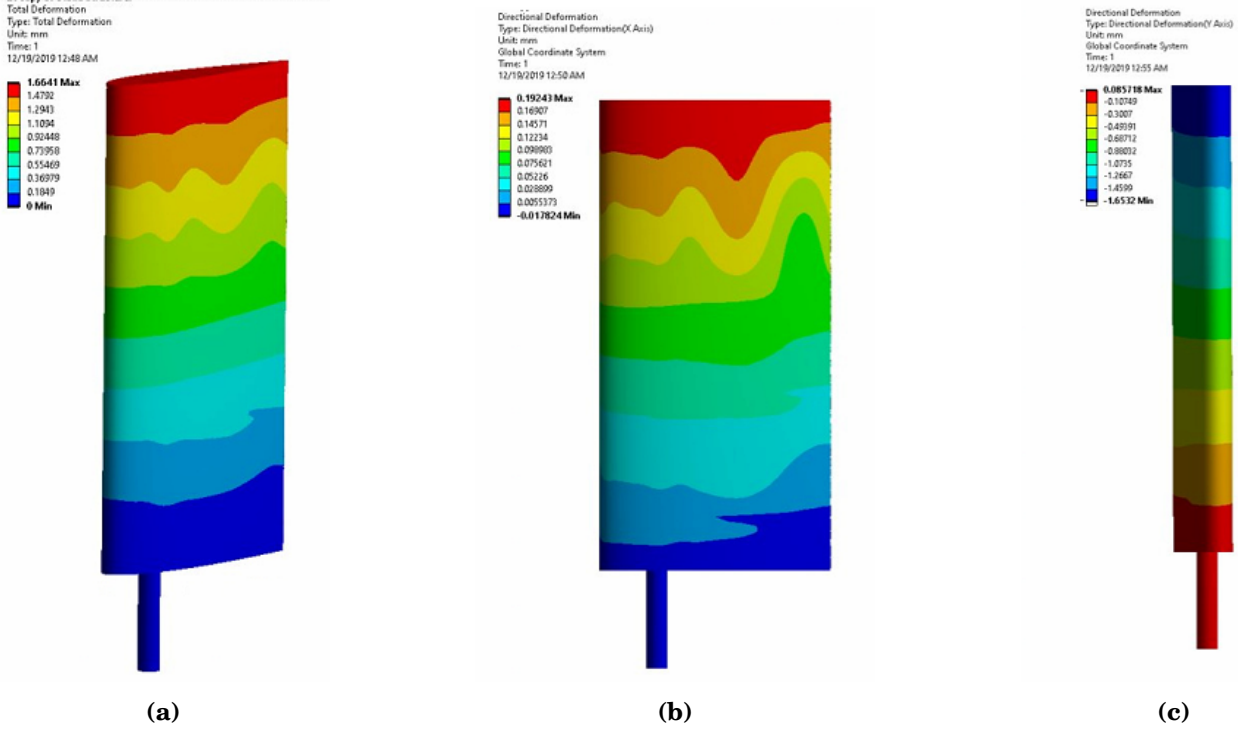


Figure 99: Validation results from Ansys for Candidate Point 1: (a) Total deformation (b) Total deformation in x-direction, (c) Total deformation in y-direction.

The normal stresses can be seen in Figure 100a, Figure 100b and Figure 100c.

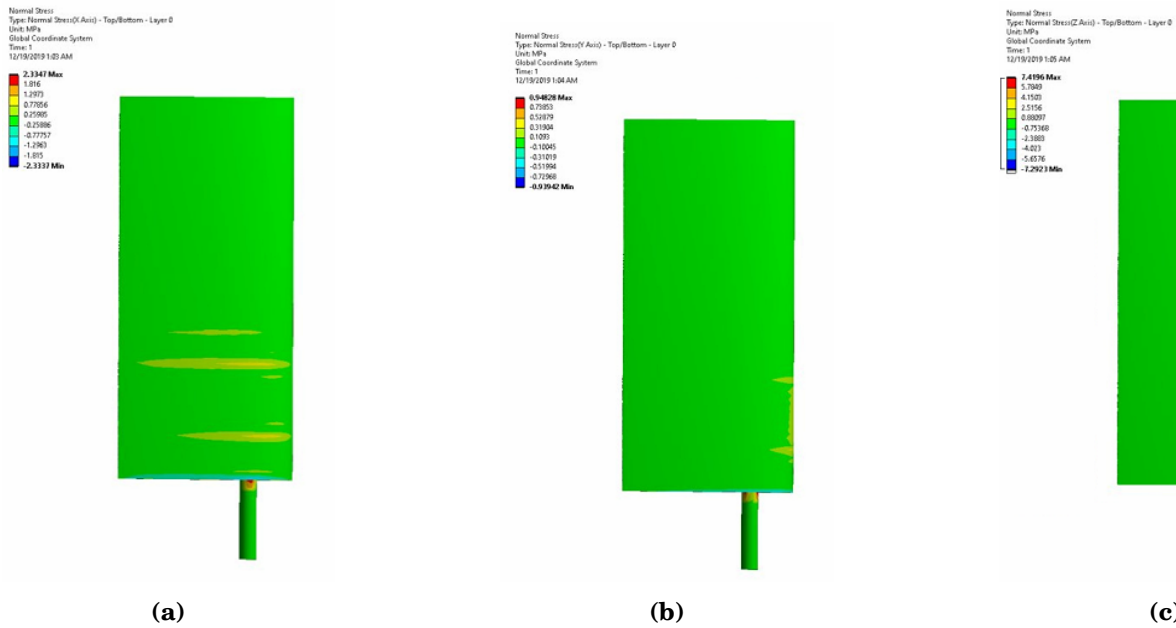


Figure 100: Validation results from Ansys for Candidate Point 1 (a) Principal stresses in x-direction, (b) Principal stresses in x-direction, (c) Principal stresses in z-direction.

Tsai-Wu and Max Stress is also evaluated, as seen in Figure 101a and Figure 101b.

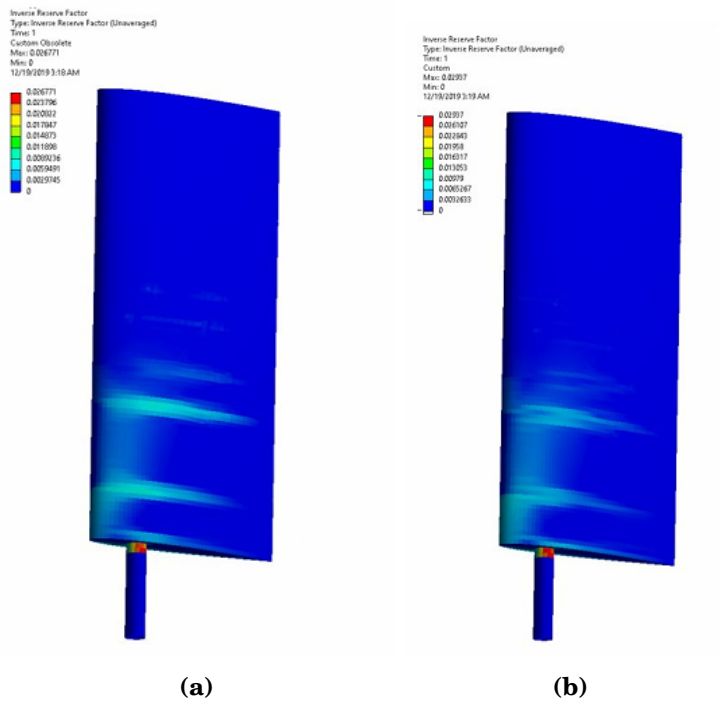


Figure 101: Validation results from Ansys for Candidate Point 1: (a) Tsai-wu failure criterion on the wingsail, (b) Maximum-stress for the chosen candidate.

E Material Data Test

Since engineering constants for lamina simulation in FEA are often difficult to find since there are numerous combinations of resin with the fibers, experimental tests are often the only way to find the right constants. In this project, most of the engineering data were estimated, but to get an idea of the data corresponded, some test specimens were tensile tested for the CFRP used on the mainsail and the ribs. All the specimens was tested according to ASTM E111-17.

E.1 Rib CFRP Specimen Preparation

10 sheets with dimension 300x300 mm of the same fiber that was used in the production of the ribs [I.6] was layered onto a cleaned and released thin steel plate. Same procedure with release, breather and vacuum bag was applied over the sheets with a vacuum hose attached from the outside of the bag. Vacuum was applied and cured according to the instructions of the CFRP [I.6]. After curing, the plate was demoulded before waterjetted to create 3 test specimens.

E.2 Mainsail CFRP Specimen Preparation

4 sheets of 300x300 mm of the same fabric that was used for casting the mainsail was layered onto a cleaned released thin steel plate, with resin [I.8] being brushed on the plate and between each layer. Thereafter, release film, breather and vacuum bag sealed with sealant tape and an vacuum hose was applied. Vacuum was applied through the vacuum hose and the bag was checked for leaks. Thereafter, the laminate was set to cure for 24 hours under vacuum and heating lamps, before it was demoulded and three test specimens was waterjetted from the laminate.

E.3 Strain Gauges

1-axis strain gauges was applied with glue in both longitudinal and transverse direction on the mid-part of each test specimen.

E.4 Tensile Test

The tensile test was done using a MTS Criterion Model 42 test machine. SiC mesh was placed onto the gripping surfaces, yet the specimens started slipping at around 500 N. Nevertheless, the test data accumulated provides enough information to determine the elastic modulus and poissons

ratio. After a preload of 50 N had been reached, a cross head speed of 2 mm/min was set. The results can be seen in Section E.5.

E.5 Results

In Figure 102, the stress vs strain for the tensile test can be seen. From this data, a mean Young's Modulus of 57928.4 MPa with a standard deviation of 2869.78 MPa and a mean Poisson's ratio of 0.05 with a standard deviation of 0.00198, was obtained, as presented in Table 19.

For Sample 2 in Figure 103, it can be seen that the readings of the transverse strain gauge almost does not change at all. It could be different causes for that; poor adhesive to the composite, poor wiring to the analog-to-digital converter (ADC), or defect strain gauge. This affects the calculation of the poisson's ratio, the affected reading is outlined in red in Table 19. For the analysis, the Youngs Modulus given in the datasheet was used, while the mean value from testing is 5 % higher than the typical value given by the supplier I.6, the values used in the analysis is in the conservative range.

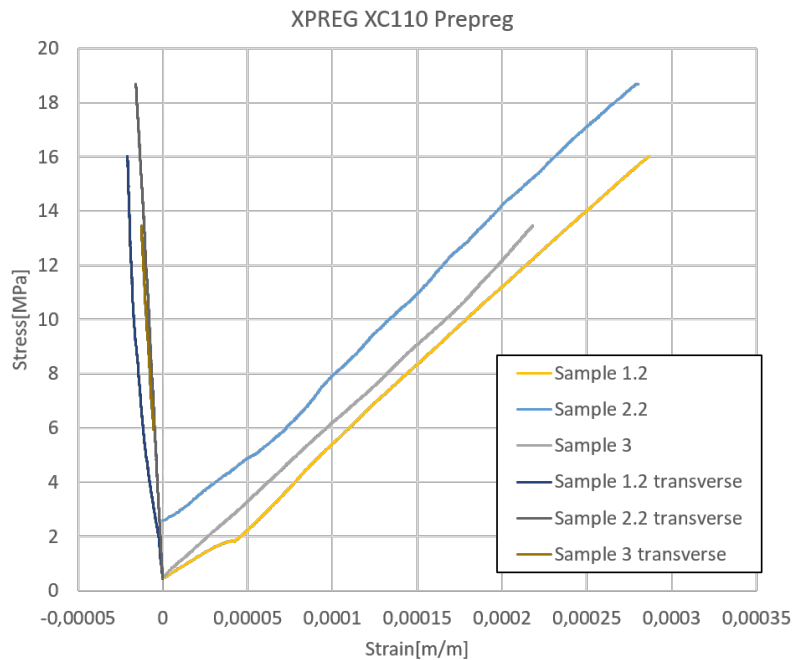


Figure 102: Material test for the XPREG XC110, showing stress vs strain.

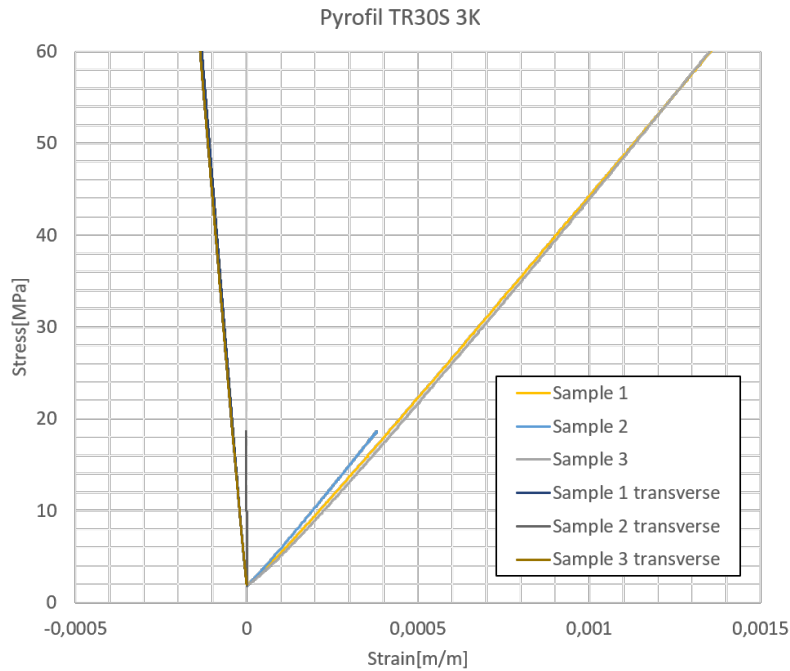


Figure 103: Material test for Pyrofil TR30S 3K, showing stress vs strain.

Table 19: Test results from the tensile tests

XPREG XC110 Prepreg					
Sample	1	2	3	Mean Value	Standard Deviation
Youngs Modulus [MPa]	56838.8	61858.9	55087.5	57928.4	2869.78
Poisson's ratio	0.049	0.053	0.052	0.05	0.00198
Pyrofil TR30S 3K					
Sample	1	2	3	Mean Value	Standard Deviation
Youngs Modulus [MPa]	44103.7	44201.4	42622.4	43642.5	722.41
Poisson's ratio	0.097	0.01	0.102	0.07	0.04

F Provided Data

In the composite research group, the following data was provided where G12, G13, G23 have been estimated based on typical values for a twill 2k Weave. This estimated were used in the final analysis.

Table 20: Provided data from research group

Prepreg	Reinforcement	E1	E2	v12	G12	G13	G23
XPREG XC110 416 g	Pyrofil TR50S HS Carbon 12k	58000	58000	0.05	3300	3300	3500
XPREG XC110 210 g	Pyrofil TR30S HS Carbon 3k	53000	53000	0.05	3300	3300	3500

G Scripts

All scripts are using Python Programming Language.

G.1 Abaqus Automatic Meshing Script

The following script was developed and used for meshing all parts in the model while doing mesh sensitivity analysis. Developed through the use of macros in Abaqus.

```
1 # -*- coding: mbcs -*-
2 # Do not delete the following import lines
3 from abaqus import *
4 from abaqusConstants import *
5 import __main__
6
7 from abaqus import getInput
8 import section
9 import regionToolset
10 import displayGroupMdbToolset as dgm
11 import part
12 import material
13 import assembly
14 import step
15 import interaction
16 import load
17 import mesh
18 import optimization
19 import job
20 import time
21 import sketch
22 import visualization
23 import xyPlot
24 import displayGroupOdbToolset as dgo
25 import connectorBehavior
```

```

26
27 meshList = [5.0]
28 meshList = getInput("Enter mesh Size:")
29 meshList = [float(i) for i in meshList.split(',') ]
30
31 onlyMesh = True
32 modelName='Model-1-20ms-Buckling'
33
34 for meshSize in meshList:
35     jobName = 'Sail_Mesh_buckling_{}_mum'.format(int(meshSize)*1000)
36     #Mesh Settings Mast
37     p = mdb.models[modelName].parts['Foil_Structual_Mast']
38     p.deleteMesh()
39     p = mdb.models[modelName].parts['Foil_Structual_Mast']
40     p.seedPart(size = meshSize, deviationFactor=0.1, minSizeFactor=0.1)
41     p = mdb.models[modelName].parts['Foil_Structual_Mast']
42     p.generateMesh()
43
44
45
46 #Mesh Settings Glue-1-
47 for i in range(1,14):
48     partName = 'Glue-{}'.format(str(i))
49     p = mdb.models[modelName].parts[partName]
50     session.viewports['Viewport: 1'].setValues(displayedObject=p)
51     p = mdb.models[modelName].parts[partName]
52     p.deleteMesh()
53     p = mdb.models[modelName].parts[partName]
54     p.seedPart(size = meshSize, deviationFactor=0.1, minSizeFactor=0.1)
55     p = mdb.models[modelName].parts[partName]
56     p.generateMesh()
57
58 #Mesh Settings MainSail
59 p = mdb.models[modelName].parts['mainsail']
60 session.viewports['Viewport: 1'].setValues(displayedObject=p)
61 p = mdb.models[modelName].parts['mainsail']
62 p.deleteMesh()
63 p = mdb.models[modelName].parts['mainsail']
64 p.seedPart(size = meshSize, deviationFactor=0.1, minSizeFactor=0.1)

```

```

65 p = mdb.models[modelName].parts['mainsail']
66 p.generateMesh()
67
68
69 #Mesh Settings Spant
70 for i in range(1,7):
71     partName = 'spant{}'.format(str(i))
72     p = mdb.models[modelName].parts[partName]
73     session.viewports['Viewport: 1'].setValues(displayedObject=p)
74     p = mdb.models[modelName].parts[partName]
75     p.deleteMesh()
76     p = mdb.models[modelName].parts[partName]
77     p.seedPart(size = meshSize, deviationFactor=0.1, minSizeFactor=0.1)
78     p = mdb.models[modelName].parts[partName]
79     p.generateMesh()
80
81
82
83
84 mdb.Job(name=jobName, model=modelName, description='', type=ANALYSIS,
85         atTime=None, waitMinutes=0, waitHours=0, queue=None, memory=90,
86         memoryUnits=PERCENTAGE, getMemoryFromAnalysis=True,
87         explicitPrecision=SINGLE, nodalOutputPrecision=SINGLE, echoPrint=OFF,
88         modelPrint=OFF, contactPrint=OFF, historyPrint=OFF, userSubroutine='',
89         scratch='D:\\Scratch', resultsFormat=ODB, multiprocessingMode=DEFAULT,
90         numCpus=4,
91         numDomains=4, numGPUs=1)
92 time.sleep(5)
93
94 #if onlyMesh == False or len(meshList)>1:
95     # mdb.jobs[jobName].submit(consistencyChecking=OFF)
96
97 status = False
98 currStat = mdb.jobs[jobName].status
99 print(currStat)
100 # while status == False:
101     # time.sleep(15)
102     # currStat = mdb.jobs[jobName].status
103     # print(status)

```

```
103 # print(currStat)
104 # if currStat == 'ABORTED' or currStat == 'COMPLETED':
105     # status = True
```

G.2 Polynomial Regression Python Script

```
1 import numpy as np
2 import pandas as pd
3 import matplotlib.pyplot as plt
4 from sklearn.metrics import r2_score
5
6
7 data = pd.read_csv('pressureData.csv',delimiter=';')
8
9
10 x = data.x.values.astype(float)*1000
11 y = data.y.values.astype(float)*1000
12 p = data.p.values.astype(float)/1000000.
13
14 def wingLine(x):
15     y = x*np.tan(np.pi*11/180.)
16     return y
17
18 # Sortdata belonging to y+
19
20 x_p = []
21 y_p = []
22 p_p = []
23
24 x_n = []
25 y_n = []
26 p_n = []
27
28 for i in range(0,len(x),1):
29     if wingLine(x[i]) < y[i]:
30         x_p = x_p + [x[i]]
31         y_p = y_p + [y[i]]
32         p_p = p_p + [p[i]]
33     elif wingLine(x[i]) > y[i]:
34         x_n = x_n + [x[i]]
35         y_n = y_n + [y[i]]
36         p_n = p_n + [p[i]]
37
38
```

```

39 #Visualisation and curve-fitting
40 plt.figure(1)
41
42 plt.plot(x_p,p_p,'.')
43 plt.xlabel('Position [mm]')
44 plt.ylabel('Pressure [MPa]')
45
46 pp = 18
47 mymodel_p = np.poly1d(np.polyfit(x_p,p_p, pp))
48
49 myline = np.linspace(0, 1190, 1000)
50
51 plt.plot(myline, mymodel_p(myline))
52 print(r2_score(p_p, mymodel_p(x_p)))
53
54 plt.legend(['Pressure data Ansys Fluent',f'Fitted Curve: R\u00b2 Score {
    r2_score(p_p, mymodel_p(x_p)):0.3f}'])
55
56
57 plt.figure(2)
58 plt.plot(x_n,p_n,'.')
59 plt.xlabel('Position [mm]')
60 plt.ylabel('Pressure [MPa]')
61
62 pn=12
63 mymodel_n = np.poly1d(np.polyfit(x_n,p_n, pn))
64
65 myline = np.linspace(0, 1190, 1000)
66
67 plt.plot(myline, mymodel_n(myline))
68 print(r2_score(p_n, mymodel_n(x_n)))
69 plt.legend(['Pressure data Ansys Fluent',f'Fitted Curve: R\u00b2 Score {
    r2_score(p_n, mymodel_n(x_n)):0.3f}'])
70
71
72
73 #Writing analytical field for Abaqus
74 abal = ''
75 nn = pp

```

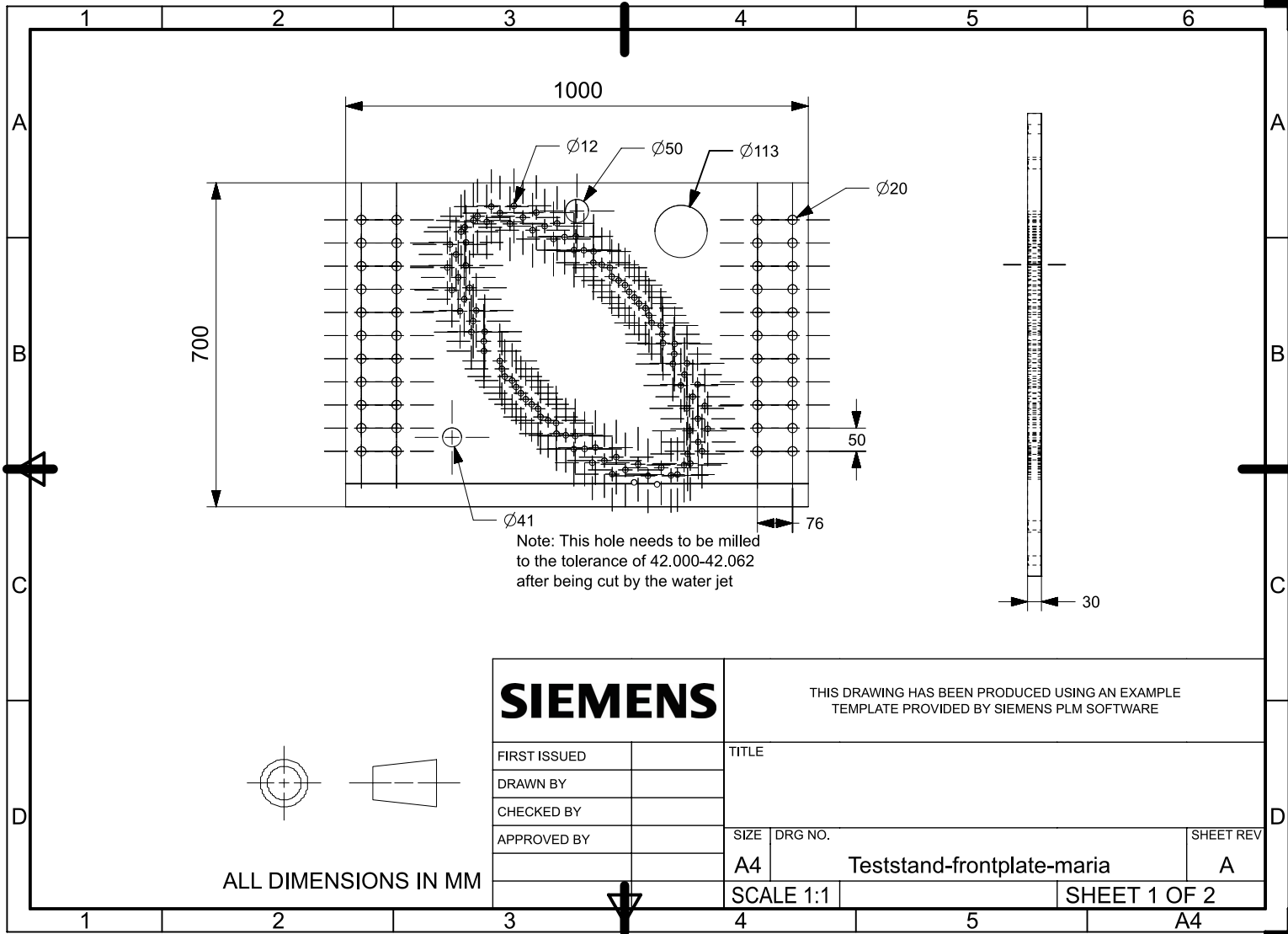
```

76
77 for i in mymodel_p:
78     if i > 0:
79         sp = '+'
80     else :
81         sp = ''
82     a1temp = f'{sp}{i}*pow( X, {nn} )'
83     aba1 = aba1+a1temp
84     nn = nn-1
85
86
87 print('Analytical Pressure field 1: '+aba1)
88
89 aba2 = ''
90 nn = pn
91
92 for i in mymodel_n:
93     if i > 0:
94         sp = '+'
95     else :
96         sp = ''
97     a2temp = f'{sp}{i}*pow( X, {nn} )'
98     aba2 = aba2+a2temp
99     nn = nn-1
100
101
102 print('Analytical Pressure field 2: '+aba2)

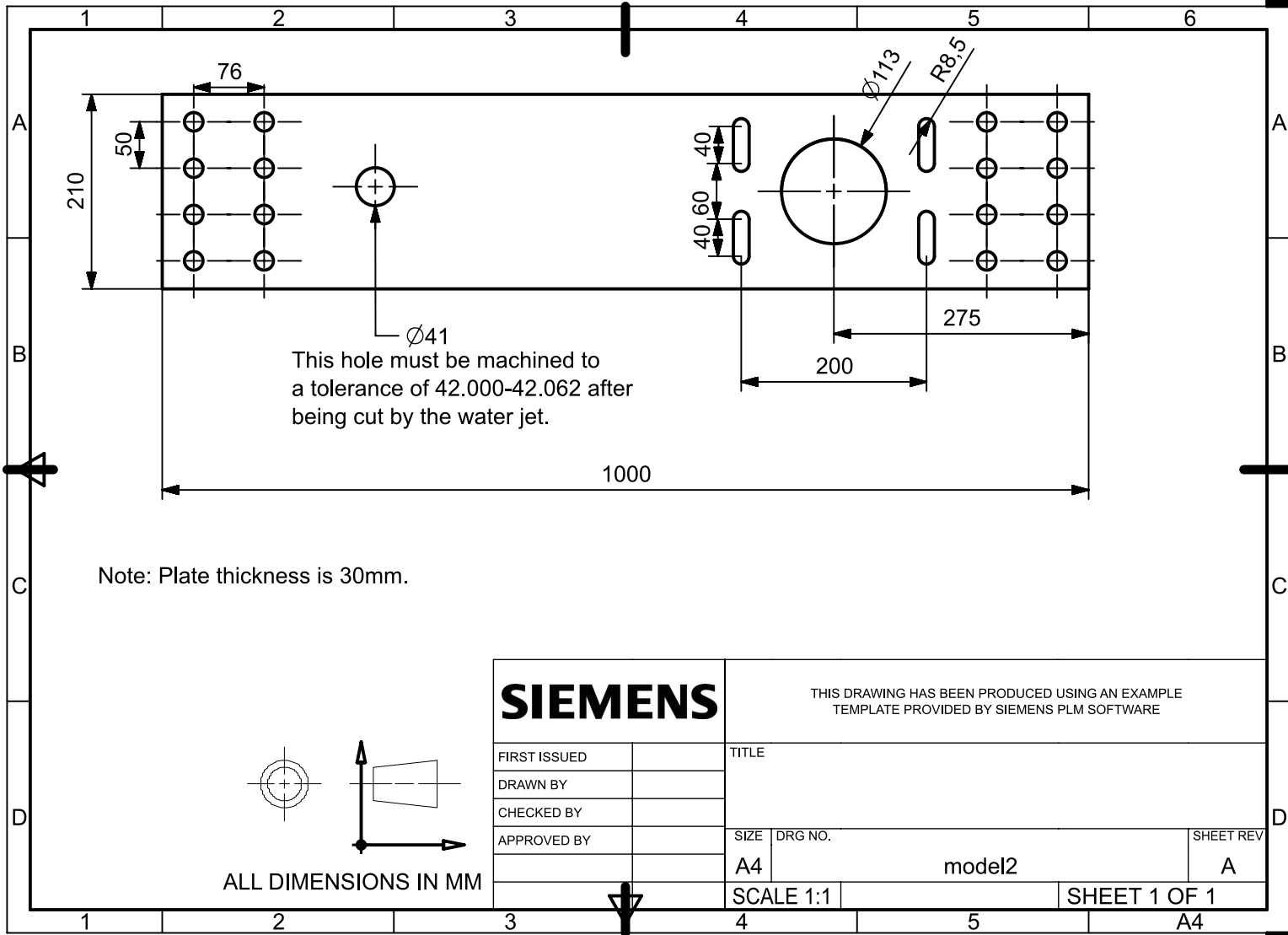
```

H Machine Drawings for Testrig

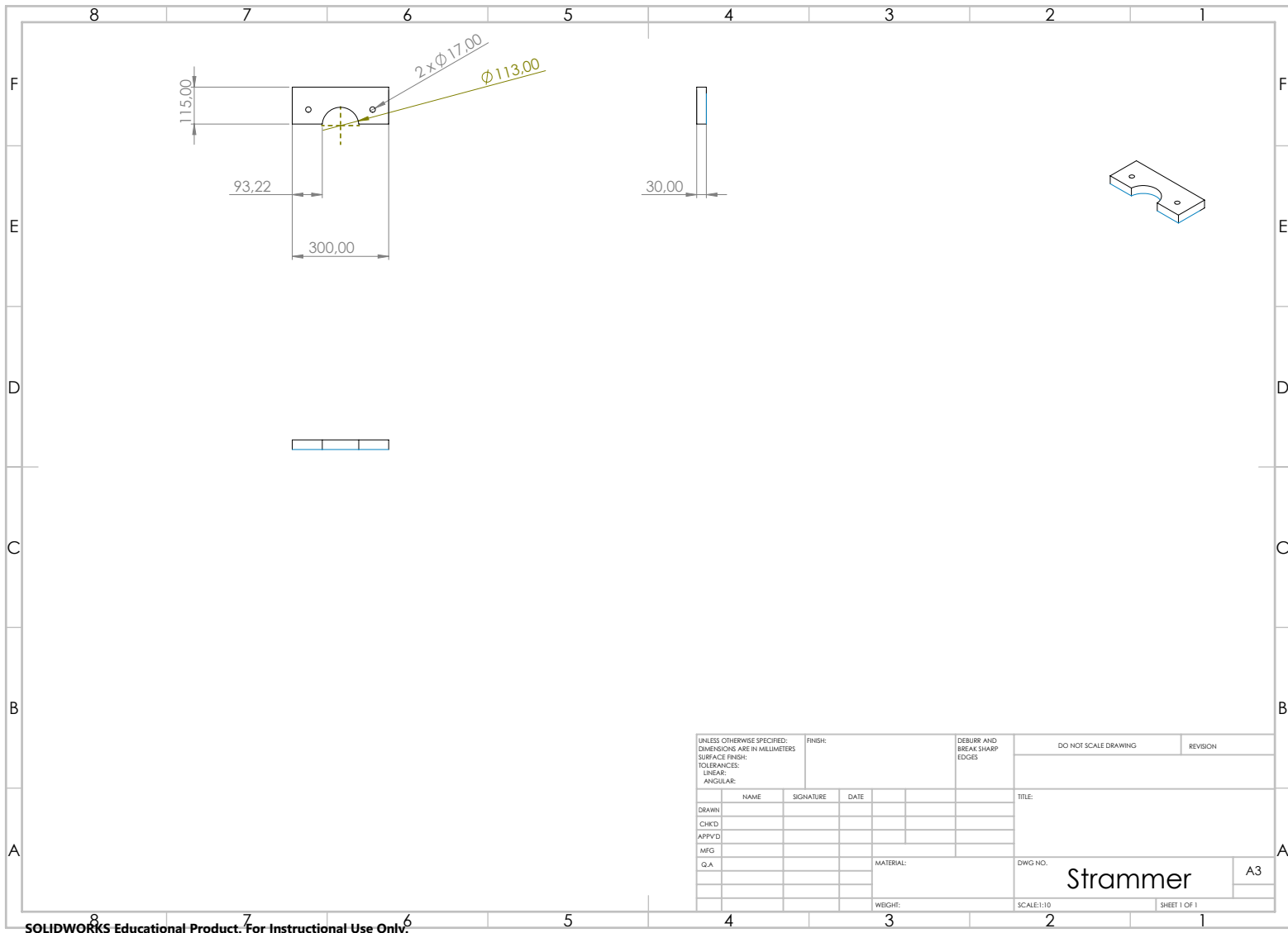
H.1 Testrig Frontplate



H.2 Testrig Backplate



H.3 Testrig Strammer



UNLESS OTHERWISE SPECIFIED: DIMENSIONS ARE IN MILLIMETERS SURFACE FINISH: TOLERANCES: LINEAR: ANGULAR:			FINISH:	DEBURR AND BREAK SHARP EDGES	DO NOT SCALE DRAWING	REVISION
DRAWN:	NAME	SIGNATURE	DATE		TITLE:	
CHECKED:						
APPROVED:						
MFG:				MATERIAL:	DWG. NO.	Strammer
Q.A.						
				WEIGHT:	SCALE: 1:10	A3
						SHEET 1 OF 1

SOLIDWORKS Educational Product. For Instructional Use Only.

I Datasheets

I.1 Cascol Indoor 3304



Erstatter: 2003-07-29

Dato: 2012-01-24

Cascol Indoor 3304



- Snekker- og sløydlimet
- Lang lagringstid
- Kort presstid

Cascol Indoor er et dispersjonslim til treliminger innendørs, ved for eksempel fugeliming og monterings-arbeider av møbler og andre trearbeider. Ikke til bærende konstruksjoner.

TEKNISKE DATA

Produkttype:	Dispersjonslim på PVAC Basis
Emballasje:	100 ml, 300 ml, 750 ml, 5 l kanne, 5 l spann
Farge:	Hvit, fargeløs når herdet
Løsningsmiddel:	Vann
Tørstoff:	47 %
Konsistens:	Tyktflytende
Densitet:	1080 kg/m ³
Ph:	5-7
Viskositet:	8000-16000 mPas, Brookfield RVT, sp. 6; 20 rpm, 25°C
Monteringstid:	0-10 min.
Fukttinnhold i materialer:	Anbefalt mellom 7-10 % + 10°C-+70°C
Påføringstemperatur:	Klasse D2
Fuktbestandighet:	600-200 g/m ² , på hardtre og eksotiske treslag anbefales det å lime begge flater.
Forbruk:	Minst 5 min. Presstrykket kan løsnes etter 10-70 min. ved + 20°C. Dersom limfugen varmes opp kortes presstiden.
Presstid:	36 mndr. i uåpnet emballasje. Oppbevares svalt. Bør omrøres godt før bruk ved lengre lagringstid.
Oppbevaring:	

FORBEHANDLING

Underlaget skal være rent, tørt, mest mulig nybearbeidet og fritt for løse partikler. Best resultat oppnås med nyslippede eller nyhøvlede materialer.

PÅFØRING

Påføres direkte fra limflasken, med tannet sparkel med rull/pensel eller mekanisk limspreder. En eller begge flatene påføres et jevnt sjikt med lim. Sammenføyning kan skje umiddelbart. Ved liming av harde materialer, og materialer som er vanskelige å lime, for eksempel teak, skal limet påføres på begge flater. Limet må alltid kjennes klebrig ved sammenføyning. Benytt ikke redskap av jern, da misfarging kan forekomme. Emner i eik kan reagere med komponentene i limet som kan gi misfarging. Vi anbefaler en pre-test ved liming av eik.

RENGJØRING

Generelt bør god renslighet overholdes. Lim på huden fjernes med tørr klut, og vask med såpe og vann. Verktøy rengjøres med vann før det er herdet. Herdet lim fjernes med Casco Limvask eller rødsprit.

A BRAND FROM
AkzoNobel



Sid. 2/2

HELSE OG MILJØ

Brannfare: Ingen
Helsefare: Produktet vurderes ikke
merkepliktig
Ytterligere info: Se Sikkerhetsdatablad

FDV

Ikke aktuelt, gjelder kun overflate-
Produkter.

Våre opplysninger er basert på laboratorieprøver og praktisk erfaring, og kan som sådan betraktes som veiledning i forbindelse med valg av produkt og arbeidsmetode. Ettersom brukerens arbeidsforhold ligger utenfor vår kontroll, påtar vi oss ikke noe ansvar for resultatene. Vårt ansvar dekker ute-lukkende personskade eller skade som faktisk har blitt bevist etter feil og mangler i ett av produktene produsert av oss.

Sertifisert iht.:



Akzo Nobel Coatings AS
Postadresse:
Postboks 565,
1411 KOLBOTN
Tlf.: +47 66 81 94 00
Fax +47 66 81 94 51
Web: www.casco.com

A BRAND FROM
AkzoNobel

I.2 Medium-Density Fiberboard

FIBRANOR TS / FIBRAPAN TS - HIGH PERFORMANCE MDF TS



FIBRANOR TS / FIBRAPAN TS - HIGH PERFORMANCE MDF TS

[Abajo /
Down](#)

TECHNICAL DATA-AVERAGE VALUES REVISION:02.01.2006

TEST METHOD	PROPERTIES	UNITS	THICKNESSES mm		
			2,5/4	>4/6	>6/8
EN 323	DENSITY (*)	Kg/m ³	820	810	800
EN 319	INTERNAL BOND	N/mm ²	1.3	1.2	1.1
EN 310	BENDING STRENGTH	N/mm ²	40	40	40
EN 310	MODULUS OF ELASTICITY	N/mm ²	2.700	2700	2.500
EN 317	THICKNESS SWELLING 24 HOURS	%	25	20	17
EN 322	MOISTURE CONTENT	%	7+/-2	7+/-2	7+/-2
EN 318	DIMENSIONAL MOVEMENT Length/ width	%	0.4	0.4	0.4
EN 318	DIMENSIONAL MOVEMENT Thickness	%	10	10	6

TOLERANCE ON NOMINAL DIMENSIONS

EN 324-1	Thickness	MM	+/-0.15
EN 324-1	Length/width	MM	+/-2 mm/m. max +/-5 mm.
EN 324-2	Squareness	MM	+/-2 mm/m.
EN 324-2	Edge straightness	MM	+/-1.5 mm/m.
EN 311	SURFACE SOUNDNESS	N/mm ²	1.2
ISO 3340	GRIT CONTENT	%Weight	Max. 0.05
EN 382-1	SURFACE ABSORPTION	MM	> 150 mm. (both faces)
	DENSIDTY PROFILE	%	>90

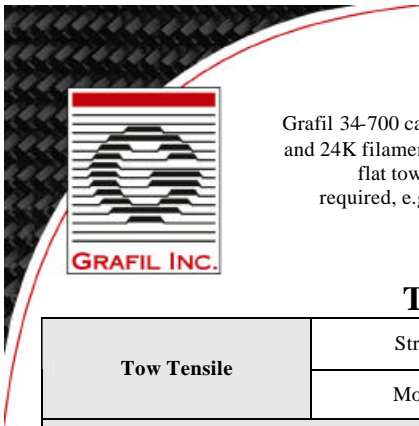
(*) Values to be considered as a rough guide

FIBRANOR TS/FIBRAPAN TS satisfies E1 CLASS requirements defined in the European Standard EN 622-1 when analysed according to EN 120 standard.



[Arriba / Up](#)

I.3 GRAFIL 34-700 Filament Winding Fiber



GRAFIL 34-700

Grafil 34-700 carbon fiber is a continuous, high strength, PAN based fiber. It is available in 12K and 24K filament count tows. They can be supplied in either round tow or flat tow formats. The flat tow (designated by 'WD') is the ideal fiber to use in applications where spreading is required, e.g., tape production. The round tow is used in applications where spreading is not necessarily required, e.g., braiding and weaving.

Typical Fiber Properties

Tow Tensile	Strength	700 ksi 4830 MPa	SRM 16
	Modulus	34 msi 234 GPa	
Typical Density		0.065 lb.in ³ 1.80 g/cm ³	SRM 15
Typical Yield	12K	620 yds/lb 800 mg/m	SRM 13
	24K	310 yds/lb 1600 mg/m	SRM 13

Typical Mechanical Properties

Tensile Properties	0°	Strength	373 ksi 2572 MPa	ASTM D3039 / 0°8ply
		Modulus	19.9 msi 137 GPa	ASTM D3039 / 0°8ply
	90°	Strength	11.17 ksi 81 MPa	ASTM D3039 / 0°16ply
		Modulus	1.34 msi 9.2 GPa	ASTM D3039 / 0°16ply
Compressive Properties	0°	Strength	198 ksi 1365 MPa	ASTM D3410 / 0°16ply
		Modulus	18.5 msi 127 GPa	ASTM D3410 / 0°16ply
	90°	Strength	30.5 ksi 210 MPa	ASTM D3410 / 0°20ply
		Modulus	1.49 msi 10.2 GPa	ASTM D3410 / 0°20ply
Flexural Properties	0°	Strength	253 ksi 1745 MPa	ASTM D790 / 0°16ply, L/D=32, Vf=61%
		Modulus	19.1 msi 132 GPa	ASTM D790 / 0°16ply, L/D=32, Vf=61%
	90°	Strength	14.9 ksi 102 MPa	ASTM D790 / 0°16ply, L/D=16, Vf=61%
		Modulus	1.28 msi 8.8 GPa	ASTM D790 / 0°16ply, L/D=16, Vf=61%
ILSS	Strength	14.1 ksi 97 GPa	ASTM D2344 / 0°16ply, L/D=4, Vf=59%	

- 250F Epoxy Prepregs
- Resin: Mitsubishi Rayon #340 resin system
- Tensile and compressive properties are normalized to 60% fiber volume

5900 88th Street
Sacramento, CA
95828, USA
Tel: 916.386.1733
Fax: 916.383.7668
Web: www.grafil.com



I.4 Mitsubishi-Rayon Pyrofil TR30S 3K

PYROFIL™

 **MITSUBISHI RAYON CO.,LTD.**

PYROFIL DEPARTMENT
1-1-1, Marunouchi, Chiyoda--Ku
Tokyo ,100-8253, Japan
Tel: +81-3-6748-7514/Fax: +81-3-3286-1380
PYROFIL WebSite: www.mrc.co.jp

Typical Properties of Carbon Fiber

PYROFIL™

	Type	Number of Filaments	Filament Diameter	Yield	Tensile Strength			Tensile Modulus			Elongation	Density
			μ m		mg/m	kg/mm2	Mpa	Ksi	ton/mm2	GPa		
HT Series	TR 30S 3L	3,000	7	200	420	4,120	600	24.0	234	34	1.8	1.79
	TR 50S 6L	6,000	7	400	500	4,900	710	24.5	240	35	2.0	1.82
	TR 50S12L	12,000	7	800								
	TR 50S15L	15,000	7	1,000								
	TR 50D12L	12,000	7	800	510	5,000	720	24.5	240	35	2.1	1.82
	TRH50 18M	18,000	6	1000	540	5,300	770	25.5	250	36	2.1	1.82
	TRH50 60M	60,000	6	3,200	490	4,830	700	25.5	250	36	1.9	1.81
	TRW40 50L	50,000	8	3,750	420	4,120	600	24.5	240	35	1.7	1.80
IM Series	MR 60H 24P	24,000	5	960	580	5,680	820	29.5	290	42	1.9	1.81
HM Series	MS 40 12M	12,000	6	600	450	4,410	640	35.0	345	50	1.3	1.77
	HR 40 12M	12,000	6	600	450	4,410	640	40.0	395	57	1.1	1.82
	HS 40 12P	12,000	5	430	470	4,610	670	46.0	455	65	1.0	1.85

GRAFIL™

	Type	Number of Filaments	Filament Diameter	Yield	Tensile Strength			Tensile Modulus			Elongation	Density
			μ m		mg/m	kg/mm2	Mpa	Ksi	ton/mm2	GPa		
HT Series	34-700	12,000	7	800	490	4,830	700	24.0	234	34	2.0	1.80
		24,000	7	1,600								
	37-800	30,000	6	1,675	560	5,520	800	26.0	255	37	2.1	1.81

Important: The technical information contained herein is not to be construed as warranties and no patent liability can be assumed. This information can be used for material selection purposes only. NOVEMBER 2013

I.5 Tencate - Carbon 205 gsm 2x2 Twill TR30S T 3K

PRODUCT DATASHEET



TENCATE ADVANCED COMPOSITES

TenCate E722 Mid temperature curing modified epoxy component prepreg

PRODUCT TYPE

120°C (248°F) cure
Toughened epoxy resin system

TYPICAL APPLICATIONS

- Motor racing
- Marine industries
- General aircraft fittings
- Sporting equipment
- Wide range of engineering applications

SHELF LIFE

Out life
60 days at @ 20°C (68°F)

Storage life
12 months @ -18°C (0°F)

Out life is the maximum time allowed at room temperature before cure.

To avoid moisture condensation:
Following removal from cold storage, allow the prepreg to reach room temperature before opening the polythene bag. Typically the thaw time for a full roll of material will be 4 to 6 hours.

PRODUCT DESCRIPTION

TenCate E722 is a toughened epoxy resin system for cures at 120°C (248°F), pre-impregnated into high performance fibres such as carbon, glass and aramid. It is designed for structural applications in the motor racing and marine industries. TenCate E722 would also suit general aircraft fittings, sporting equipment, and a wide range of engineering applications. TenCate E722 is compatible for co-cure with TenCate EF72, a 120°C (248°F) cure resin film and TenCate Amlite SC72A syntactic core.

TENCATE E722 PRODUCT BENEFITS/FEATURES

- Excellent drapeability – complex shapes easily formed
- Good surface finish
- Medium tack level – easily laminates to mould surface
- Low volatile content – no solvents used during processing
- 60 day shelf life at ambient temperature
- Autoclave, vacuum bag or press curable

TYPICAL NEAT RESIN PROPERTIES

Density 1.21 g/cm³ (75.5 lbs/ft³) at 23°C (73.4°F)
T_g (DMTA) after 1 hour @ 120°C (248°F)..... Onset: 120°C (248°F); Peak tan δ: 138°C (280°F)

TYPICAL LAMINATE PROPERTIES

HS0838 – CARBON 205 GSM 2X2 TWILL TR30S T 3K - 0/90° CONFIGURATION WOVEN LAMINATES

Property	Condition	Method	Results	
Tensile Strength (Warp)	RTD	ISO 527-4	595 MPa	86 ksi
Tensile Modulus (Warp)	RTD	ISO 527-4	56.1 GPa	8.1 Msi
Poisson's Ratio (Warp)	RTD	ISO 527-4	0.04	
Tensile Strength (Weft)	RTD	ISO 527-4	580 MPa	84 ksi
Tensile Modulus (Weft)	RTD	ISO 527-4	52.4 GPa	7.6 Msi
Poisson's Ratio (Weft)	RTD	ISO 527-4	0.04	
In Plane Shear Strength	RTD	EN 6031	112 MPa	16 ksi
In Plane Shear Modulus	RTD	EN 6031	3.57 GPa	0.5 Msi
Poisson's Ratio	RTD	EN 6031	0.8	
Compression Strength (Warp)	RTD	EN 2850	567 MPa	82 ksi
Compression Modulus (Warp)	RTD	EN 2850	52.5 GPa	7.6 Msi
Compression Strength (Weft)	RTD	EN 2850	563 MPa	82 ksi
Compression Modulus (Weft)	RTD	EN 2850	49.4 GPa	7.2 Msi
ILSS (Warp)	RTD	ISO 14130	68.1 MPa	10 ksi
ILSS (Weft)	RTD	ISO 14130	68.7 MPa	10 ksi

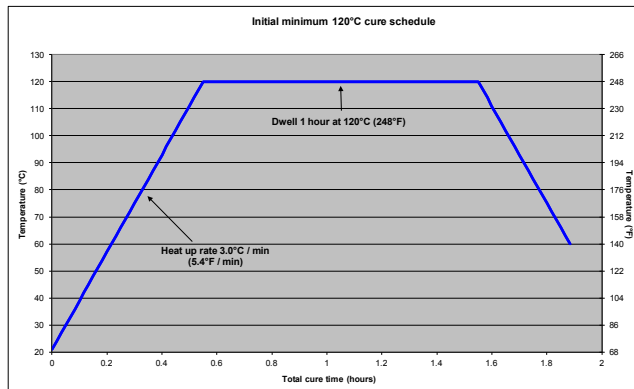
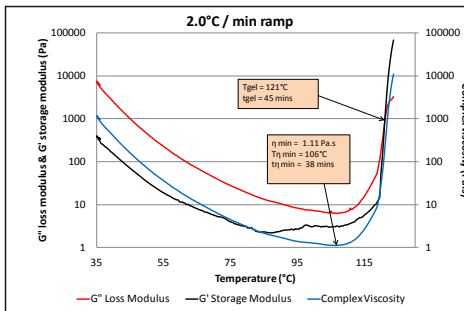
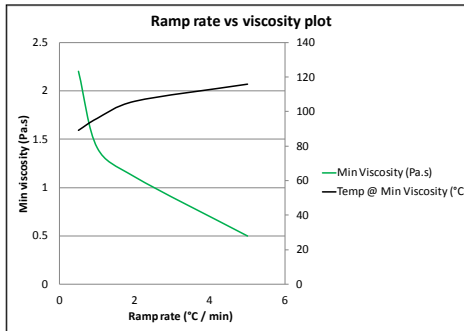
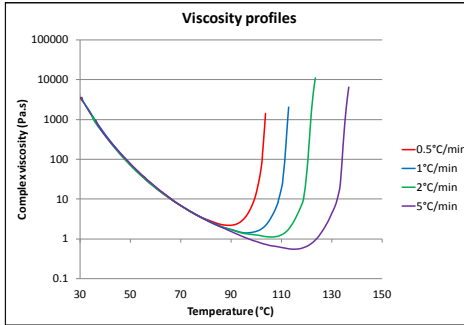
* Cured 1 hour at 120°C (248°F) at 50% Vf.

PRODUCT DATASHEET



TENCATE ADVANCED COMPOSITES

TenCate E722 Mid temperature curing modified epoxy component prepreg



PRODUCT DATASHEET



TENCATE ADVANCED COMPOSITES

TenCate E722 Mid temperature curing modified epoxy component prepreg

RECOMMEND CURE CYCLE

- TenCate E722 can be successfully moulded by vacuum bag, autoclave, or matched die moulding techniques.
- Increase autoclave pressure to 1.4 bar (20 psi) with vacuum applied.
- Vent to atmosphere and raise pressure to 6.2 bar (90 psi) (or max allowed by the core material).
- Increase air temperature at 3°C (5.4°F) / min and hold for 1 hour at 120°C (248°F).
- Allow to cool to 50°C (122°F) before removal of pressure.

CURE PROPERTIES: VISCOSITY PROFILE (30°C TO 140°C OR 86°F TO 284°F)

Ramp rate [°C (°F) / min]	Min viscosity (Pa.s)	Temp @ min viscosity (°C/°F)
0.5 (1)	2.2	89°C (192°F)
1 (1.8)	1.41	96°C (205°F)
2 (3.6)	1.11	106°C (223°F)
5 (9.0)	0.5	116°C (241°F)

HANDLING SAFETY

Observe established precautions for handling epoxy resins and fibrous materials – wear gloves.

For further information refer to Material Safety Data Sheet.

PROCESSING

Cut patterns to size and lay up the laminate in line with design instructions taking care not to distort the prepreg. If necessary, the tack of the prepreg may be increased by gentle warming with hot air. The lay-up should be vacuum debulked at regular intervals using a P3 (pin pricked) release film on the prepreg surface, vacuum of 980 mbar (29 ins Hg) is applied for 20 minutes.

For autoclave cures, use of a non-perforated release film on the prepreg surface trimmed to within 25-30mm of prepreg edge is recommended for the cure cycle, a vacuum bag should be installed using standard techniques.

EXOTHERM

In certain circumstances, such as the production of thick section laminates rapid heat up rates or highly insulating masters, TenCate E722 can undergo exothermic heating leading to rapid temperature rise and component degradation in extreme cases.

Where this is likely, a cure incorporating an intermediate dwell of 1 hour at 90°C (194°F) is recommended in order to minimize the risk.

Revised 08/2013

TenCate AmberTool™ and all other related characters, logos and trade names are claims and/or registered trademarks TenCate and/or its subsidiaries. Use of trademarks, trade names and other IP rights of TenCate without express written approval of TenCate is strictly prohibited.

Page 3 of 3

TENCATE_E722_V7_DS_082813

TENCATE ADVANCED COMPOSITES

Amber Drive, Langley Mill
Nottingham, NG16 4BE UK
Tel: +44 (0)1773 530899
Fax: +44 (0)1773 768687

Campbellweg 30
7443 PV Nijverdal NL
Tel: +31 548 633 933
Fax: +31 548 633 299

18410 Butterfield Blvd.
Morgan Hill, CA 95037 USA
Tel: +1 408 776 0700
Fax: +1 408 776 0107

www.tencate.com

www.tencateadvancedcomposites.com
www.tencateindustrialcomposites.com
E-mail: tcac-us@tencate.com (USA)
E-mail: ambersales@tencate.com (Europe)

ISO 9001
ISO 14001
Registered
AS 9100

I.6 XPREG XC110 Out-Of-Autoclave Component Prepreg System



XC110 prepreg is laid into a temperature stable mould. This part uses only 2 plies in total.



Once laminated, the part is vacuum bagged and cured in an oven at 120°C under vacuum.



The cured part has a pin-hole free 'class A' surface finish straight from the mould.

XC110 | OUT-OF-AUTOCCLAVE COMPONENT PREPREG SYSTEM

XPREG® XC110 is an advanced prepreg system designed specifically for out-of-autoclave (vacuum bag, oven cure) processing. The special resin formulation has been developed to produce cured laminates with a 'class A' surface finish and minimal void content when over-cured under vacuum pressure only.

Components made using the XC110 resin system offer mechanical properties comparable to autoclave-cure systems (such as XPREG® XC130) without the need for expensive autoclave plant or the associated cycle costs. The system is also ideally suited for large components which exceed the capacity of typical autoclaves, such as boat hulls and turbine blades.

XC110 prepreps can be backed-up with unidirectional reinforcement (from the XC130 range) and are fully compatible with our XA120 adhesive film meaning that even the most complex composite structures - including honeycomb cores - can be achieved out-of-autoclave.

RECOMMENDED USES

XC110 is the recommended system for both structural and cosmetic applications where components will be cured without an autoclave.

The combination of excellent mechanical performance, visual quality appearance and class-A surface finish make XC110 prepreps suitable for a wide range of applications from large-scale structural components to high-precision cosmetic parts.

High Performance

- UAV/drones
- Motorsport
- Bike frames
- Racing boats
- Skis, boards

Large Scale

- Boat hulls
- Wind energy
- Mass transit
- Light aircraft

Cosmetic/Lifestyle

- Interior trim
- Phone cases
- Furniture
- Stands/display

CURING

XPREG® XC110 is designed to be oven cured in a vacuum bag at full vacuum pressure however it can also be cured in an autoclave or hot-press. Minimum vacuum pressure is 10mbar.

For best results, an accurately controlled multi-stage temperature cycle with final cure temperature of 120°C should be followed:

STANDARD CURE CYCLE

Step	Start Temp	Ramp Rate	Duration	End Temp	Elapsed Time
1	~ 20°C	1°C /min	00:50	70°C	00:50
2	70°C	Soak	04:00	70°C	04:50
3	70°C	2°C /min	00:25	120°C	05:15
4	120°C	Soak	01:00	120°C	06:15
5	120°C	Natural Cool	--	~20°C	07:15



For detailed information, including alternative cure cycles from 85°C see the *XC110 Processing Handbook*.

SUITABLE MOULDS/TOOLING

Moulds/tools should be epoxy-based composite moulds, epoxy tooling board or metal. In all cases, moulds must be temperature stable to a minimum of 85°C but ideally to 120°C.

Although it is possible to use Vinylester tools (such as Uni-Mould™) they are not recommended due to the increased possibility of surface imperfections (pin holes) which can occur when XPREG® XC110 is cured in the presence of vinylester.

Polyurethane tooling board should never be used with any XPREG® prepreg due to the cure inhibition of polyurethane on epoxy on elevated temperature.

Fully Compatible

- Carbon or glass fibre prepreg moulds (e.g. XPREG® XT135)
- Epoxy tooling board (e.g. EP700 with S120 Board Sealer)
- High temp epoxy hand-layup moulds (e.g. EG160 / EMP160)
- Aluminium / stainless steel moulds
- Toughened glass (for flat sheet/panels)

NOT Recommended

- Vinylester composite moulds (e.g. Uni-Mould™)

NOT Compatible

- Polyester composite moulds
- Polyurethane model/tooling board

For detailed information on mould suitability and preparation, see the *XC110 Processing Handbook*.

STANDARD REINFORCEMENTS

XPREG® XC110 is available off-the-shelf using standard reinforcements of 210g 3k and 450g 12k carbon fibre.

SKU	Fibre	Weight (gsm)	Weave	Width (mm)
XC110-C331T2-210(1250)	Pyrofil TR305 High Strength Carbon 3k	210	2x2	1250
XC110-1232T2-450(1250)	Pyrofil TR505 High Strength Carbon 12k	450	2x2	1250

A range of alternative reinforcements including multiaxial and unidirectional can be produced on request, subject to MOQ.

TECHNICAL SPECIFICATION

GENERAL PROPERTIES

Cure temperature range	85°C to 120°C
Maximum service temperature	115°C (after post cure)
Out-life (at 20°C)	30 days
Freezer-life (at -18 °C)	12 months
VOC content	Very low (solvent free)

CURED MECHANICAL PROPERTIES

Tests performed on XC110-C331T2-210(1250) laminate cured out-of-autoclave

Property	Test Standard	Units	Result
Compressive strength	BS EN ISO 14126 : 1999	MPa	483
Tensile strength	BS EN ISO 527-4 : 1997	MPa	521
Tensile modulus	BS EN ISO 527-4 : 1997	GPa	55.1
Flexural strength	BS EN ISO 14125 : 1998	MPa	777
Flexural modulus	BS EN ISO 14125 : 1998	GPa	46.7
Interlaminar shear strength	BS EN 2563 : 1997	MPa	64.7
Tg Onset (DMA)	ASTM 1-0003 Issue 3	°C	121
Tg Peak (DMA)	ASTM 1-0003 Issue 3	°C	135

STORAGE & HANDLING

When not in use, XPREG® prepregs should be kept frozen at -18°C (0°F) in sealed plastic packaging. When ready to use, the material should be removed from the freezer and allowed to thaw fully to room temperature before being removed from the packaging.

Remaining material should be re-sealed before returning to the freezer to avoid the risk of moisture uptake.

PROCESSING GUIDE

XPREG® XC110 is supported by a highly detailed processing guide to help users achieve the best results from this advanced material.

The guide includes information on recommended laminating and vacuum bagging procedures, tooling and mould preparation, process specific cure cycles, working with core materials and adhesive films, and troubleshooting tips.

SAFETY INFORMATION

This material contains uncured epoxy resin which can cause allergic reactions with skin contact. Repeated and prolonged skin contact must be avoided.

Please refer to the product safety data sheet before working with this material.



XC110 | OUT-OF-AUTOCLAVE COMPONENT PREPREG

OTHER XPREG® SYSTEMS

XT135	Out-of-autoclave tooling prepreg system ideal for use with XC110. Maximum service temp of 135°C.
XA120	Adhesive film fully compatible with XC110.
XC130	Autoclave cure, visual quality, high performance prepreg with a service temperature of 130°C. Co-curable with XC110.
XT180	Autoclave cure tooling prepreg with low CTE, long out-life and 180°C service temperature.
XT210	Aerospace industry autoclave cure tooling prepreg with low CTE and very high 210°C service temperature.

Disclaimer

This data is not to be used for specifications. Values listed are for typical properties and should not be considered minimum or maximum.

Our technical advice, whether verbal or in writing, is given in good faith but Easy Composites Ltd gives no warranty; express or implied, and all products are sold upon condition that purchasers will make their own tests to determine the quality and suitability of the product for their particular application and circumstances.

Easy Composites Ltd shall be in no way responsible for the proper use and service of the product, nor for the safeguarding of personnel or property, all of which is the duty of the user. Any information or suggestions are without warranty of any kind and purchasers are solely responsible for any loss arising from the use of such information or suggestions. No information or suggestions given by us shall be deemed to be a recommendation to use any product in conflict with any existing patent rights. Before using any of our products, users should familiarise themselves with the relevant technical and safety datasheets provided by Easy Composites Ltd.



XPREG® is distributed exclusively by Easy Composites Ltd from centres in the UK and China.

Easy Composites Ltd

Units 39-40, Park Hall Business Village,
Stoke on Trent, Staffordshire, ST3 5XA
United Kingdom
Tel. +44 (0)1782 454499
Email sales@easycomposites.co.uk
Web www.easycomposites.co.uk

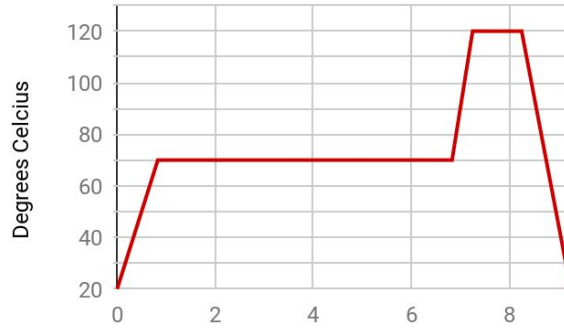
Easy Composites (Beijing) Ltd

No.20# A , U Gu Mid Area
Liandong, Majuqiao, Beijing
101102, **China**
Tel. +86 (0) 1057485810
Email sales@easycomposites.asia
Web www.easycomposites.asia

I.7 XPREG XC110 Out-Of-Autoclave Component Prepreg System - Processing Guide

Extended Soak Cycle

This cure cycle is recommended for use on laminates above 4 plies, or components of high complexity, with the extended initial soak of 6hrs this capitalises on the full flow time available and will yield the lowest void content possible in nearly all applications, the only downside of this cycle against the 'Standard' cure cycle is the processing time as it is 2 Hours longer at 9hr 15min.



Step #	Start Temp	Ramp Rate	Time	End Temp	Elapsed Time
1	~20°C	1°C/min	00:50	70°C	00:50
2	70°C	Soak	06:00	70°C	06:50
3	70°C	2°C/min	00:25	120°C	07:15
4	120°C	Soak	01:00	120°C	08:15
5	120°C	Natural Cool	--	~20°C	09:15

Low Temp Cycle

This cure cycle is recommended when the maximum temperature capability of either the mould or the oven is lower than 120°C used in the 'Standard' cure. This cycle does not reflow the resin to the same degree and may in rare cases lead to an increased void content and reduce surface finish. The reduced final cure temperature increases the process time and reduces the final HDT (max temp) of the laminate unless subsequently post-cured.



Step #	Start Temp	Ramp Rate	Time	End Temp	Elapsed Time
1	~20°C	1°C/min	00:50	70°C	00:50
2	70°C	Soak	04:00	70°C	04:50
3	70°C	2°C/min	00:08	85°C	04:58
4	85°C	Soak	10:00	85°C	14:15
5	85°C	Natural Cool	--	~20°C	15:00

I.8 EPIKOTE Resin MGS RIMR 135 Data Sheet



Technical Data Sheet

Issued: August 2006

EPIKOTE™ Resin MGS™ RIMR 135 and EPIKURE™ Curing Agent MGS™ RIMH 134–RIMH 137

CHARACTERISTICS

Approval	German Lloyd
Application	Specially designed for infusion processes (RMT, SCRIMP/VARI); rotor blades for wind turbines, boat and shipbuilding, sports equipment
Operational Temperature	-60 °C up to +50 °C (-76 °F up to 122 °F) without heat treatment -60 °C bis +80 °C (-76 °F up to 176 °F) after heat treatment
Processing	At temperatures between 10 °C and 50 °C (50-122 °F) due to the very low mixing viscosity especially suited for infusion, injection and pultrusion
Features	Very low viscosity, excellent initial curing properties at room temperature, pot life from approx. 0,5 hours to approx. 4 hours, short curing times at high temperatures
Storage	Shelf life of 24 months in originally sealed containers

APPLICATION

Very low viscosity laminating resin system with different pot lives for processing of glass, carbon and aramide fibers. Due to its good mechanical properties, this system is suitable for the production of components featuring high static and dynamic loadability.

The range of pot lives is between approx. 0,5 hour and 3-4 hours. The parts can be worked and demoulded after curing at room temperature. Curing at higher temperatures (up to approx. 80-100 °C, 176-212 °F) is possible, depending on layer thickness and geometry of the parts to be manufactured. The curing times can be reduced to a few minutes by this.

Adding internal parting agents, such as zinc stearate, etc., has proven useful for pultrusion processes. Profiles with good surface qualities are obtained. Depending on profile geometry, mould temperatures in the range of 180-230 °C (356-446 °F) are possible, thus permitting high drawing speeds.

The mixing viscosity is very low, which is especially advantageous for infusion and injection processes. It may be lowered to approx. 150 mPas by heating the resin mass (see diagram). This means that even complicated molded parts with long flow paths can be easily infused. The temperature rise with hardener RIMH 137 remains very low up to a mold temperature of approx. 30 °C, so that even parts of greater thickness can be produced at elevated temperatures.

The infusion resin system does not contain any unreactive components. The raw materials used feature a

very low vapor pressure. This permits processing of the material under vacuum even at elevated temperatures (VARIM process). Compatibility problems are not to be expected in combination with UP gelcoats, various paints (e.g. PUR-based), etc. However, comprehensive tests are indispensable.

The relevant industrial safety regulations for the handling of epoxy resins and hardeners and our instructions for safe processing are to be observed.

The resin and hardeners can be stored for at least 24 months in their carefully sealed original containers. The resin and hardeners may crystallise at temperatures below +15 °C (59 °F). The crystallisation is visible as a clouding or solidification of the contents of the container. Before processing, the crystallisation must be removed by warming up. Slow warming up to approx. 50-60 °C (122-140 °F) in a water bath or oven and stirring or shaking will clarify the contents of the container without any loss of quality. Use only completely transparent products. Before warming up, open containers slightly to permit equalization of pressure. Caution during warm-up! Do not warm up over an open flame! While stirring up, use safety equipment (gloves, eyeglasses, respirator).

SPECIFICATIONS

		Infusion Resin RIM 135
Density	[g/cm ³]	1,13 - 1,17
Viscosity	[mPas]	700 - 1.100
Epoxy equivalent	[g/equivalent]	166 - 185
Epoxy value	[equivalent/100g]	0,54 - 0,60
Refractory index		1,548- 1,552

		Hardener RIMH 134	Hardener RIMH 137
Density	[g/cm ³]	0,93 - 1,00	0,93 - 0,98
Viscosity	[mPas]	10 - 80	10 - 50
Amine Value	[mg KOH/g]	550 - 700	400 - 600
Refractory index		1,4900 - 1,5000	1,460 - 1,463

Measuring conditions: measured at 25 °C / 77 °F

PROCESSING DETAILS

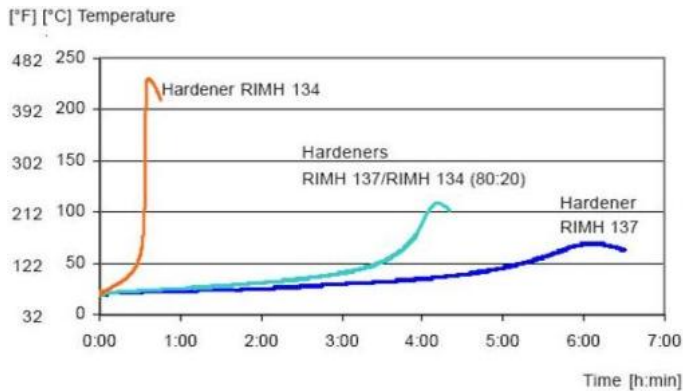
	Infusion Resin RIMR 135	Hardeners RIMH 134-137
Average EP - Value	0,56	-
Average amine equivalent	-	52

MIXING RATIOS

	Infusion Resin RIMR 135 : Hardener RIMH 134 – RIMH 137
Parts by weight	100 : 30 ± 2
Parts by volume	100 : 36 ± 2

The specified mixing ratios must be observed as exactly as possible. Adding more or less hardener will not effect a faster or slower reaction - but in incomplete curing which cannot be corrected in any way. Resin and hardener must be mixed very thoroughly. Mix until no clouding is visible in the mixing container. Pay special attention to the walls and the bottom of the mixing container.

TEMPERATURE DEVELOPMENT



Quantity: 100 g / 20 °C (77 °F)

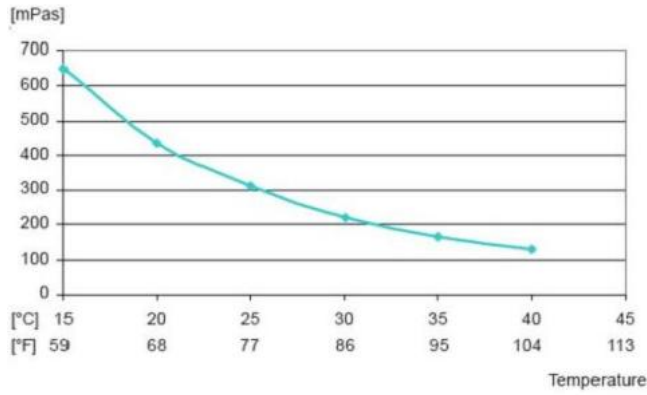
The optimum processing temperature is in the range between 20 °C and 25 °C (68-77 °F). Higher processing temperatures are possible, but will shorten pot life. A rise in temperature of 10 °C (50 °F) will halve the pot life. Water (for example very high humidity or contained in fillers) causes an acceleration of the resin/hardener reaction. Different temperatures and humidities during processing have no significant effect on the strength of the hardened product.

Do not mix large quantities - particularly of highly reactive systems - at elevated processing temperatures. The heat flow from the mixing container is very low, so the contents will heat up fast because of the dissipating reaction heat (exothermic resin-hardener reaction). This can result in temperatures of more than 200 °C (392 °F) in the mixing container, which may cause smoke-intensive burning of the resin mass.

VISCOSITY

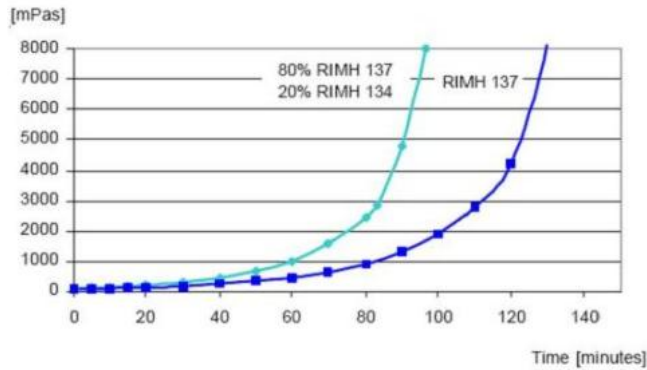
Viscosity of mixture at different temperatures

Infusion resin RIM 135 with mixture of Hardeners RIMH 137 (80 %) /RIMH 134 (20 %)



Viscosity development

Infusion resin RIM 135 with mixture of Hardeners RIMH 137 (80 %) /RIMH 134 (20 %) and Hardener RIMH 137



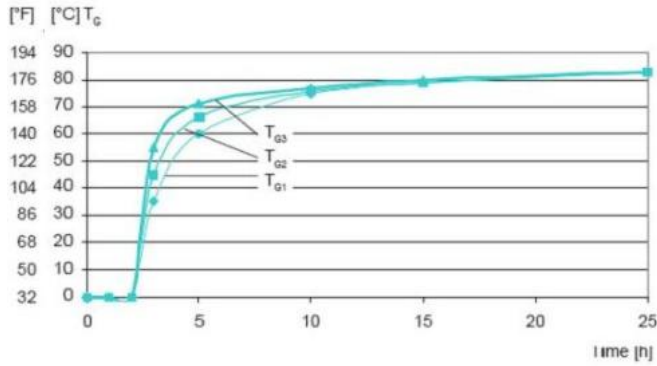
Measuring conditions:

Temperature: 40°C (104 °F); measuring gap 0,2 mm

T_g DEVELOPMENT

Development of glass transition temperature (T_g) at 60 °C

Infusion resin RIM 135 with mixture of Hardeners RIMH 137 (80 %) /RIMH 134 (20 %)

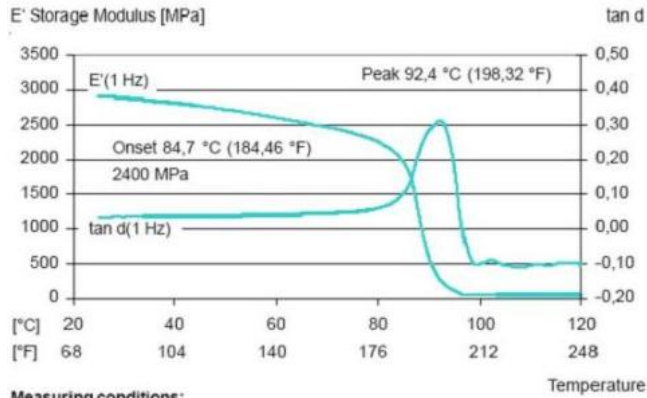


DMA

DMA Measuring after heat treatment

DMA-T_g (peak) tan delta

Infusion resin RIM 135 with mixture of Hardeners RIMH 137 (80 %) /RIMH 134 (20 %)



Measuring conditions:
 Sample thickness: 2 mm
 Heat rate: 2 K/min

MECHANICAL DATA

Mechanical Data of Neat Resin		
Density	[g/cm ³]	1,18 - 1,20
Flexural strength	[N/mm ²]	90 - 120
Modulus of elasticity	[kN/mm ²]	2,7 - 3,2
Tensile strength	[N/mm ²]	60 - 75
Compressive strength	[N/mm ²]	80 - 90
Elongation of break	[%]	8 - 16
Impact strength	[KJ/m ²]	70 - 80
Water absorption at 23 °C	24 h [%]	0,10 - 0,20
	7 d [%]	0,20 - 0,50
Fatigue strength under reversed bending stresses acc. to DLR Brunsw.	10%	exp. > 1 x 10 ⁶
	90%	exp. > 2 x 10 ⁶
Curing: 24 h at 23° C (74° F) + 15 h at 60° C (140° F), partly cured/full cure Typical data according to WL 5.3203 Parts 1 and 2 of the GERMAN AVIATION MATERIALS MANUAL		

Advice: Mechanical data are typical for the combination of laminating resin RIMR 135 with hardener RIMH 137. Data can differ in other applications.

Data of Reinforced Resin – Static Tests Standard Climate

Reinforced with:		GRC Glass Fibre	CRC Carbon Fibre	SRC Aramide Fibre
Flexural strength	[N/mm ²]	510 - 560	720 - 770	350 - 380
Tensile strength	[N/mm ²]	460 - 500	510 - 550	400 - 480
Compressive strength	[N/mm ²]	410 - 440	460 - 510	140 - 160
Interlaminar shear strength	[N/mm ²]	42 - 46	47 - 55	29 - 34
Modulus of elasticity	[kN/mm ²]	20 - 24	40 - 45	16 - 19
<p>GRC samples: 16 layers of glass fabric, 8H satin, 296 g/m² (8.7 oz/sq.yd.), 4 mm (0.16 in) thick CRC samples: 8 layers of carbon fabric, plain, 200 g/m² (5.9 oz/sq.yd.) 2 mm (0.08 in) thick SRC samples: 15 layers of aramide fabric, 4H satin, 170 g/m² (5.0 oz/sq.yd.) , 4 mm (0.16 in) thick</p> <p>Fibre content of samples during processing/testing: 40-45 vol% Data calculated for fibre content of 43 vol%</p> <p>Typical data according to WL 5.3203 Parts 1 and 2 of the GERMAN AVIATION MATERIALS MANUAL</p> <p>Sample Preparation: Curing: 24 h at 23 °C (74 °F) +15 h at 80 °C (180 °F)</p>				

© and ™ Licensed trademarks of Hexion Inc.

DISCLAIMER

The information provided herein was believed by Hexion Inc. ("Hexion") to be accurate at the time of preparation or prepared from sources believed to be reliable, but it is the responsibility of the user to investigate and understand other pertinent sources of information, to comply with all laws and procedures applicable to the safe handling and use of the product and to determine the suitability of the product for its intended use. All products supplied by Hexion are subject to Hexion's terms and conditions of sale. **HEXION MAKES NO WARRANTY, EXPRESS OR IMPLIED, CONCERNING THE PRODUCT OR THE MERCHANTABILITY OR FITNESS THEREOF FOR ANY PURPOSE OR CONCERNING THE ACCURACY OF ANY INFORMATION PROVIDED BY HEXION,** except that the product shall conform to Hexion's specifications. Nothing contained herein constitutes an offer for the sale of any product.

PDS-8246- (Rev.3/23/2015 3:45:24 AM)

I.9 TEKNOSEAL 4002 Sealer Data Sheet



TEKNISK DATABLAD
7 18-09-2017

TEKNOSEAL 4002-XX

Side 1 av 2

Sealer for sprøytepåføring

TEKNOSEAL 4002 er en vannfortynnbar sealer til industriell behandling av MDF/HDF utendørs kvalitet til vinduer og dører.

TEKNOSEAL 4002 har god forseglingseffekt mot opptak av vann/fuktighet og sikrer dimensjonsstabilitet.

TEKNISKE DATA

Bindemiddel:	Syntetisk bindemiddel
Flyktige organiske forbindelser (VOC):	Se sikkerhetsdatablad.
Teoretisk forbruk:	6-8 m ² /l
Farger:	Fargeløs

PÅFØRINGSINFORMASJON

Forbehandling: Substratet må være rent og fritt for trestøv og forurensinger. Emnene må alltid forbehandles med et Teknos grunningsprodukt, og kanter og utfresninger pensles med TEKNOSEAL 4002 før sprøytepåføring for å sikre optimal forseglingseffekt.

Påføring: Airmix (sprøytepåføring) eller uten luft med hånd eller i automatisk sprøyteutstyr.

Påføringsforhold: Produktet leveres klart til bruk. Rør godt i produktet før bruk.

Lagtykkelse:	175-200 µm vått
Optimal temperatur for produktet og omgivelsene:	18-22 °C
Optimal relativ luftfuktighet:	ca. 50 %

Sprøyteforhold:	<u>Dyse</u>	<u>Trykk</u>	<u>Luftmengde</u>
	Airless 0,28 mm	100-110 bar	
	Aircoat 0,28 mm	80-100 bar	1,0-1,5 bar

Systembehandling: Behandlede emner sluttbehandles med topcoat før de utsettes for vær og vind.

Tørketider: Ved 20 °C og 50 % relativ luftfuktighet:

Berøringstørr:	1-2 timer
Tørketid før sliping*/neste strøk:	2-3 timer

* Ettersom lagtykkelsen er avgjørende for produktets effektivitet, er det viktig å ikke slippe overflaten for mye. Eventuell sliping skal derfor holdes på et minimum, og det er særdeles viktig at det ikke slipes igjennom filmen.

Tørketiden kan reduseres ved å bruke spesielle tørkesystemer for å redusere tørketiden. Tørketidene er omtrentlige og kan variere i henhold til trekvalitet, temperatur, luftfuktighet, ventilasjon og lagtykkelse.

Rengjøring: Utstyret rengjøres med vann.

SIKKERHETSDATA Se sikkerhetsdatablad.

I.10 TEKNOTHERM 4350 Topcoat Datasheet



TECHNICAL DATA SHEET
5 25.09.2013

TEKNOTHERM 4350 Stoving topcoat 4350-00

PAINT TYPE	Stoving topcoat.		
USE	Topcoat for steel and light alloy metals.		
SPECIAL PROPERTIES	Excellent adhesion to steel. Provides a scratch- and impact resistant surface. Resistant to water, oil, weak acids and bases. Resistant to yellowing when stoved. Outdoor resistant.		
TECHNICAL DATA			
Solids	Approx. 52 %		
Total mass of solids	1026 g/l		
Volatile organic compound (VOC)	418 g/l		
Recommended film thickness and theoretical spreading rate	Dry film (µm) 35	Wet film (µm) 70	Theoretical spreading rate (m ² /l) 12 - 16
Curing	Suggested curing time/object temperature		
	Flash off time:	Approx. 10 minutes	
	Stoving time:	30 minutes at 150 °C 15 minutes at 170 °C 10 minutes at 180 °C	
Thinner	See page 2.		
Clean up	TEKNOSOLV 6340-00.		
Finish	Can be supplied in full gloss and semi-gloss.		
Colours	Colours are produced by using colour-mixing machine. As RAL, NCS-S and other references are stored in the computer memory; delivery times are kept to a minimum. If the colour has to be matched exactly to a previously supplied batch or a different product, this variant should not be used.		
Primer	Max. adhesion and protection against corrosion is obtained by using TEKNOTHERM PRIMER 4010.		
Packing	Is supplied in 10 litre containers with a content of 9 litres of paint + colouring paste.		
Delivery	The colour production system enables individual orders to be processed very quickly.		
Storage	See additional information.		
HEALTH AND SAFETY	See Safety Data Sheet.		

PTO

I.11 SprayMax 2k Clear Coat

Technical Data Sheet



Peter Kwasny GmbH, Heilbronner Str. 96
74831 Gundelsheim / Deutschland
Telefon: +496269 95-0, Fax: +496269 95-80
www.spraymax.com / www.kwasny.com / info@kwasny.de

SprayMax® 2K Clear coat semi gloss 400 ml Art. Nr. 680067



Product

Description / Purpose

2K clear coat with very high chemical, gasoline, and weathering resistance for high-quality and longterm sealing of repair paint jobs and new paint jobs on cars and motorcycles.

Properties

- Maximum resistance to abrasion and scratching
- Very smooth flow
- Very good polish ability
- No colour deviation
- Outstanding painting surface
- Suitable even at higher ambient temperatures
- Ideally suited for large surfaces

Material base

Two-component acrylic resins
Activator: aliphatic isocyanates

Gloss level

semi gloss

VOC Value (EU)

36+/-2 gloss units at 60° measuring angle
710 g/l

Substrate

Solvent and waterborne base coat systems, old paint coats dried according to manufacturer's instructions (cleaned and sanded).



Processing

Protection measures



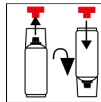
Wear personal protection equipment.
(respiratory mask/gloves/goggles)
For more information, see safety data sheet.

Shake



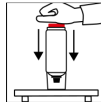
Before activating, shake can thoroughly for 2 minutes from when the mixing balls are heard.

Place red button



Remove the red button from the cap. Turn the can by 180° and fit the button onto the pin.

Press red button



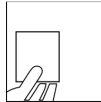
Turn the can upside down and place on a firm surface. Press the red button with the palm of your hand until it clicks into place.

Shake



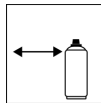
After activating, shake can again thoroughly for 2 minutes, again from when the mixing balls are heard.

Spray to test



After shaking the can, test spray and check compatibility with the surface and the colour.

Spraying distance



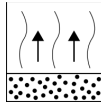
15 cm - 20 cm

Spray passes



Dry film thickness 40 µm
(approx. 1 - 2 spray coats)

Flash-off time



Flash time: approx. 10 - 15 min between each spray coat

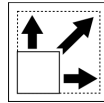
Processing conditions



Optimum application at 18°C - 25°C and a relative humidity from 40 - 50 %.



Coverage



approx. 0,5 - 0,75 m² at 30 - 50 µm dry film thickness

Drying



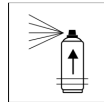
TG1 dust dry: 12 min
TG3 dry to touch: 80 min

The stated values refer to the above mentioned processing conditions. The level of dryness is determined pursuant to DIN 53150.



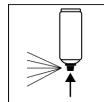
IR- drying possible,
Observe equipment description

Pot life



Approx. 48 h at 20 °C room temperature and a relative humidity of approx. 40 - 50 %. The processing time depends on the ambient temperature. Higher temperatures reduce the pot life, lower temperatures will prolong it.

Finish



After painting, turn the can upside down and spray the valve until empty.

Additional Information

Shelf Life



36 months (not activated)
The usage period refers to an unused can that is stored correctly at a temperature of 15 – 25 °C and a relative humidity below 60%. The can must be stored and transported in an upright position in a dry place where it is protected against chemical and mechanical influences. The safety information on the can and all statutory provisions applicable for the storage site must be observed.

I.12 Chemlease 2185 Release Agent



Chemlease[®] 2185 Semi-Permanent Release Agent

Description

Chemlease[®] 2185 is a one-part, room-temperature curing material that provides a long-wearing release film with proper mold preparation and application. It gives easy, multiple releases, and does not require an extended cure. It is a ready-to-use liquid dispersion.

Mold Preparation/Cleaning

Because Chemlease[®] semi-permanent release agents polymerize on the mold surface, all traces of prior release agents, sealers and buffers/polishes must be removed from the mold.

This method will remove not only wax release agents, but also waxes, silicones and water solubles that are contained in buffing and rubbing compounds. This includes "jewelers' rouge." To clean the mold following buffing, take the following steps:

1. Using liberal quantities of clean water, wipe the mold with a clean, soft, lint-free cotton cloth (tee-shirt-type material) and wipe until dry.
2. Soak a clean, soft, lint-free cloth with a Chemlease[®] Mold Cleaner.
3. Apply the cleaner to the mold surface.
4. Before the cleaner dries, use a second clean cloth to wipe off the dissolved wax and other contaminants.
5. Continue steps 3 and 4 until the surface is free of wax. When all traces of prior release agent have been removed, the hand/thumb will skid, and not slip, across the mold surface.

Application

Always use in a well-ventilated area. Consult MSDS prior to use. The ideal temperature of the mold for application is between 65-80°F/18-27°C.

If Chemlease[®] 2185 is applied below 65°F/18°C, allow a longer time than generally recommended for room-temperature curing. If applied when the mold surface is over 80°F/27°C, curing will be faster.

1. Shake or mix well before and during use. Soak a clean, soft, lint-free cotton cloth (tee-shirt type material) until it is thoroughly wet.
2. Starting at one end of the mold, wipe a generous wet film over a 2 x 2 foot section.
3. Repeat until the mold is completely covered. (see note after "5" which applies to very large molds)
4. Check the treated mold for any area that appears uncoated (where haze is not present). Coat as above.

5. After the product has dried to a haze on the mold surface, polish with a clean, dry, lint-free cotton cloth until a high gloss is obtained. To ensure that no release agent is re-deposited onto the mold, change cloth frequently.

Note: Do not allow any product to remain dry (hazed) for any longer than 30 minutes as it will become very difficult to buff out

6. Repeat steps 1-6 an additional four times for a total of five coats of Chemlease[®] 2185. This will allow the release agent to seal any mold pores and will give the necessary film thickness to permit multiple releases. A final polish with a clean cotton cloth will achieve a higher, Class A, gloss.
7. A cure time of 30 minutes is recommended prior to molding parts.

Touch-Up Coats

As parts are removed from the mold, abrasion will gradually wear away the release film. When slight sticking is noticed, maintain the film by applying one or two touch-up coats (as required) as described above.

Molders should experience no buildup with Chemlease[®] 2185. Previously-applied Chemlease[®] does not have to be removed prior to touch-up. If the mold surface contains buildup of materials such as styrene, internal mold releases, UV absorbers, gel coats, "top coats" or other mold contaminants, clean the mold with a Chemlease[®] Mold Cleaner as specified under Mold Preparation/Cleaning.

Packaging

Chemlease[®] 2185 is available in a variety of package sizes. Please contact Chem-Trend customer service for details.

Safety Data

Safety Data Sheets are available for all Chemlease[®] products and should be consulted prior to use of the product.

Further Information

Request information on our complete range of materials: custom-formulated release agents for polyurethane molding; tire lubes and bladder coatings; Mono-Coat[®] semi-permanent release coatings; aerosol formulations; mold cleaners and sealers; specialized coatings and application equipment.

While the technical information and suggestions for use contained herein are believed to be accurate and reliable, nothing stated in this bulletin is to be taken as a warranty either expressed or implied.

